

# **Regional, seasonal, and predictable Arctic sea ice change**

**Ingrid H. Onarheim**



Thesis for the degree of philosophiae doctor (PhD)  
at the University of Bergen

2017

Date of defence: 07.12.2017



# Abstract

The loss of Arctic sea ice is one of the most prominent and best quantified indicators of ongoing global climate change. Satellite passive microwave observations since 1979 indicate significant negative sea ice extent trends in all months, accompanied by pronounced interannual variability. The recent changes in the Arctic sea ice cover have profound environmental, societal, and ecological impacts, and have led to an increased demand for reliable sea ice predictions. This thesis considers observed regional, seasonal, and predictable Arctic sea ice variability and trends, and particularly assesses the impact of Atlantic water on the recent winter sea ice area variability and loss.

Updated through 2016, the recent Arctic sea ice extent decline is most pronounced in summer along the Russian and North American shelves. Winter trends are currently smaller and generally further south. The largest winter sea ice extent loss has occurred in the Atlantic sector, particularly in the Barents Sea and Nansen Basin, where the sea ice extent is currently less than half of the pre-satellite mean (1850–1978). The recent winter sea ice extent trend and interannual variability in the Arctic Ocean, carried by the Barents Sea and Nansen Basin, largely depend on variations in the advection of Atlantic heat. Based on recent winter observations, it is shown that the warm Atlantic water in the Nansen Basin typically melts sea ice advected from the Arctic Ocean. In contrast, most sea ice forms locally in the Barents Sea and the inflow of Atlantic water mainly inhibits sea ice freezing there.

Rooted in observations, the thesis presents and evaluates prognostic frameworks to predict winter sea ice variability in the Barents Sea and Nansen Basin. It is shown that the Barents Sea ice area may be skillfully predicted, both qualitatively and quantitatively, up to two years in advance based on observed ocean heat transport and regional sea ice area. By using observed hydrography upstream, the Nansen Basin sea ice area appears skillfully predictable up to three years in advance. Anomalously strong meridional winds also impact interannual sea ice variability, and partly explain model imperfection.

The recent loss of Arctic sea ice is unprecedented in all seasons considering the available historical record since 1850. Both climate models and extrapolation of present trends project the Arctic sea ice extent loss to continue toward 2100. In particular, the Barents Sea is expected to be ice-free year-round by the end of the century. If the current sea ice extent trends persist, the Arctic Ocean will become ice-free in summer, and trends gradually have to increase toward the winter season and in regions presently fully ice covered in winter. In summary, this thesis demonstrates that the recent observed Arctic winter sea ice extent variability and trends mainly reflect variations in the Atlantic inflow to the Arctic, and can skillfully be predicted one to three years in advance. More generally, the thesis documents from observations how the ongoing pan-Arctic shift toward a seasonal sea ice cover is increasingly concerned with wintertime change.



# Contents

<b>Acknowledgements</b>	<b>i</b>
<b>Abstract</b>	<b>iii</b>
<b>1 Outline</b>	<b>1</b>
<b>2 Scientific background</b>	<b>2</b>
2.1 Recent change in Arctic sea ice . . . . .	2
2.1.1 Contributors to sea ice variability and change . . . . .	4
2.1.2 Recent change in a longer perspective . . . . .	5
2.2 Atlantic water inflows to the Arctic Ocean . . . . .	7
2.2.1 Fram Strait branch . . . . .	8
2.2.2 Barents Sea branch . . . . .	8
2.2.3 Long-term variability . . . . .	9
2.3 Predictions and projections . . . . .	10
2.3.1 Sea ice predictions . . . . .	10
2.3.2 Sea ice projections . . . . .	11
<b>3 This study</b>	<b>13</b>
3.1 Motivation and objectives . . . . .	13
3.2 Data and methods . . . . .	14
3.2.1 Observations . . . . .	14
3.2.2 Models . . . . .	16
<b>4 Summary of papers</b>	<b>17</b>
4.1 Paper I: Loss of sea ice during winter north of Svalbard . . . . .	17
4.2 Paper II: Skillful prediction of Barents Sea ice cover . . . . .	17
4.3 Paper III: Toward an ice-free Barents Sea . . . . .	18
4.4 Paper IV: Sea ice variability and predictability in the Nansen Basin . . . . .	18
4.5 Paper V: Seasonal and regional manifestation of Arctic sea ice loss . . . . .	19
<b>5 Perspectives and outlook</b>	<b>20</b>
5.1 Simulated sea ice extent trends . . . . .	22
<b>References</b>	<b>25</b>
<b>Manuscripts</b>	<b>39</b>



# 1. Outline

This thesis consists of an introductory part and five scientific papers. The introduction gives a general scientific background including an overview of recent changes in the Arctic sea ice cover, variations in the inflow of Atlantic water to the Arctic, and a brief review of Arctic sea ice prediction models (Section 2). Motivation and objectives are provided in Section 3 followed by data and methods. A brief summary of the papers is given in Section 4, before perspectives and an outlook are presented in Section 5.

The manuscripts included in this thesis are:

- **PAPER I: Loss of sea ice during winter north of Svalbard.**  
I.H. Onarheim, L.H. Smedsrud, R.B. Ingvaldsen, and F. Nilsen.  
*Tellus A*, 66, 23933, 2014.
- **PAPER II: Skillful prediction of Barents Sea ice cover.**  
I.H. Onarheim, T. Eldevik, M. Årthun, R.B. Ingvaldsen, and L.H. Smedsrud.  
*Geophysical Research Letters*, 42, 5364–5371, 2015.
- **PAPER III: Toward an ice-free Barents Sea.**  
I.H. Onarheim and M. Årthun.  
*Geophysical Research Letters*, 44, 8387–8395, 2017.
- **PAPER IV: Sea ice variability and predictability in the Nansen Basin.**  
I.H. Onarheim, T. Eldevik, L.H. Smedsrud, and M. Steele.  
*Manuscript*.
- **PAPER V: Seasonal and regional manifestation of Arctic sea ice loss.**  
I.H. Onarheim, T. Eldevik, L.H. Smedsrud, and J.C. Stroeve.  
*In revision, Journal of Climate*.

## 2. Scientific background

The increase in atmospheric CO<sub>2</sub> concentrations since the industrial revolution has contributed to increased air and ocean temperatures globally, and consequent changes in, e.g., atmosphere and ocean circulation, sea level, ocean acidification, precipitation, and storm activity [IPCC, 2013]. One of the most striking and best quantified changes is the loss of Arctic sea ice [Figure 2.1; Comiso and Parkinson, 2004; ACIA, 2005], which is considered as an early-warning sign of anthropogenic global warming [Holland and Bitz, 2003; Comiso and Parkinson, 2004; Min et al., 2008]. Sea ice is a unique feature of the polar oceans and plays an important role in the energy balance of the Earth. The shrinking Arctic sea ice cover is not only an indicator of climate change, but also an active player in the ongoing change [e.g., Perovich et al., 2008]. Increased understanding of the Arctic sea ice decline, seasonally and regionally, and its interactions with the ocean and atmosphere, is essential in order to understand and predict future change.

This chapter introduces recent observed changes in the Arctic sea ice cover focusing on regional and seasonal variability, and addresses drivers of the sea ice loss, and long-term variability since 1850 (Section 2.1). The main focus herein is on winter sea ice variability and change in the Atlantic sector of the Arctic, i.e., the Atlantic-Arctic, and the inflow of Atlantic water to the Arctic Ocean and its link to the Arctic sea ice cover are thus described in Section 2.2. A brief overview of Arctic sea ice prediction and projection models and related challenges are presented in Section 2.3.

### 2.1 Recent change in Arctic sea ice

Satellite observations of Arctic sea ice since the late 1970s demonstrate a rapid decrease in Arctic sea ice extent (i.e., the cumulative area of all grid cells having at least 15% sea ice concentration; Serreze et al. [2007]). Besides the reduction in sea ice coverage, the sea ice is also thinning [Kwok and Rothrock, 2009], the volume is declining [Haine et al., 2015], drift speeds and deformation rates are increasing [Rampal et al., 2009; Spreen et al., 2011], the amount of multiyear ice is decreasing [Comiso, 2002; Maslanik et al., 2007; Nghiem et al., 2007], and the melt season is extending [Stroeve et al., 2014a]. The Arctic sea ice cover is thus changing from a thick stable ice pack to a thinner more fragile sea ice cover that is more mobile and more prone to break up and melt.

The loss of Arctic sea ice is largest at the end of the summer melt season [Stroeve et al., 2012a; Serreze and Stroeve, 2015] when the sea ice extent is at its minimum. Typically, only the central parts of the Arctic Ocean are ice covered in summer (Figure 2.1), and the ice edge is relatively zonal [Bitz et al., 2005]. The average monthly September sea ice extent has decreased at a linear rate of 13.2% per decade over the satellite record (1979–2017) relative to the 1981–2010 average [NSIDC, 2017a], but the reduction rate

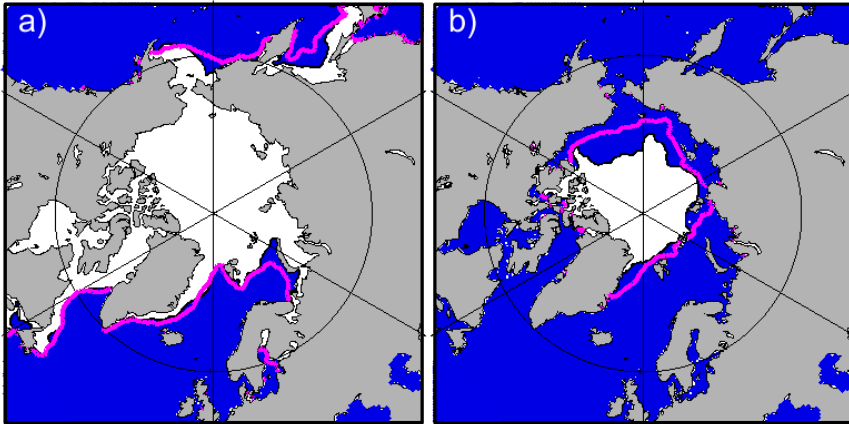


**Figure 2.1:** Observed Northern Hemisphere sea ice extent in March 2017 (a) and September 2017 (b). White indicates sea ice (more than 15% sea ice concentration), and pink contours show the median sea ice edge (15% sea ice concentration), 1981–2010. Data are from the National Snow and Ice Data Center [Cavalieri *et al.*, 1996; Maslanik and Stroeve, 1999].

has accelerated in recent years [e.g., Comiso *et al.*, 2008; Stroeve *et al.*, 2012a]. Record low summer sea ice extents were reached in 2007 and 2012, and the 10 lowest September sea ice extents have all occurred during the past 11 years. The September sea ice extent in 2017 (Figure 2.1b) was the seventh lowest September extent on record.

Despite a general focus on the summer sea ice decline, the loss of Arctic sea ice is not limited to summer [Meier *et al.*, 2005]. Negative trends in sea ice extent are now statistically significant in all months of the year, although generally less extensive in winter [Serreze *et al.*, 2007; Cavalieri and Parkinson, 2012]. The Arctic sea ice cover reaches its maximum in March when the sea ice extends well into the northern Atlantic and Pacific oceans (Figure 2.1a). The Arctic winter sea ice edge typically spans  $25^\circ$  of latitude [Bitz *et al.*, 2005], with the northernmost sea ice edge in the Barents Sea and northwest of Svalbard (Figure 2.1a). The monthly March sea ice extent shows a linear rate of decline of 2.7% per decade, 1979–2017, with the three most recent years being the three lowest on record [NSIDC, 2017b]. The sea ice extent in March 2017 was the lowest March extent in the satellite record, with particularly large ice-free areas in the Barents Sea and Sea of Okhotsk.

The recent loss of Arctic summer sea ice extent is widespread throughout the Arctic Ocean, particularly along the Russian and North American coasts [Figure 2.1b; Comiso *et al.*, 2008]. As a consequence, the Northwest Passage became completely ice-free for the first time in 2007 [Cressey, 2007], and climate model projections indicate a prolongation of the ice-free season of several months in both the Northwest Passage and Northern Sea Route during the twenty-first century [Khon *et al.*, 2010]. This could offer a faster and cheaper shipping route between Atlantic and Pacific harbors [Hassol, 2004; Smith and Stephenson, 2013].

The decreasing sea ice extent in winter is, in contrast, generally associated with larger open water areas in the North Atlantic and North Pacific oceans, i.e., south of the Arctic Ocean (Figure 2.1a). Despite an overall smaller sea ice decline in winter, regional winter

trends can be extensive [Cavaliere and Parkinson, 2012]. The largest reduction in winter ice extent has occurred in the Barents Sea due to reduced local sea ice formation [Årthun *et al.*, 2012]. The Bering Sea in the northern Pacific is the only region with increasing winter sea ice extent since 1979 [Cavaliere and Parkinson, 2012].

The distinct regional and seasonal differences in Arctic sea ice extent trends reflect the complex nature of the Arctic climate system. Regional variations are, however, masked out in pan-Arctic sea ice studies. Detailed assessments concerned with regional sea ice change in all seasons are essential in order better to understand, predict, and adapt to future sea ice loss. The winter season has in particular received little attention, and detailed examinations of past, present, and future winter sea ice variability and change are lacking.

### 2.1.1 Contributors to sea ice variability and change

The Arctic sea ice cover is influenced by a wide range of dynamical and thermodynamical factors, including atmospheric and oceanic temperatures, winds, waves, and ocean currents [e.g., Wadhams, 2000]. Sea ice typically freezes on the Arctic shelves in winter but drifts across the Arctic Ocean in the transpolar drift stream and exits the Arctic Ocean through Fram Strait [Kwok, 2009]. Sea ice also tends to converge in the anticyclonic Beaufort Gyre. The sea ice circulation is largely driven by surface winds [Thorndike and Colony, 1982], typically at 2% of the wind speed [Spreen *et al.*, 2011]. Variations in sea ice circulation influence the amount of sea ice export from the Arctic Ocean. Gudkovich [1961a,b] describe a cyclonic and an anticyclonic sea ice regime, where the cyclonic circulation regime is associated with larger sea ice and freshwater transport through Fram Strait due to export of thick sea ice [Polyakov *et al.*, 1999]. Large sea ice export from the Arctic Ocean generally contributes to low September sea ice minima [Smedsrud *et al.*, 2017], and particularly in 2007 [Zhang *et al.*, 2008].

The Arctic sea ice cover is also affected by variability and change in thermodynamical forcing. The ocean and atmosphere carry heat from the tropics to the polar regions, and both contribute importantly to the mass budget of Arctic sea ice [Maykut and Untersteiner, 1971; Graversen *et al.*, 2011]. The Atlantic water is the main oceanic heat source for the Arctic Ocean [Aagaard and Greisman, 1975; Carmack *et al.*, 2015], but is generally separated from the sea ice cover by a cold and fresh surface layer (described in more detail in Section 2.2). Still, the inflow of warm Atlantic water to the Arctic influences the variability in Arctic summer sea ice extent on multidecadal time scales [Zhang, 2015]. Pacific water entering the Arctic Ocean through the Bering Strait also provides heat contributing importantly to Arctic sea ice melt [Shimada *et al.*, 2006; Woodgate *et al.*, 2010].

The recent loss of Arctic sea ice has been attributed to a combination of anthropogenic forcing and internal climate variability [e.g., Lindsay and Zhang, 2005; Kay *et al.*, 2011; IPCC, 2013]. By assessing climate model simulations anthropogenic forcing is found to be the dominant factor and responsible for more than half of the observed trend in summer [Kay *et al.*, 2011; Stroeve *et al.*, 2012b; Ding *et al.*, 2017]. Based on observations, Notz and Marotzke [2012] also infer that the Arctic sea ice retreat is externally driven, and recently, Notz and Stroeve [2016] demonstrated that the ongoing Arctic sea ice loss strongly follows the trend of increasing atmospheric CO<sub>2</sub> concentrations. Internal climate variability may, however, trigger abrupt reductions of the Arctic sea ice cover in

the twenty-first century [Holland et al., 2006].

Arctic sea ice loss is affected by changes in radiative fluxes [Graversen et al., 2011; Lindsay and Zhang, 2005], increased solar heating of the upper ocean [Perovich et al., 2007; Steele et al., 2008], changes in cloud cover [Francis and Hunter, 2006; Kay et al., 2008], shifts in the North Atlantic Oscillation [NAO; Lindsay and Zhang, 2005] and Arctic Oscillation [AO; Rigor et al., 2002], changes in sea ice circulation [Comiso et al., 2008; Ogi and Wallace, 2012; Smedsrud et al., 2017], and warming ocean conditions in the Bering Strait [Woodgate et al., 2006], Fram Strait [Beszczynska-Möller et al., 2012], Barents Sea [Árthun et al., 2012], and the eastern Eurasian Basin [Polyakov et al., 2017]. The Arctic winter sea ice growth has recently been very low due to anomalously high air temperatures and low cumulative freezing degree days [Ricker et al., 2017]. Graham et al. [2017] show that the number of winter warming events in the Arctic has increased over the past few decades, and that the events appear to last longer. Storms transporting warm and humid air masses contribute importantly to reduced sea ice freezing in winter [Boisvert et al., 2016]. Thinner sea ice at the end of the winter season makes the ice cover more vulnerable to melt in summer. Preconditioning by a thin sea ice cover was found to contribute to the record low September sea ice extents in 2007 [Zhang et al., 2008] and 2012 [Parkinson and Comiso, 2013].

The reduction of Arctic sea ice is enhanced by the ice-albedo feedback [Perovich et al., 2008; Zhang et al., 2008]; when more sea ice melts in spring and summer, larger open water areas are exposed to solar radiation, and the consequent increased absorption of solar heating leads to enhanced sea ice melt. Steele and Dickinson [2016] show that the ice cover has to retreat before the peak of atmospheric heat flux in order to achieve the highest sea surface temperatures. Self-acceleration can, however, not explain the recent observed sea ice decline [Notz and Marotzke, 2012]. Negative feedbacks, including the fact that thin ice freezes more rapid than thick ice [Bitz and Roe, 2004], that open water loses excess heat to the atmosphere rapidly in winter, and that ice forming late in the season carries a thinner insulating snow cover [Notz, 2009], explain parts of the recovery processes.

Understanding the recent loss of Arctic sea ice, regionally and seasonally, is of large importance as the sea ice decline has been found to have both local and remote consequences, including amplified Arctic surface warming [Serreze and Barry, 2011], changes in atmospheric circulation patterns locally and probably remotely [Francis and Vavrus, 2012; Jaiser et al., 2012; Screen, 2017], possible slow-down of the Atlantic Meridional Overturning Circulation [AMOC; Sévellec et al., 2017], timing of onset of Greenland surface melt [Stroeve et al., 2017], and changes in polar ecosystems [Post et al., 2013]. The expanding open water areas can also have profound effects on resource management and maritime activity [Emmerson and Lahn, 2012], and provide potential for new trans-Arctic shipping routes [Smith and Stephenson, 2013]. Detailed examinations of regional Arctic sea ice variability and change are needed to enhance the prognostic capability of future change and its potential drivers.

### 2.1.2 Recent change in a longer perspective

Historical observations are essential in order to put recent observed sea ice extent trends into a broader context and to better understand internal climate variability. A new monthly gridded data set of observed Arctic sea ice concentrations since 1850 [Walsh

*et al.*, 2015, hereafter referred to as the 1850 onward data set] shows that the recent loss of Arctic sea ice is unprecedented since 1850 in both summer and winter [Figure 2.2; *Walsh et al.*, 2017]. Prior to the recent sea ice loss, the ice cover was characterized by large interannual variability and relatively little decadal to multidecadal variability [Figure 2.2; *Walsh et al.*, 2015, 2017]. By assessing observations from 1953 to 1984, *Mysak and Manak* [1989], however, found interdecadal to decadal variability in the Arctic sea ice cover. The time scale of variability varied regionally, and fluctuations in the western Arctic had cycles of 4–6 years, whereas the Barents and Kara seas showed pronounced decadal variability [*Mysak and Manak*, 1989], the latter consistent with *Kvingedal* [2005]. Moreover, sea ice oscillations with periods of 60–80 years are observed in the Nordic Seas, and associated with variations in the subpolar North Atlantic [*Divine and Dick*, 2006].

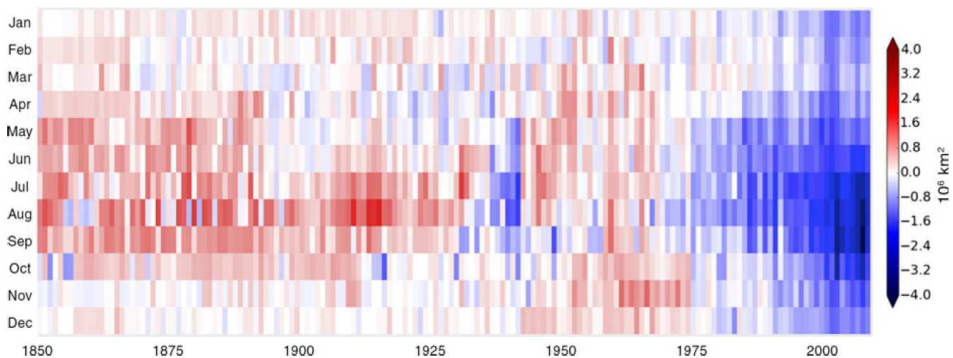


**Figure 2.2:** Monthly Arctic sea ice extent anomalies from the 1850 onward data set, 1850–2013. From *Walsh et al.* [2017].

Sea ice extent variations since 1850 are generally more pronounced in summer than in winter [Figure 2.2; *Walsh et al.*, 2015, 2017]. The summer sea ice cover decreased toward the 1940s, increased to the 1970s, and has decreased since. This is consistent with positive sea ice extent trends reported by *Walsh and Johnson* [1979] over the 1953–1977 period. Decreased summer Arctic sea ice extent in the 1930s–40s has also been reported by *Zakharov* [1997], *Polyakov et al.* [2003], and *Mahoney et al.* [2008], and linked to the early twentieth-century warming in the Arctic. *Bengtsson et al.* [2004] suggest that the early warming was due to increased inflow of warm waters to the Barents Sea, with correspondingly smaller sea ice extent and increased atmospheric temperatures. There is, however, no clear signal of a reduced sea ice extent in the Barents Sea in the 1930s and 1940s [*Vinje*, 2001; *Mahoney et al.*, 2008], and most of the change is carried by the Greenland Sea [*Walsh et al.*, 2017] and Russian Arctic [*Polyakov et al.*, 2003; *Mahoney et al.*, 2008]. The sea ice extent in the eastern Arctic thereafter increased, possibly due to increasing anthropogenic aerosols [*Gagné et al.*, 2017]. The 1850 onward data set is described in more detail in Section 3.

## 2.2 Atlantic water inflows to the Arctic Ocean

The Atlantic Ocean is the major carrier of ocean heat from the tropics to the polar regions. Warm and saline Atlantic water originating in the North Atlantic flows poleward in the Nordic Seas as a two-branch structure, the Norwegian Atlantic Current [NwAC; *Orvik and Nøller, 2002*]. Near 70°N the eastern barotropic branch [*Orvik et al., 2001*] bifurcates; one branch continues northward along the western coast of Svalbard as the West Spitsbergen Current, and one branch enters the Barents Sea as the North Cape Current [Figure 2.3; *Loeng et al., 1997*], hereafter referred to as the Fram Strait branch and Barents Sea branch, respectively. The Fram Strait branch converges with the western NwAC branch near 77°N [*Walczowski et al., 2005*]. Individually the Barents Sea branch and the Fram Strait branch carry approximately 50 TW of heat to the Barents Sea and eastern Fram Strait [*Ingvaldsen et al., 2002; Schauer et al., 2008*].

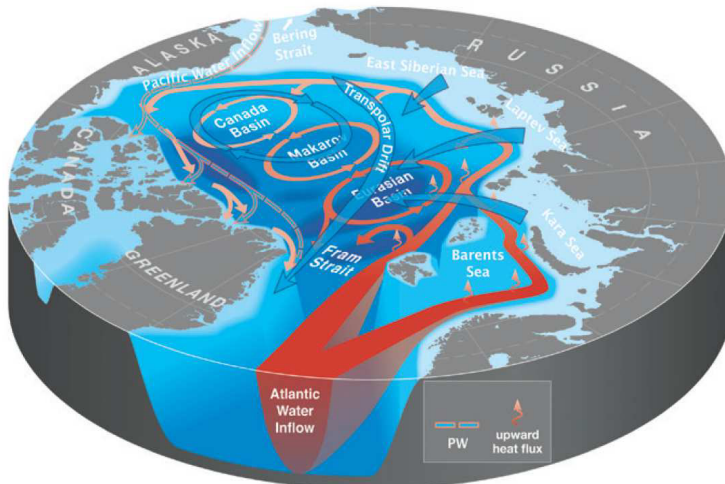


**Figure 2.3:** Schematic of Arctic Ocean circulation of Atlantic water (red), surface water (blue), intermediate Pacific water (pink/blue). From *Carmack et al.* [2015].

After water mass modification in the Barents Sea and Fram Strait (described in more detail below) the Fram Strait and Barents Sea branches partly rejoin in the northern Kara Sea and continue cyclonically in a boundary current along the Arctic Basin, strongly following the bathymetry [Figure 2.3; *Nansen, 1902; Aagaard, 1989; Rudels et al., 1994*]. The Atlantic water forms an intermediate layer of relatively warm water (warmer than 0°C; *Aagaard [1989]; Rudels et al. [1994]; McLaughlin et al. [2009]*), typically separated from the sea ice and the atmosphere by a fresh and cold surface layer with a cold halocline at its base. Freshwater is supplied to the Arctic Ocean and its low salinity surface layer by melting of sea ice, river discharge from Eurasian rivers [at increasing rates; *Peterson et al., 2002*], inflow of Pacific waters, and net precipitation [*Serreze et al., 2006; Haine et al., 2015*]. Several mechanisms are suggested to contribute to the formation of the cold halocline, including advection of cold shelf waters and local winter convection [*Rudels et al., 1996; Steele and Boyd, 1998*].

Due to the cold halocline throughout most of the Arctic Ocean, the vertical heat loss from the Atlantic water to the sea ice is typically small [Maykut and Untersteiner, 1971; Krishfield and Perovich, 2005; Fer, 2009]. There are, however, large spatial and temporal variations, and large heat losses can occur over rough topography [Rippeth *et al.*, 2015], in regions with strong currents or tidal forcing [Sirevaag and Fer, 2009], and during storms [Meyer *et al.*, 2017; Peterson *et al.*, 2017]. The Atlantic water cools and freshens substantially as it passes through the Arctic Ocean, and modified Atlantic water eventually exits the Arctic Ocean through western Fram Strait [Figure 2.3; Aagaard *et al.*, 1985; Mauritzen, 1996; Meincke *et al.*, 1997].

### 2.2.1 Fram Strait branch

The West Spitsbergen Current flows north in the deep Fram Strait and carries roughly 3 Sv ( $1 \text{ Sv} = 10^6 \text{ m}^3\text{s}^{-1}$ ) of Atlantic water northward [Beszczynska-Möller *et al.*, 2012]. Due to the complex bathymetry in Fram Strait, the current splits into at least three branches north of  $79^\circ\text{N}$  [Quadfasel *et al.*, 1987]; the Svalbard Branch, following the upper part of the slope north of Svalbard, the Yermak Branch, following the western flank of the Yermak Plateau, and a third branch recirculating to the south in Fram Strait [Perkin and Lewis, 1984; Aagaard *et al.*, 1987; Schauer *et al.*, 2004]. The Svalbard branch continues eastward along the slope of the Eurasian continent and provides heat and salt to the Arctic Ocean [Perkin and Lewis, 1984].

Sea ice from the Laptev, Kara, and Barents seas typically drifts into the region north of Svalbard [Kwok *et al.*, 2013; Itkin *et al.*, 2017]. The poleward flowing Atlantic water keeps the west coast of Svalbard ice-free [Kvingedal, 2005], but encounters the advected sea ice north of Svalbard [Untersteiner, 1988]. In contrast to most of the Arctic Ocean, the Atlantic water north of Svalbard is still close to the surface [Rudels *et al.*, 1996]. The Atlantic water thus melts the opposing sea ice [Untersteiner, 1988], and the winter sea ice extent north of Svalbard co-varies with observed Atlantic water temperatures [Piechura and Walczowski, 2009]. The melting of sea ice results in the formation of an upper mixed layer of cooled and freshened Atlantic water [Rudels *et al.*, 1996]. Below the mixed layer, the warm and saline Atlantic layer maintains most of its characteristics and continues into the Arctic Ocean, where it gradually cools and freshens [Perkin and Lewis, 1984; Saloranta and Haugan, 2004; Sirevaag and Fer, 2009].

### 2.2.2 Barents Sea branch

Atlantic water in the North Cape Current enters the Barents Sea between Norway and Bjørnøya, known as the Barents Sea Opening. The inflow of roughly 2 Sv [Skagseth *et al.*, 2008] is strongly affected by the local wind field which induces changes in sea level pressure and associated currents [Ingvaldsen *et al.*, 2004a,b]. Within the shallow Barents Sea (average depth of 230 m), the Atlantic water mainly follows a counterclockwise circulation before exiting the Barents Sea through the strait between Novaya Zemlya and Frans Josef Land [Figure 2.3; Loeng, 1991]. The Atlantic water experiences substantial cooling en route [Midttun, 1985; Häkkinen and Cavalieri, 1989; Áρθun and Schrum, 2010], and the heat transport through the northern exit is consequently small [Gammelsrød *et al.*, 2009].

The Barents Sea is a transition zone between warm and saline Atlantic water to the

south and colder and slightly fresher Arctic water to the north [e.g., *Smedsrud et al.*, 2013]. The region is practically ice-free in summer [*Kvingedal*, 2005], and most of the sea ice forms locally in winter. Some sea ice is, however, advected to the Barents Sea from the passage between Svalbard and Franz Josef Land [typically 5% of the Fram Strait area export; *Kwok*, 2009]. The Atlantic heat entering the western Barents Sea determines the amount of sea ice extent freezing in winter and strongly controls the extent of the ice-free Atlantic domain [*Árthun et al.*, 2012]. The Atlantic heat transport variability in the Barents Sea Opening is dominated by variations in volume transport and leads the sea ice variability by 1–2 years [*Árthun et al.*, 2012], however, the sea ice extent correlates well also with the Atlantic water temperature [*Árthun et al.*, 2012; *Schlichtholz*, 2011].

### 2.2.3 Long-term variability

The temperature and salinity of the Atlantic inflows to the Arctic Ocean show pronounced seasonal, interannual, and decadal to multidecadal variability [e.g., Figure 2.4; *Skagseth et al.*, 2008; *Beszczyńska-Möller et al.*, 2012; *Zhang*, 2015]. Particularly warm inflow periods were observed in the late 1920s to 1950s and in recent decades. The low-frequency temperature variability co-varies with the Atlantic Multidecadal Oscillation (AMO) index, i.e., the large-scale sea surface temperature variations in the Atlantic [Figure 2.4; *Skagseth et al.*, 2008]. Increased heat transport to the Barents Sea and Fram Strait recently, is due to a combination of warmer waters and stronger currents [*Schauer et al.*, 2004; *Árthun et al.*, 2012]. The warm and cold inflow periods are reflected within the Arctic Ocean [*Polyakov et al.*, 2004], and temperatures were unprecedented in the 2000s [*Polyakov et al.*, 2012]. The recent warming in the Arctic Ocean is associated with a salinification and shoaling of the Atlantic layer in the Eurasian Basin [*Polyakov et al.*, 2004, 2017]. Understanding the influence from variations in Atlantic heat on the Arctic sea ice cover is accordingly important in order to predict future change.

The observed temperature variability in the Barents Sea and Fram Strait largely results from the northward propagation of ocean heat anomalies from the eastern North Atlantic into the Nordic Seas toward the Arctic Ocean [*Holliday et al.*, 2008; *Polyakov et al.*, 2005]. Anomalies may also be generated within the Nordic Seas [*Furevik*, 2001]. Despite of cooling and freshening northwards, heat and salt anomalies can be traced around the Nordic Seas [*Árthun and Eldevik*, 2016; *Árthun et al.*, 2017] and further into the Arctic Ocean along the boundary of the Eurasian Basin [*Polyakov et al.*, 2005]. Anomalies traveling from the Svinøy section (northwestward from the Norwegian coast at 63°N) to the Barents Sea Opening take about two years [*Skagseth et al.*, 2008], whereas it takes about three years to reach the present sea ice edge [*Árthun et al.*, 2017]. Moreover, a warm pulse of Atlantic water that entered the Arctic Ocean in the early 1990s reached the Canada Basin in the 2000s [*Polyakov et al.*, 2010]. Variations in the Atlantic inflow has been linked to the dynamics of the North Atlantic subpolar gyre circulation [*Hátún et al.*, 2005]. The northward propagating nature of ocean heat and salt anomalies provides potential for predicting ocean and sea ice conditions several years in advance [*Yeager et al.*, 2015; *Árthun et al.*, 2017].

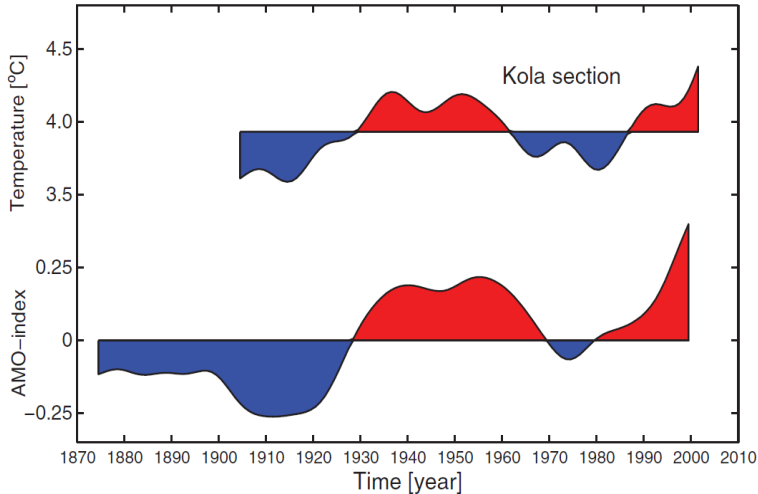


**Figure 2.4:** Observed temperature in the Kola section, Barents Sea (upper), and the Atlantic Multidecadal Oscillation index (AMO, lower). The AMO index is based on the sea surface temperature in the region  $0\text{--}60^\circ\text{N}$ ,  $7.5\text{--}75^\circ\text{W}$ . The time series are filtered using a two-way 14-year Hamming window. From *Skagseth et al.* [2008].

## 2.3 Predictions and projections

As larger areas of the Arctic Ocean become ice-free and accessible for longer time periods, the interest in maritime activities and resource extraction [Emmerson and Lahn, 2012] and the potential for new trans-Arctic shipping routes [Smith and Stephenson, 2013] increase. There is an urgent need for skillful sea ice predictions, months to years in advance, in order to accommodate increased human activities in the Arctic [Eicken, 2013]. Predictions and projections from a few years to centuries in advance are also of considerable interest and relevance to society. For practical purposes there is a demand for regional predictions in all seasons.

Sea ice predictability is generally provided by persistence or advection of sea ice anomalies, or by interaction with the atmosphere and ocean [e.g., Guemas et al., 2016]. Providing skillful sea ice predictions is, however, challenging due to for instance sparsity of observations and inadequate understanding and representation of physical processes. The atmosphere is typically an important driver on short time scales, whereas the ocean becomes more important on longer times scales [Griffies and Bryan, 1997; Yeager and Robson, 2017]. The prediction focus in this thesis is on Atlantic-Arctic sea ice predictability provided by the ocean over time periods from years to decades. However, we here also briefly introduce seasonal atmospheric prediction models. Initialized model experiments are not considered herein.

### 2.3.1 Sea ice predictions

The chaotic nature of atmospheric circulation patterns makes sea ice predictions based on the atmospheric state challenging, even a few months in advance [e.g., Holland et al., 2011; Stroeve et al., 2014b; Guemas et al., 2016]. Seasonal Arctic sea ice

predictions tend to be focused on the summer sea ice extent [e.g., *Schröder et al.*, 2014; *Day et al.*, 2014; *Kapsch et al.*, 2014]. Since 2008, the Sea Ice Outlook (SIO; <https://www.arcus.org/sipn/sea-ice-outlook>) has collected sea ice predictions of the September sea ice extent a few months in advance, from both numerical, heuristic, statistical, and mixed approaches. *Stroeve et al.* [2014b] show that seasonal predictions of the September sea ice extent are most accurate in years where the extent is near the long-term trend. Between 2008 and 2015, predictions from statistical and ice-ocean-atmosphere models were slightly better, collectively, than the others predictions [*Hamilton and Stroeve*, 2016]. Still, skillful September sea ice predictions appear challenging in years where the weather plays a large role [*Hamilton and Stroeve*, 2016].

The ocean has compared to the atmosphere a large inertia and large heat capacity, and is thus potentially a major source of climate predictability years to decades in advance [*Schlichtholz*, 2011; *Zhang*, 2015; *Yeager et al.*, 2015]. Already in 1909, *Helland-Hansen and Nansen* [1909] suggested that temperature conditions in the Barents Sea were predictable based on upstream hydrographic conditions. Later both *Venegas and Mysak* [2000] and *Vinje* [2001] suggested that sea ice variations in the Barents Sea were affected by the northward flowing waters in the Norwegian Sea. More recently, the potential for predicting the Barents Sea ice cover based on observed ocean heat was explored in more detail [e.g., *Schlichtholz*, 2011; *Árthun et al.*, 2012].

The observed poleward propagation of ocean heat anomalies from the subpolar North Atlantic to the Arctic Ocean [e.g., *Holliday et al.*, 2008; *Árthun et al.*, 2017] has recently been used to predict the Atlantic-Arctic winter sea ice extent up to a decade in advance. Estimates from both observations [*Árthun et al.*, 2017] and models [*Yeager et al.*, 2015] predict increased winter sea ice extent (pentadal to decadal tendencies) in the Atlantic-Arctic during the next few years. The increase is expected due to colder waters flowing northward. Although the observed Atlantic heat shows large potential for Arctic sea ice predictability, the predictions are limited to the regions where the sea ice cover is directly influenced by Atlantic water, i.e., typically in the Barents Sea and near Svalbard.

### 2.3.2 Sea ice projections

Coupled global climate models are the main tool used to project Arctic sea ice change on timescales from decades to centuries. Through the fifth phase of the Climate Model Intercomparison Project (CMIP5), a comprehensive suite of global climate model simulations has been coordinated, with more than 50 models contributing [*Taylor et al.*, 2012]. Projections for the twenty-first century are forced with prescribed emission forcing scenarios, referred to as representative concentration pathways (RCPs), including a high forcing scenario (RCP8.5) and a medium forcing scenario (RCP4.5), described in *Moss et al.* [2010]. The external forcing plays a dominant role in the future evolution of the Arctic sea ice cover [*Notz and Marotzke*, 2012].

On average the current climate models simulate a slower rate of sea ice retreat than what has been observed since 1979 [*Stroeve et al.*, 2007; *Massonnet et al.*, 2012]. The CMIP5 models do, however, simulate trends that are more consistent with observations than the CMIP3 models [*Stroeve et al.*, 2012b]. The negative trends in Arctic sea ice extent are projected to continue in the foreseeable future [e.g., *Zhang and Walsh*, 2006], and according to the models ice-free summers (sea ice extent less than  $10^6$  km<sup>2</sup>) are projected within the middle of this century [*Notz and Stroeve*, 2016]. The projections are,

however, associated with large uncertainties as a combination of model biases [Stroeve *et al.*, 2012b], internal variability [Kay *et al.*, 2011; Swart *et al.*, 2015], and scenario uncertainty [Liu *et al.*, 2013]. The projection uncertainty cannot be reduced to less than 20 years due to large internal variability, and the uncertainty related to emission scenario adds another five years of uncertainty [Jahn *et al.*, 2016]. As the prediction uncertainty remains large, understanding the processes influencing Arctic sea ice variability and trends is of great importance for improving sea ice predictions and projections.

## 3. This study

This thesis assesses regional and seasonal Arctic sea ice variability and change in the past, present, and future by combining observations, simulations, and conceptual models. The work is particularly focused on the winter sea ice cover in the Barents Sea and Nansen Basin, i.e., the inflow regions of Atlantic water to the Arctic Ocean.

### 3.1 Motivation and objectives

The recent loss of Arctic sea ice displays pronounced regional and seasonal variations [Cavalieri and Parkinson, 2012], with currently largest changes occurring at the end of the summer melt season [e.g., Serreze and Stroeve, 2015]. Most studies are concerned with pan-Arctic sea ice changes limited to the summer season. Changes in winter sea ice have received little attention due to its overall smaller trends, however, changes are now pronounced also in winter. This thesis considers regional and seasonal aspects of the recent Arctic sea ice loss, with a particular focus on winter change. In order to understand the uniqueness of ongoing trends and put recent changes into a larger perspective, the thesis also examines available historical observations of sea ice variability since 1850, and it presents projections for the future.

The largest Arctic winter sea ice extent decline has occurred in the Atlantic-Arctic. The main focus herein is thus on the Barents Sea and Nansen Basin; regions of large financial importance for Norway. A tight link between Atlantic water and winter sea ice in the Atlantic-Arctic has been demonstrated in previous studies [e.g., Helland-Hansen and Nansen, 1909; Untersteiner, 1988; Schlichtholz, 2011; Årthun *et al.*, 2012]. Skillful sea ice predictions have, however, not yet been achieved. In order to improve the understanding of Atlantic-Arctic sea ice predictability, this thesis further examines the impact of Atlantic water on the regional winter sea ice variability. The thesis aims to provide skillful sea ice predictions, rooted in observations, of the Atlantic-Arctic winter sea ice variability based on a physical-based understanding of the climate system.

The main questions that are addressed in this thesis can be summarized as:

- To what extent can winter sea ice variability and trends in the Barents Sea and Nansen Basin be explained by and predicted from observed Atlantic water characteristics upstream?
- What is the future fate of the Barents Sea ice cover?
- What characterizes regional and seasonal variations in the Arctic sea ice cover in the past, present, and future?

Results are mainly based on an assessment of observations of sea ice concentration from remote sensing (Paper I–V), and on hydrography and current observations of Atlantic water (Paper I, II, and IV). Simulations from a regional ice-ocean model (Paper II) and global climate models (Paper III) are also utilized, and conceptual models are developed in Paper II and IV.

## 3.2 Data and methods

Accurate, high resolution data over long time periods are required in order to understand and predict the variability of the climate system. The Arctic is a remote region, and the harsh environment makes observations challenging, particularly in winter. Assessing a combination of observations and models are thus often advantageous in order to get the most robust insights. However, they have both their strengths and weaknesses. Observations measure the climate system directly, but are often strongly limited in time and space. Models provide, in contrast, complete data sets in time and space, but are limited by the models' capabilities to realistically simulate the real world, and often by their spatial resolution. This thesis mainly examines observations, but model output is analyzed in Paper II to evaluate an analytical framework, and in Paper III to go beyond the observational record.

### 3.2.1 Observations

The spatial and temporal coverage of Arctic sea ice observations was scarce before satellite observations of sea ice began in October 1978. Since 1978 satellite passive microwave imagery has monitored the Arctic sea ice cover, providing (near) daily gridded data sets of sea ice concentration for the Arctic and Antarctic at approximately 25-km resolution [e.g., *Cavalieri et al.*, 1996]. The sensors monitor passive microwave emissions emitted from the Earth's surface which can pass through clouds and are not affected by the polar night. Sea ice concentration is then generated from the satellite observed brightness temperature. A variety of different sea ice algorithms converting brightness temperature to sea ice concentration exists, e.g., the Goddard NASA Team, Goddard Bootstrap, and Hadley HadISST algorithms. The algorithms provide slightly different estimates of the sea ice concentrations, particularly in areas with new ice or in meltponded areas in summer [*Comiso et al.*, 2017]. The trends are, however, in good agreement between the different estimates [*Comiso et al.*, 2017]. Herein, we make use of the monthly Goddard NASA Team product [*Cavalieri et al.*, 1996], which is commonly used in studies assessing Arctic sea ice variability and change.

Uncertainties in the sea ice concentration products are generally largest during summer when melt ponds are present, and in regions with thin sea ice or low sea ice concentration [e.g., *Meier and Notz*, 2010]. The accuracy of the sea ice concentration is usually within  $\pm 5\%$  in winter, and  $\pm 20\%$  in summer [*Cavalieri et al.*, 1992; *Meier and Notz*, 2010]. Uncertainty also appears due to different sensors operating over different time periods (the Nimbus-7 Scanning Multichannel Microwave Radiometer (SMMR), the Defense Meteorological Satellite Program (DMSP) -F8, -F11 and -F13 Special Sensor Microwave/Imagers (SSM/Is), and the DMSP-F17 Special Sensor Microwave Imager/Sounder (SSMIS)). Despite the uncertainties of the satellite products, the data record

provides one of the most complete and reliable indicators of ongoing climate change. We note that there is no similarly long observational record for sea ice thickness, and observed sea ice concentration products are thus the focus herein.

A new observational based data set by *Walsh et al.* [2015] provides monthly Northern Hemisphere sea ice concentrations since 1850 on a  $0.25^\circ$  grid. The 1850 onward data set consists of satellite passive microwave data since 1979, where the concentration estimates are calculated by combining the Bootstrap and NASA Team algorithms [*Meier et al.*, 2013]. Before the satellite era all available historical sources of sea ice observations since 1850 are incorporated, including ship observations, compilations by naval oceanographers, whaling log books, and analysis by national ice services. The data set improves on the previously published data set that begins in 1901 by *Chapman and Walsh* [1991]; it adds newly available observations, extends the record in time, and refines the method used to merge data from different sources [*Walsh et al.*, 2015]. See *Walsh et al.* [2015, 2017] for a more detailed description of the various data sources.

As the observational coverage of Arctic sea ice before 1979 is sparse, particularly in winter, the gridded 1850 onward product is constructed from a limited number of observations by applying interpolation and analog mapping techniques. In some cases there is no overlap between the different data sources, and over long time periods observations are limited both spatially and temporally [*Walsh et al.*, 2015]. Satellite observations typically underestimate summer sea ice concentrations compared to more manual methods of sea ice observations [*Partington et al.*, 2003], and some (lacking) variability may be an artifact of few observations. *Connolly et al.* [2017] recently indicated that the decadal to multidecadal variability in the 1850 onward data set is considerably underestimated. They argue that the different data sources are not always directly comparable, and that the tight relation between sea ice extent and surface air temperature over the satellite era does not apply in the longer time period. The uncertainty in the 1850 onward data set is not yet quantified [*Walsh et al.*, 2015], and the 1850 onward data set thus has to be used with caution, particularly in the early time period and in winter. We note, however, that the Atlantic-Arctic is one of the most well-observed areas as the region has been visited for more than 500 years [*van Linschoten*, 1601], and sealing and hunting started in the 1850s [*Vinje*, 2001].

The poleward flow of Atlantic water in the North Atlantic and Nordic Seas has been monitored in several regularly sampled sections over many years to decades [e.g., *Holliday et al.*, 2009]. Herein, we assess observed Atlantic properties in the Barents Sea Opening, and in sections westward from Sørkapp (the southern tip of Svalbard), Gimsøy (at  $69^\circ\text{N}$  along the Norwegian coast), and Svinøy. Observations are provided by the Institute of Marine Research, Norway. Temperature and salinity observations in the Barents Sea Opening are available since 1977, whereas volume transport has been measured by current meter moorings since 1997. Temperature and salinity have been measured at Sørkapp since 1977 through an annually repeated conductivity-temperature-depth (CTD) section in fall. At Gimsøy and Svinøy CTD sections are conducted four to five times per year since 1976, and current measurements are available at Svinøy since 1995. The Sørkapp, Gimsøy, and Svinøy sections are herein not assisted by current observations. A more detailed description of the instrumentation is given in the manuscripts and references therein.

Also included in the thesis are observations from the Norwegian Young Sea Ice Cruise (N-ICE2015) north of Svalbard from January to June 2015 [*Granskog et al.*, 2016]. The

field campaign provides the most comprehensive data set of ocean, sea ice, snow, atmosphere, and biochemical conditions in the Nansen Basin in winter and spring. Paper IV and references therein provide an overview of the field campaign and instrumentation.

### 3.2.2 Models

Numerical models are the main tool to assist direct observations and improve the understanding of past, present, and future climate variability and change. The models are numerical representations of the climate system where the simulations are computed by solving mathematical formulations that describe the climate system. A broad range of models exists; both regional and global models that are either fully coupled or partly coupled. The global models provide geographically and physically consistent estimates, but their spatial resolution is fairly coarse. Regional models have typically lower computational costs and can therefore have higher spatial resolution. The atmosphere, ocean, and sea ice interact freely in fully coupled models, whereas for instance ice-ocean coupled models are forced with prescribed atmospheric forcing [e.g., *Schrum and Backhaus, 1999*]. Provided realistic forcing, the models can reproduce climate variables that are sparsely observed.

Climate models are used to simulate past, present, and future climate. Pre-industrial control simulations are typically run over long time periods with constant external forcing, whereas historical simulations are run with observed prescribed external forcing, and future projections are forced with different emission scenarios. The models are typically evaluated against available observations. *Notz [2015]*, however, demonstrate that a model that matches observations in the past and present does not necessarily provide realistic projections of the future evolution.

As coupled global climate models (also known as coupled general circulation models or Earth system models) are the key tool to assess and project the future evolution of the Arctic sea ice cover [e.g., *Notz and Stroeve, 2016*], coordinated experiments have recently been conducted to produce climate projections from several climate models [*Meehl et al., 2007*]. Projections of the evolution of the climate system typically consider different emission scenarios [*Moss et al., 2010*]. Large uncertainty also arises due to large internal variability [*Jahn et al., 2016*] caused by the chaotic nature of the climate system. Averaging together ensembles of simulations is thus commonly used to cancel out internally generated fluctuations. The model spread provided by internal variability is, however, irreducible [*Jahn et al., 2016*].

Herein, output from a regional coupled ice-ocean model for the Barents Sea, 1948–2007, is assessed in Paper II. In Paper III output from commonly used models from the CMIP5 ensemble are examined. Both pre-industrial control simulations (500–1800-year simulations), historical simulations (1850–2005), and future simulations run with RCP8.5 (2006–2100) and RCP4.5 forcing (2006–2080) are utilized. A more detailed description of the models is given in Paper II and III and references therein.

## 4. Summary of papers

### 4.1 Paper I: Loss of sea ice during winter north of Svalbard

Paper I examines satellite observed sea ice changes in the area north of Svalbard. The regional sea ice decline is statistically significant in all months, but largest in winter. The large winter change in the Nansen Basin is in contrast to the remaining Arctic Ocean which undergoes largest change in summer, with the Barents Sea as the only exception. Paper I shows that regionally, trends in the Arctic Ocean sea ice cover are substantial also in winter.

The recent winter sea ice loss north of Svalbard is most pronounced above the core of the warm Atlantic water. By assessing observations and reanalysis, and utilizing heat budget estimates it is argued that the recent loss of winter sea ice north of Svalbard is due to a warming of the inflowing Atlantic water. The sea ice loss leads to larger open water areas which allow for increased heat loss to the atmosphere, and thereby increased atmospheric temperatures. The Atlantic water thus exerts a dominant influence on the recent Arctic winter sea ice decline.

The analysis considers changes in sea ice concentration and area, but corresponding changes in sea ice thickness are not assessed. A thinner and more mobile sea ice cover drifting into the region north of Svalbard may, however, also contribute to the observed change. Moreover, it is not known to what degree the volume transport and northward water mass transformation of the Atlantic water have varied. For a more detailed assessment of the recent sea ice loss north of Svalbard, observations of e.g., sea ice thickness, sea ice drift speed, mixed layer characteristics, and current velocity, or the use of a numerical or conceptual model would be helpful.

### 4.2 Paper II: Skillful prediction of Barents Sea ice cover

The Barents Sea ice cover contributes importantly to the recent observed winter sea ice variability and trend in the Arctic Ocean. Paper II assesses the predictability of the annual mean Barents Sea ice cover, which variability is carried by the winter. The sea ice cover in the Barents Sea largely reflects the inflow of warm Atlantic water through the Barents Sea Opening. Rooted in observations and based on first principles a predictive framework of interannual Barents Sea ice variability is presented. The framework states that the Barents Sea ice area is predictable up to two years in advance based on its past observed sea ice area and heat transport.

The proposed framework is evaluated against observed sea ice area and heat transport since 1997, and by a 60-year simulation from a regional ice-ocean model. The predictions explain approximately 50% of the observed sea ice variance one year in advance, and beat both persistence and linear trend predictions. The framework is thus found to be skillful. Variability that is not accounted for by the framework can largely be explained by regional simultaneous meridional winds. Winds are, however, not predictable a year in advance, and cannot be accounted for by the proposed framework. The proposed framework is, to the authors' knowledge, the first physical-based prediction model that skillfully predicts the Barents Sea ice cover.

### **4.3 Paper III: Toward an ice-free Barents Sea**

Paper III provides the first detailed examination of the past, present, and future winter sea ice extent in the Barents Sea. The current sea ice extent and trends in the Barents Sea are unprecedented in the available historical record since 1850, and the most recent 30-year trend is an uncommon feature in long climate model control simulations (3800 years in total). The present record low winter Barents Sea ice cover thus appears as an extreme event in a longer perspective.

Future projections with a strong climate forcing scenario indicate that the Barents Sea ice cover will continue to decrease toward 2100. According to a large ensemble simulation, the Barents Sea reaches ice-free conditions for the first time between 2061 and 2088, and remains ice-free throughout the year by the end of the twenty-first century. The prediction uncertainty of 28 years is due to large internal variability. The sea ice cover also demonstrates pronounced interannual to decadal variability toward 2100, which may reflect variations in the Atlantic inflow.

### **4.4 Paper IV: Sea ice variability and predictability in the Nansen Basin**

Inspired by Paper I, Paper IV is concerned with the recent observed winter sea ice variability and water mass transformation in the Nansen Basin. Based on observations from multiple drifting ice camps in the Nansen Basin in winter and spring 2015, it is found that the upper Atlantic water cools and freshens due to melting of sea ice and heat loss to the atmosphere as it encounters the sea ice edge north of Svalbard. It is herein, for the first time, shown that the transformed Atlantic water forms a barotropic homogeneous low salinity surface layer that flows in tandem with the warm Atlantic water below. The competition between the inflowing Atlantic water and sea ice advection determines variations in the regional winter sea ice cover.

Rooted in observations, a conceptual model founded on heat and salt conservation is developed. Despite of scarce observations the framework is found to capture both the climatological balance and the interannual winter sea ice variability in the Nansen Basin. Moreover, the proposed framework provides skillful sea ice predictions up to three years in advance based on observed Atlantic water characteristics along the Norwegian coast. Other variables associated with the melting of sea ice including the characteristics of the advected sea ice cover, also influence the interannual sea ice variability. Still, the

northward propagation of ocean heat and salt anomalies appears as skillful predictors for the Nansen Basin winter sea ice cover, highlighting a strong influence from Atlantic water on interannual and long-term Nansen Basin winter sea ice variability.

## 4.5 Paper V: Seasonal and regional manifestation of Arctic sea ice loss

Paper V examines regional and seasonal Northern Hemisphere sea ice extent variability and change in the past, present, and future. Based on satellite observations, the recent Northern Hemisphere sea ice extent is characterized by pronounced seasonal and regional variations; summer variability and change dominate in the perennially ice covered seas, whereas winter variability and change are most pronounced generally further south. Based on the distinct differences regionally and seasonally, Paper V classifies regions into three groups of sea ice variability and trends: summer, winter, and transition modes. The summer (winter) mode regions experience largest sea ice variability and change in summer (winter), whereas regions with sea ice variability and change in both summer and winter are in transition mode.

According to available observations since 1850, the distinct summer and winter mode regions have generally been consistent over the past 160 years. As a consequence of the ongoing sea ice loss in all seasons, however, the current summer mode regions are transforming to transition mode. The current winter mode regions gradually lose their winter sea ice, and are going toward ice-free conditions year-round. If the current Northern Hemisphere sea ice loss persists, trends will have to increase toward the winter season also in the current summer mode regions. Paper V thus indicates that in a warming climate, the Northern Hemisphere winter sea ice cover will become gradually more important as the summer sea ice cover disappears.

## 5. Perspectives and outlook

Based on available observations, this thesis documents substantial regional and seasonal variations in the Arctic sea ice cover. Arctic winter sea ice extent variability, predictability, and trends, carried mainly by the Barents Sea and Nansen Basin, are the main focus herein (Figure 5.1). These regions experience, in contrast to other parts of the Arctic Ocean, largest sea ice decline in winter. A tight link between the Atlantic-Arctic sea ice cover and the poleward flowing warm Atlantic water has previously been established [e.g., *Helland-Hansen and Nansen*, 1909; *Schlichtholz*, 2011; *Smedsrud et al.*, 2013]. For the Barents Sea specifically, *Árthun et al.* [2012] demonstrate that the recent winter sea ice loss is due to increased Atlantic heat transport through the Barents Sea Opening. Here, we examine the Atlantic water branch that enters the Arctic Ocean through Fram Strait, and show based on observations that the recent loss of winter sea ice north of Svalbard is also largely caused by the inflowing Atlantic water (Paper I). The Atlantic water thus appears as a major contributor to the recent observed Arctic winter sea ice decline.

The Atlantic water has also been anticipated to have predictive potential for the Atlantic-Arctic [e.g., *Helland-Hansen and Nansen*, 1909; *Schlichtholz*, 2011], as upstream temperature changes propagate northward along the Atlantic water pathway [e.g., *Holliday et al.*, 2008]. Models predicting the regional sea ice cover have, however, been lacking. Based on an adequate understanding of air-ice-sea interaction in the Barents Sea and Nansen Basin we assess the regional winter sea ice predictability. Rooted in observations and based on first principles we propose conceptual models to describe the winter sea ice variability, and demonstrate for the first time that the winter sea ice area in the Barents Sea (Paper II) and Nansen Basin (Paper IV) can be skillfully predicted up to three years in advance based on observed Atlantic water characteristics upstream. The thesis thus identifies the Atlantic water as a main predictor for Arctic winter sea ice variability. Future observations of the Atlantic water inflow are essential in order to accommodate the increased need for regional Arctic sea ice predictions [*Eicken*, 2013]. An adequate representation of the Atlantic inflow in climate models also appears important in order for them to simulate the regional sea ice variability well. *Li et al.* [2017] find that the CMIP5 models generally underestimate the Atlantic heat transport into the Barents Sea and, hence, overestimate the sea ice extent.

The analytical frameworks presented in this thesis are concerned with regions dominated by advection of warm Atlantic water. However, the Barents Sea is a shallow shelf sea encompassed by landmasses, whereas the Nansen Basin is part of the deep Arctic Ocean. As a consequence, the sea ice advection to the Barents Sea is small and most of the sea ice forms locally in winter. In contrast, large amounts of sea ice are advected into the region north of Svalbard [*Kwok*, 2009; *Itkin et al.*, 2017]. Paper II thus assesses a re-

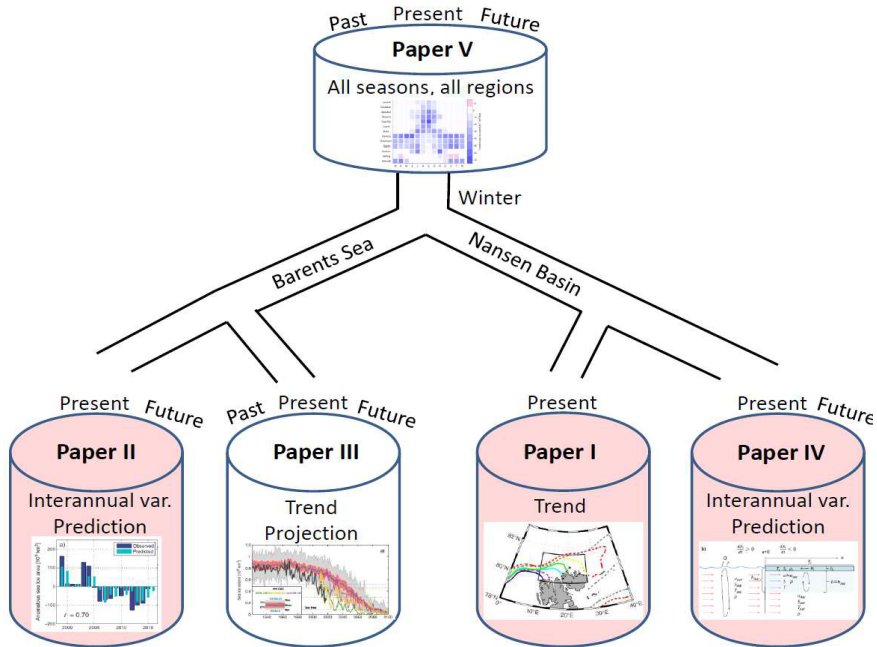


**Figure 5.1:** Schematic summarizing the papers included in this thesis. Paper V assesses past, present, and future sea ice variability and change in the Northern Hemisphere, regionally and seasonally. Detailed assessments of winter sea ice variability and change in the Barents Sea and Nansen Basin are provided in Paper II and III, and Paper I and IV, respectively. Red boxes indicate that the papers examine Atlantic water observations.

gion where the Atlantic domain mostly governs the boundary of the area of open water, whereas Paper IV is concerned with the competition between inflowing Atlantic water and drifting sea ice. The two proposed frameworks thus consider two different situations, where in Paper II warm water mainly inhibits freezing, whereas in Paper IV warm water mainly melts approaching sea ice. The frameworks may be applicable to other regional seas where warm water is advected near the surface and sea ice is present, for instance near the Bering Strait where warm Pacific waters enter the Arctic Ocean and flow poleward toward the ice edge [Woodgate *et al.*, 2010]. The Bering Strait heat inflow is found to be key in predicting the timing of retreat and advance of sea ice in the Chukchi Sea [Serreze *et al.*, 2016]. If the ongoing Atlantification of the Arctic Ocean [Polyakov *et al.*, 2017] persists into the future, the proposed frameworks may also become applicable to larger parts of the Arctic shelves.

During the last decade predictions of Arctic sea ice have advanced rapidly. Besides providing important information for end users concerned with management and industry decisions, Atlantic-Arctic sea ice predictions are of particular interest as variations in the sea ice cover potentially affect mid-latitude weather and climate [Inoue *et al.*, 2012; Liptak and Strong, 2014; Sorokina *et al.*, 2016], and Arctic ecosystems and fisheries [Dalpadado *et al.*, 2014]. Sea ice predictions presented in Paper IV toward 2020 are in agreement with pentadal [Arthur *et al.*, 2017] and decadal [Yeager *et al.*, 2015] predictions of the Atlantic-Arctic winter sea ice cover, and with the observed and predicted

cooling of the subpolar North Atlantic [*Hermanson et al.*, 2014]. In order to ensure relevant products for policymakers and industry, better collaboration between the sea ice prediction community and end users is essential [*Murphy*, 1993]. More advanced metrics including spatial distributions, sea ice thickness, and the duration of the sea ice cover on different timescales should also be considered. We note that a major challenge with prediction models is that the climate system is rapidly changing, and that formulations that hold for the past and present may not hold for the future [*Hamilton and Stroeve*, 2016]. Statistical models based on regression or dynamical models with parametrization may thus not be valid in a new Arctic. A thorough understanding of mechanisms and the use of simple conceptual models thus appear essential.

The present Barents Sea climate system is relatively well understood and the tight link between Atlantic water and sea ice is well established [e.g., *Smedsrud et al.*, 2013]. Paper III provides, however, the first detailed assessment of past, present, and future winter sea ice variability and change in the Barents Sea. The recent Barents Sea winter ice extent and trends are unprecedented in the available historical record since 1850. By assessing a large ensemble climate model simulation, it is found that the main part of the recent Barents Sea ice loss is due to internal variability, in agreement with *Li et al.* [2017]. The simulations, moreover, show that the Barents Sea may be ice-free by the end of the century, but that internal variability leads to a large spread in models projections of ice-free conditions. Substantial interannual to decadal variability is also present toward 2100, possibly reflecting variations in the inflowing Atlantic water.

Paper I–IV suggest that detailed assessments regionally and seasonally are essential in order to better understand recent and future Arctic sea ice extent variability and change. Paper V provides a pan-Arctic perspective of observed regional and seasonal sea ice extent changes since 1850, and demonstrates pronounced regional differences between winter and summer. Although the current sea ice loss is largest in summer [e.g., *Serreze and Stroeve*, 2015], Paper V emphasizes that the Arctic sea ice cover is becoming more seasonal, and that changes will continue to increase in new regions and toward the winter season in a warming climate. The present dominance of Atlantic-Arctic winter sea ice variability and loss is thus expected to decrease in the future.

The recent Arctic sea ice extent variability is well documented in this thesis. Corresponding changes in sea ice thickness are, however, not addressed in much detail. The lack of observed Arctic sea ice thickness represents a large uncertainty in quantifying the ongoing sea ice change. Based on submarine sonar measurements *Rothrock et al.* [1999] calculate a reduction of approximately 40% in volume over the last few decades, and simulations indicate significant negative trends in sea ice volume of 3–4% per decade [*Gregory et al.*, 2002; *Hilmer and Lemke*, 2000; *Schweiger et al.*, 2011]. Detailed examinations of Arctic sea ice volume are needed to assist the regional and seasonal sea ice extent trends quantified herein. To further address the large seasonal and regional variations of the Arctic sea ice cover, detailed regional analysis similar to Paper III should also be performed.

## 5.1 Simulated sea ice extent trends

This thesis has assessed the regional and seasonal Arctic sea ice extent evolution toward 2100 by extrapolating current regional trends into the future (Paper V). Climate models

are, however, the key tool to assess the future evolution of the Arctic sea ice cover [Notz and Stroeve, 2016]. An assessment of projected regional and seasonal sea ice extent change by climate models could provide increased understanding of the future sea ice evolution, and be compared to the estimated evolution in Paper V.

Stroeve *et al.* [2012b] show that the CMIP5 models as a group underestimate the recent observed sea ice extent trends in all seasons (Figure 5.2a). The smaller simulated trends indicate that the observed sea ice loss is a statistically rare event or that the models are deficient in their response to anthropogenic forcing [Stroeve *et al.*, 2007].

Based on 107 CMIP5 ensemble members (1979–2015; 1979–2005 are historical simulations, whereas 2005–2015 are forced with the RCP4.5 emission scenario), Figure 5.2 demonstrates a large spread in monthly CMIP5 sea ice extent trends. The CMIP5 ensemble mean correctly simulates the seasonal cycle in the sea ice extent trends with larger trends in summer than winter [Figure 5.2a; Stroeve *et al.*, 2012b]. We find, however, that the individual ensemble members are often not able to simulate the observed seasonal cycle of the sea ice extent trends (Figure 5.2c–d). The seasonal cycle of simulated sea ice extent trends fall within three groups: Ensemble members that correctly simulate the seasonal cycle with large trends in summer and smaller trends in winter (Figure 5.2b), members that have similar trends throughout the year with no distinct peaks (Figure 5.2c), and members that have largest trends in winter and smallest trends in summer (Figure 5.2d). In total 29 out of the 107 ensemble members simulate larger trends in March than September over the 1979–2015 period (not shown), strongly contrasting the observed change.

Due to large internal variability it may not be surprising that the magnitude of the observed sea ice extent trends is not correctly simulated. One may, however, expect that the seasonal cycle of the simulated trends would match the observed. The fact that 27% of the models have larger trends in March than September may be related to different sea ice models. Stroeve *et al.* [2007] find that climate models with more sophisticated sea ice models to a larger degree capture recent observed trends. A comparison of the individual models' sea ice extent and thickness could also provide increased insight into the incorrect simulated seasonal cycle of sea ice extent trends. For instance, if the sea ice cover extends too far into the North Atlantic or Pacific oceans in winter there is potential for large winter sea ice extent trends. We note that the models examined in Paper III have similar seasonal cycle to the observed (not shown), and were specifically evaluated against the observed Barents Sea ice cover.

As the observed pan-Arctic seasonal cycle of sea ice extent trends, 1979–2015, is incorrectly simulated by more than 1/4 of the CMIP5 models, an assessment of their regional and seasonal evolution toward 2100 may not be reliable. At least, a more thorough evaluation of the individual models' performance would be beneficial before the simulated change is compared to the estimates presented in Paper V. We note, however, again that a model with a realistic representation of the present sea ice cover does not imply a correct representation of the future evolution [Notz, 2015].

In order to skillfully project future seasonal and regional changes in the Arctic sea ice cover, climate models need adequate representation of the most important physical processes. Currently, prediction models based on process understanding, as presented in Paper II and IV, appear essential in order to skillfully predict the future. This thesis demonstrates that a realistic representation of the Atlantic inflow to the Atlantic-Arctic is key in order to correctly simulate the Atlantic-Arctic winter sea ice variability. In

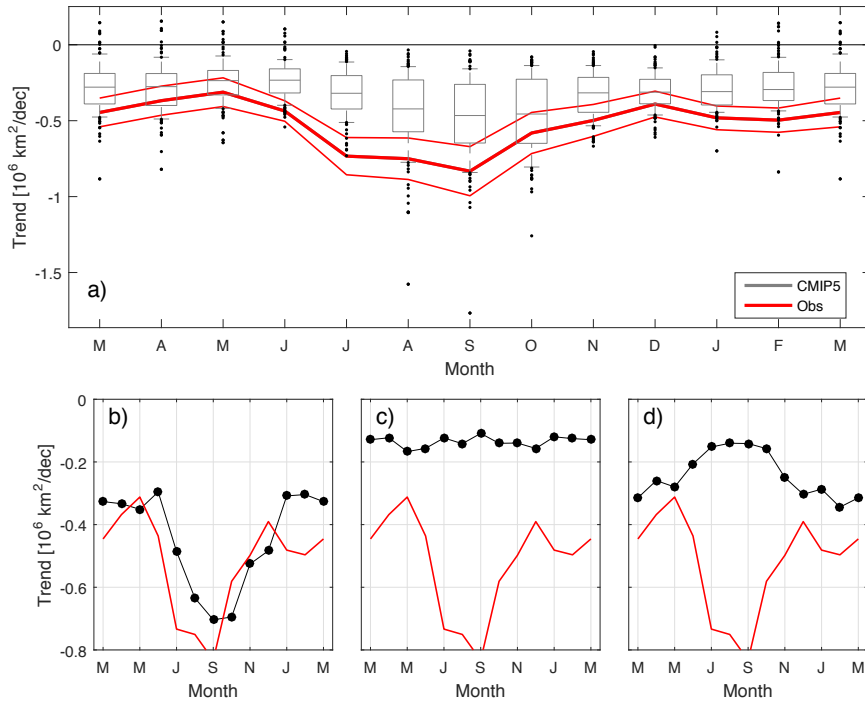


**Figure 5.2:** Monthly Northern Hemisphere sea ice extent trends, 1979–2015, centered around September in observations (red) and CMIP5 models (black). a) The CMIP5 ensemble mean median (central horizontal line in black boxes), quartiles (edges of the boxes), 10 and 90 percentiles (whiskers), and trends that are more extreme than the 10 and 90 percentiles (dots) are indicated. Thin red lines show the 95% confidence interval of the observed trends. b–d) Observed (red) and simulated (black) monthly sea ice extent trends in three CMIP5 ensemble members, representing members with larger summer than winter trends (b), similar trends in all months (c), and largest trends in winter (d).

regions being less dominated by ocean forcing other predictors must be identified in order to skillfully predict the future sea ice evolution.

By quantifying and characterizing observed regional and seasonal variations in the Arctic sea ice cover, this thesis suggests that assessing a combination of observations, simulations, and conceptual models is essential in order to understand the recent observed sea ice change, predict the future evolution, and evaluate its consequences. The thesis demonstrates that the recent observed Arctic winter sea ice variability and loss are carried by the Atlantic-Arctic. Currently, the Atlantic water contributes importantly to the Arctic winter sea ice decline (Paper I) and acts as a skillful predictor of winter sea ice variability in the Barents Sea (Paper II) and Nansen Basin (IV). In a warming climate, however, the Barents Sea may become ice-free year-round (III). As the Arctic becomes ice-free in summer, sea ice variability and trends increase in new regions toward the winter season, and sea ice variability and trends in winter become increasingly important (Paper V).

# References

- Aagaard, K. (1989), A synthesis of the Arctic Ocean circulation, *Rapp. P.-V. Reun.-Cons. Int. Explor. Mer*, 188, 11–22.
- Aagaard, K., and P. Greisman (1975), Toward new mass and heat budgets for the Arctic Ocean, *J. Geophys. Res.*, 80(27), 3821–3827.
- Aagaard, K., J. Swift, and E. Carmack (1985), Thermohaline circulation in the Arctic Mediterranean seas, *J. Geophys. Res.*, 90(C3), 4833–4846.
- Aagaard, K., A. Foldvik, and S. Hillman (1987), The West Spitsbergen Current: Disposition and water mass transformation, *J. Geophys. Res.*, 92(C4), 3778–3784.
- ACIA (2005), *Arctic Climate Impact Assessment*, Cambridge Univ. Press, Cambridge, UK.
- Årthun, M., and T. Eldevik (2016), On anomalous ocean heat transport toward the Arctic and associated climate predictability, *J. Clim.*, 29(2), 689–704.
- Årthun, M., and C. Schrum (2010), Ocean surface heat flux variability in the Barents Sea, *J. Mar. Syst.*, 83(1–2), 88–98.
- Årthun, M., T. Eldevik, L. H. Smedsrud, Ø. Skagseth, and R. B. Ingvaldsen (2012), Quantifying the influence of Atlantic heat on Barents Sea ice variability and retreat, *J. Clim.*, 25, 4736–4743.
- Årthun, M., T. Eldevik, E. Viste, H. Drange, T. Furevik, H. L. Johnson, and N. S. Keenlyside (2017), Skillful prediction of northern climate provided by the ocean, *Nat. Commun.*, 8, 15,875.
- Bengtsson, L., V. A. Semenov, and O. M. Johannessen (2004), The early twentieth-century warming in the Arctic – a possible mechanism, *J. Clim.*, 17(20), 4045–4057.
- Beszczynska-Möller, A., E. Fahrbach, U. Schauer, and E. Hansen (2012), Variability in Atlantic water temperature and transport at the entrance to the Arctic Ocean, 1997–2010, *ICES J. Mar. Sci.*, 69(5), 852–863.
- Bitz, C., and G. Roe (2004), A mechanism for the high rate of sea ice thinning in the Arctic Ocean, *J. Clim.*, 17(18), 3623–3632.
- Bitz, C., M. Holland, E. Hunke, and R. Moritz (2005), Maintenance of the sea-ice edge, *J. Clim.*, 18(15), 2903–2921.

- Boisvert, L. N., A. A. Petty, and J. C. Stroeve (2016), The impact of the extreme winter 2015/16 arctic cyclone on the Barents–Kara seas, *Mon. Wea. Rev.*, *144*(11), 4279–4287.
- Carmack, E., I. Polyakov, L. Padman, I. Fer, E. Hunke, J. Hutchings, J. Jackson, D. Kelley, R. Kwok, C. Layton, et al. (2015), Toward Quantifying the Increasing Role of Oceanic Heat in Sea Ice Loss in the New Arctic, *Bull. Am. Meteorol. Soc.*, *96*(12), 2079–2105.
- Cavalieri, D. J., and C. L. Parkinson (2012), Arctic sea ice variability and trends, 1979–2010, *The Cryosphere*, *6*(4), 881–889.
- Cavalieri, D. J., J. Crawford, M. Drinkwater, W. J. Emery, D. T. Eppler, L. D. Farmer, M. Goodberlet, R. Jentz, A. Milman, C. Morris, R. Onstott, A. Schweiger, R. Shuchman, K. Steffen, C. T. Swift, C. Wackerman, and R. L. Weaver (1992), NASA Sea Ice Validation Program for the DMSP SSM/I: Final Report, *Tech. rep.*, National Aeronautics and Space Administration, Washington, D. C., NASA Technical Memorandum 104559, 126 pp.
- Cavalieri, D. J., C. L. Parkinson, P. Gloersen, and H. Zwally (1996), Sea ice concentrations from Nimbus-7 SMMR and DMSP SSM/I passive microwave data, *Digital media, National Snow and Ice Data Center*.
- Chapman, W. L., and J. E. Walsh (1991), Arctic and Southern Ocean Sea Ice Concentrations, Version 1, Boulder, Colorado USA. NSIDC: National Snow and Ice Data Center.
- Comiso, J. C. (2002), A rapidly declining perennial sea ice cover in the Arctic, *Geophys. Res. Lett.*, *29*(20), 1956.
- Comiso, J. C., and C. L. Parkinson (2004), Satellite observed changes in the Arctic, *Phys. Today*, *57*(8), 38–44.
- Comiso, J. C., C. L. Parkinson, R. Gersten, and L. Stock (2008), Accelerated decline in the Arctic sea ice cover, *Geophys. Res. Lett.*, *35*(1), L01,703.
- Comiso, J. C., W. N. Meier, and R. Gersten (2017), Variability and trends in the Arctic Sea ice cover: Results from different techniques, *J. Geophys. Res.*, *122*, 6883–6900.
- Connolly, R., M. Connolly, and W. Soon (2017), Re-calibration of Arctic sea ice extent datasets using Arctic surface air temperature records, *Hydrol. Sci. J.*, *62*(8), 1317–1340.
- Cressey, D. (2007), Arctic melt opens Northwest passage, *Nature*, *449*, 267.
- Dalpadado, P., K. R. Arrigo, S. S. Hjøllo, F. Rey, R. B. Ingvaldsen, E. Sperfeld, G. L. van Dijken, L. C. Stige, A. Olsen, and G. Ottersen (2014), Productivity in the Barents Sea—response to recent climate variability, *PLoS one*, *9*(5), e95,273.
- Day, J., E. Hawkins, and S. Tietsche (2014), Will Arctic sea ice thickness initialization improve seasonal forecast skill?, *Geophys. Res. Lett.*, *41*(21), 7566–7575.

- Ding, Q., A. Schweiger, M. L'Heureux, D. S. Battisti, S. Po-Chedley, N. C. Johnson, E. Blanchard-Wrigglesworth, K. Harnos, Q. Zhang, R. Eastman, et al. (2017), Influence of high-latitude atmospheric circulation changes on summertime Arctic sea ice, *Nat. Clim. Change*, 7(4), 289–295.
- Divine, D. V., and C. Dick (2006), Historical variability of sea ice edge position in the nordic seas, *J. Geophys. Res.*, 111(C1), C01,001.
- Eicken, H. (2013), Ocean science: Arctic sea ice needs better forecasts, *Nature*, 497(7450), 431–433.
- Emmerson, C., and G. Lahn (2012), *Arctic opening: Opportunity and risk in the High North*, LLOYD's report.
- Fer, I. (2009), Weak vertical diffusion allows maintenance of cold halocline in the central Arctic, *Atmos. Oceanic Sci. Lett.*, 2(3), 148–152.
- Francis, J. A., and E. Hunter (2006), New insight into the disappearing Arctic sea ice, *Eos*, 87(46), 509–511.
- Francis, J. A., and S. J. Vavrus (2012), Evidence linking Arctic amplification to extreme weather in mid-latitudes, *Geophys. Res. Lett.*, 39(6), L06,801.
- Furevik, T. (2001), Annual and interannual variability of Atlantic Water temperatures in the Norwegian and Barents Seas: 1980–1996, *Deep Sea Res.*, 48(2), 383–404.
- Gagné, M.-È., J. C. Fyfe, N. P. Gillett, I. V. Polyakov, and G. M. Flato (2017), Aerosol-driven increase in Arctic sea ice over the middle of the 20th Century, *Geophys. Res. Lett.*, (14), 7338–7346.
- Gammelsrød, T., Ø. Leikvin, V. Lien, W. P. Budgell, H. Loeng, and W. Maslowski (2009), Mass and heat transports in the NE Barents Sea: Observations and models, *J. Mar. Syst.*, 75(1), 56–69.
- Graham, R. M., L. Cohen, A. A. Petty, L. N. Boisvert, A. Rinke, S. R. Hudson, M. Nicolaus, and M. A. Granskog (2017), Increasing frequency and duration of Arctic winter warming events, *Geophys. Res. Lett.*, 44(13), 6974–6983.
- Granskog, M. A., P. Assmy, S. Gerland, G. Spreen, H. Steen, and L. H. Smedsrud (2016), Arctic research on thin ice: Consequences of Arctic sea ice loss, *Eos*, 97.
- Graversen, R. G., T. Mauritsen, S. Drijfhout, M. Tjernström, and S. Mårtensson (2011), Warm winds from the Pacific caused extensive Arctic sea-ice melt in summer 2007, *Clim. Dyn.*, 36(11–12), 2103–2112.
- Gregory, J. M., P. Stott, D. Cresswell, N. Rayner, C. Gordon, and D. Sexton (2002), Recent and future changes in Arctic sea ice simulated by the HadCM3 AOGCM, *Geophys. Res. Lett.*, 29(24).
- Griffies, S. M., and K. Bryan (1997), Predictability of North Atlantic multidecadal climate variability, *Science*, 275(5297), 181–184.

- Gudkovich, Z. (1961a), Relation of the ice drift in the Arctic Basin to ice conditions in the Soviet Arctic seas, *Tr. Okeanogr. Kom. Akad. Nauk SSSR*, 11, 14–21, (In Russian).
- Gudkovich, Z. (1961b), On the nature of Pacific currents in the Bering Strait and the causes of seasonal variations in their intensity, *Okeanologiya*, 1(4), 608–612, (In Russian).
- Guemas, V., E. Blanchard-Wrigglesworth, M. Chevallier, J. J. Day, M. Déqué, F. J. Doblas-Reyes, N. S. Fučkar, A. Germe, E. Hawkins, S. Keeley, et al. (2016), A review on Arctic sea-ice predictability and prediction on seasonal to decadal time-scales, *Q. J. R. Meteorol. Soc.*, 142(695), 546–561.
- Haine, T. W., B. Curry, R. Gerdes, E. Hansen, M. Karcher, C. Lee, B. Rudels, G. Spreen, L. de Steur, K. D. Stewart, et al. (2015), Arctic freshwater export: Status, mechanisms, and prospects, *Global Planet. Change*, 125, 13–35.
- Häkkinen, S., and D. J. Cavalieri (1989), A study of oceanic surface heat fluxes in the Greenland, Norwegian, and Barents Seas, *J. Geophys. Res.*, 94(C5), 6145–6157.
- Hamilton, L. C., and J. Stroeve (2016), 400 predictions: the SEARCH Sea Ice Outlook 2008–2015, *Polar Geogr.*, 39(4), 274–287.
- Hassol, S. (2004), *Impacts of a warming Arctic: Arctic climate impact assessment*, 140 pp., Cambridge University Press: Cambridge, UK, <http://www.amap.no/arctic-climate-impact-assessment-acia>.
- Hátún, H., A. B. Sandø, H. Drange, B. Hansen, and H. Valdimarsson (2005), Influence of the Atlantic subpolar gyre on the thermohaline circulation, *Science*, 309(5742), 1841–1844.
- Helland-Hansen, B., and F. Nansen (1909), The Norwegian Sea, *Fiskdir. Skr. Ser. Havunders.*, 11(2), 1–360.
- Hermanson, L., R. Eade, N. H. Robinson, N. J. Dunstone, M. B. Andrews, J. R. Knight, A. A. Scaife, and D. M. Smith (2014), Forecast cooling of the Atlantic subpolar gyre and associated impacts, *Geophys. Res. Lett.*, 41(14), 5167–5174.
- Hilmer, M., and P. Lemke (2000), On the decrease of Arctic sea ice volume, *Geophys. Res. Lett.*, 27(22), 3751–3754.
- Holland, M. M., and C. M. Bitz (2003), Polar amplification of climate change in coupled models, *Climate Dynamics*, 21(3–4), 221–232.
- Holland, M. M., C. M. Bitz, and B. Tremblay (2006), Future abrupt reductions in the summer Arctic sea ice, *Geophys. Res. Lett.*, 33(23), L23,503.
- Holland, M. M., D. A. Bailey, and S. Vavrus (2011), Inherent sea ice predictability in the rapidly changing Arctic environment of the Community Climate System Model, version 3, *Climate Dyn.*, 36(7–8), 1239–1253.

- Holliday, N. P., S. Hughes, S. Bacon, A. Beszczynska-Möller, B. Hansen, A. Lavin, H. Loeng, K. Mork, S. Østerhus, T. Sherwin, et al. (2008), Reversal of the 1960s to 1990s freshening trend in the northeast North Atlantic and Nordic Seas, *Geophys. Res. Lett.*, *35*(3), L03,614.
- Holliday, N. P., S. L. Hughes, and A. Beszczynska-Möller (2009), ICES report on ocean climate 2008, ICES Cooperative Research Report, 298. 66 pp.
- Ingvaldsen, R., H. Loeng, and L. Asplin (2002), Variability in the Atlantic inflow to the Barents Sea based on a one-year time series from moored current meters, *Cont. Shelf Res.*, *22*(3), 505–519.
- Ingvaldsen, R. B., L. Asplin, and H. Loeng (2004a), The seasonal cycle in the Atlantic transport to the Barents Sea during the years 1997–2001, *Cont. Shelf Res.*, *24*(9), 1015–1032.
- Ingvaldsen, R. B., L. Asplin, and H. Loeng (2004b), Velocity field of the western entrance to the Barents Sea, *J. Geophys. Res.*, *109*(C3), C03,021.
- Inoue, J., M. E. Hori, and K. Takaya (2012), The role of Barents Sea ice in the wintertime cyclone track and emergence of a warm-Arctic cold-Siberian anomaly, *J. Clim.*, *25*(7), 2561–2568.
- IPCC (2013), *Climate Change 2013: The Physical Science Basis: Contribution of Working Group I to the Fifth Assessment Report of the Intergovernmental Panel on Climate Change*, Cambridge University Press, Cambridge, United Kingdom and New York, NY, USA.
- Itkin, P., G. Spreen, B. Cheng, M. Doble, F. Girard-Ardhuin, J. Haapala, N. Hughes, L. Kaleschke, M. Nicolaus, and J. Wilkinson (2017), Thin ice and storms: Sea ice deformation from buoy arrays deployed during N-ICE2015, *J. Geophys. Res.*, *122*, 4661–4674.
- Jahn, A., J. E. Kay, M. M. Holland, and D. M. Hall (2016), How predictable is the timing of a summer ice-free Arctic?, *Geophys. Res. Lett.*, *43*(17), 9113–9120.
- Jaiser, R., K. Dethloff, D. Handorf, A. Rinke, and J. Cohen (2012), Impact of sea ice cover changes on the Northern Hemisphere atmospheric winter circulation, *Tellus A*, *64*(1), 11,595.
- Kapsch, M.-L., R. G. Graversen, T. Economou, and M. Tjernström (2014), The importance of spring atmospheric conditions for predictions of the Arctic summer sea ice extent, *Geophys. Res. Lett.*, *41*(14), 5288–5296.
- Kay, J. E., T. L’Ecuyer, A. Gettelman, G. Stephens, and C. O’Dell (2008), The contribution of cloud and radiation anomalies to the 2007 Arctic sea ice extent minimum, *Geophys. Res. Lett.*, *35*(8), L08,503.
- Kay, J. E., M. M. Holland, and A. Jahn (2011), Inter-annual to multi-decadal Arctic sea ice extent trends in a warming world, *Geophys. Res. Lett.*, *38*(15), L15,708.

- Khon, V., I. Mokhov, M. Latif, V. Semenov, and W. Park (2010), Perspectives of Northern Sea Route and Northwest Passage in the twenty-first century, *Clim. Change*, 100(3–4), 757–768.
- Krishfield, R. A., and D. K. Perovich (2005), Spatial and temporal variability of oceanic heat flux to the Arctic ice pack, *J. Geophys. Res.*, 110(C7), C07,021.
- Kvingedal, B. (2005), Sea-ice extent and variability in the Nordic Seas, 1967–2002, in *The Nordic Seas: An Integrated Perspective*, vol. 158, edited by H. Drange, T. Dokken, T. Furevik, R. Gerdes, and W. Berger, pp. 137–156, Amer. Geophys. Union.
- Kwok, R. (2009), Outflow of Arctic Ocean sea ice into the Greenland and Barents Seas: 1979–2007, *J. Clim.*, 22(9), 2438–2457.
- Kwok, R., and D. Rothrock (2009), Decline in Arctic sea ice thickness from submarine and ICESat records: 1958–2008, *Geophys. Res. Lett.*, 36(15), L15,501.
- Kwok, R., G. Spreen, and S. Pang (2013), Arctic sea ice circulation and drift speed: Decadal trends and ocean currents, *J. Geophys. Res.*, 118(5), 2408–2425.
- Li, D., R. Zhang, and T. R. Knutson (2017), On the discrepancy between observed and CMIP5 multi-model simulated Barents Sea winter sea ice decline, *Nat. Commun.*, 8, 14,991.
- Lindsay, R., and J. Zhang (2005), The thinning of Arctic sea ice, 1988–2003: Have we passed a tipping point?, *J. Clim.*, 18(22), 4879–4894.
- Liptak, J., and C. Strong (2014), The winter atmospheric response to sea ice anomalies in the Barents Sea, *J. Climate*, 27(2), 914–924.
- Liu, J., M. Song, R. M. Horton, and Y. Hu (2013), Reducing spread in climate model projections of a September ice-free Arctic, *Proc. Natl. Acad. Sci.*, 110(31), 12,571–12,576.
- Loeng, H. (1991), Features of the physical oceanographic conditions of the Barents Sea, *Polar Res.*, 10(1), 5–18.
- Loeng, H., V. Ozhigin, and B. Ådlandsvik (1997), Water fluxes through the Barents Sea, *ICES J. Mar. Sci.*, 54(3), 310–317.
- Mahoney, A. R., R. G. Barry, V. Smolyanitsky, and F. Fetterer (2008), Observed sea ice extent in the Russian Arctic, 1933–2006, *J. Geophys. Res.*, 113(C11), C11,005.
- Maslanik, J., and J. Stroeve (1999), updated daily. Near-Real-Time DMSP SSMIS Daily Polar Gridded Sea Ice Concentrations, Version 1, Boulder, Colorado USA. NASA National Snow and Ice Data Center Distributed Active Archive Center.
- Maslanik, J., C. Fowler, J. Stroeve, S. Drobot, J. Zwally, D. Yi, and W. Emery (2007), A younger, thinner Arctic ice cover: Increased potential for rapid, extensive sea-ice loss, *Geophys. Res. Lett.*, 34(24), L24,501.

- Massonnet, F., T. Fichefet, H. Goosse, C. M. Bitz, G. Philippon-Berthier, M. M. Holland, and P.-Y. Barriat (2012), Constraining projections of summer Arctic sea ice, *The Cryosphere*, 6(6), 1383.
- Mauritzen, C. (1996), Production of dense overflow waters feeding the North Atlantic across the Greenland-Scotland Ridge. Part 1: Evidence for a revised circulation scheme, *Deep-Sea Res.*, 43(6), 769–806.
- Maykut, G. A., and N. Untersteiner (1971), Some results from a time-dependent thermodynamic model of sea ice, *J. Geophys. Res.*, 76(6), 1550–1575.
- McLaughlin, F. A., E. C. Carmack, W. J. Williams, S. Zimmermann, K. Shimada, and M. Itoh (2009), Joint effects of boundary currents and thermohaline intrusions on the warming of Atlantic water in the Canada Basin, 1993–2007, *J. Geophys. Res.*, 114(C1), C00A12.
- Meehl, G. A., C. Covey, K. E. Taylor, T. Delworth, R. J. Stouffer, M. Latif, B. McAvaney, and J. F. Mitchell (2007), The WCRP CMIP3 multimodel dataset: A new era in climate change research, *Bull. Amer. Meteor. Soc.*, 88(9), 1383–1394.
- Meier, W., and D. Notz (2010), A note on the accuracy and reliability of satellite-derived passive microwave estimates of sea-ice extent, in *CliC Arctic Sea Ice Working Group Consensus Document*, pp. 1–4, World Climate Research Program, The Climate and Cryosphere (CliC), Tromsø, Norway.
- Meier, W., J. Stroeve, F. Fetterer, and K. Knowles (2005), Reductions in Arctic sea ice cover no longer limited to summer, *Eos*, 86(36), 326–326.
- Meier, W., F. Fetterer, M. Savoie, S. Mallory, R. Duerr, and J. Stroeve (2013), updated 2016. NOAA/NSIDC Climate Data Record of Passive Microwave Sea Ice Concentration, Version 2, Boulder, Colorado USA. NSIDC: National Snow and Ice Data Center.
- Meincke, J., B. Rudels, and H. Friedrich (1997), The Arctic Ocean–Nordic Seas thermohaline system, *ICES J. Mar. Sci.*, 54(3), 283–299.
- Meyer, A., I. Fer, A. Sundfjord, and A. K. Peterson (2017), Mixing rates and vertical heat fluxes north of Svalbard from Arctic winter to spring, *J. Geophys. Res.*, 122(6), 4569–4586.
- Midttun, L. (1985), Formation of dense bottom water in the Barents Sea, *Deep Sea Res.*, 32(10), 1233–1241.
- Min, S.-K., X. Zhang, F. W. Zwiers, and T. Agnew (2008), Human influence on Arctic sea ice detectable from early 1990s onwards, *Geophys. Res. Lett.*, 35(21), L21,701.
- Moss, R. H., J. A. Edmonds, K. A. Hibbard, M. R. Manning, S. K. Rose, D. P. Van Vuuren, T. R. Carter, S. Emori, M. Kainuma, T. Kram, et al. (2010), The next generation of scenarios for climate change research and assessment, *Nature*, 463(7282), 747–756.
- Murphy, A. H. (1993), What is a good forecast? An essay on the nature of goodness in weather forecasting, *Wea. Forecasting*, 8(2), 281–293.

- Mysak, L. A., and D. M. Manak (1989), Arctic sea-ice extent and anomalies, 1953–1984, *Atmos. Ocean*, *27*(2), 376–405.
- Nansen, F. (1902), *The oceanography of the North Polar Basin*, vol. 3, Longmans, Green, and Company, in Norwegian North Polar Expedition 1893–1896: Scientific Results.
- Nghiem, S., I. Rigor, D. Perovich, P. Clemente-Colón, J. Weatherly, and G. Neumann (2007), Rapid reduction of Arctic perennial sea ice, *Geophys. Res. Lett.*, *34*(19), L19,504.
- Notz, D. (2009), The future of ice sheets and sea ice: Between reversible retreat and unstoppable loss, *Proc. Nat. Ac. Sci.*, *106*(49), 20,590–20,595.
- Notz, D. (2015), How well must climate models agree with observations?, *Phil. Trans. R. Soc. A*, *373*(2052), 20140,164.
- Notz, D., and J. Marotzke (2012), Observations reveal external driver for Arctic sea-ice retreat, *Geophys. Res. Lett.*, *39*(8), L08,502.
- Notz, D., and J. Stroeve (2016), Observed Arctic sea-ice loss directly follows anthropogenic CO<sub>2</sub> emission, *Science*, *354*(6313), 747–750.
- NSIDC (2017a), Arctic sea ice 2017: Tapping the brakes in September, Available online at: <https://nsidc.org/arcticseaicenews/2017/10/>.
- NSIDC (2017b), Another record, but a somewhat cooler Arctic Ocean, Available online at: <https://nsidc.org/arcticseaicenews/2017/04/>.
- Ogi, M., and J. M. Wallace (2012), The role of summer surface wind anomalies in the summer Arctic sea ice extent in 2010 and 2011, *Geophys. Res. Lett.*, *39*(9), L09,704.
- Orvik, K. A., and P. Niiler (2002), Major pathways of Atlantic water in the northern North Atlantic and Nordic Seas toward Arctic, *Geophys. Res. Lett.*, *29*(19), 1896.
- Orvik, K. A., Ø. Skagseth, and M. Mork (2001), Atlantic inflow to the Nordic Seas: current structure and volume fluxes from moored current meters, VM-ADCP and SeaSoar-CTD observations, 1995–1999, *Deep Sea Res.*, *48*(4), 937–957.
- Parkinson, C. L., and J. C. Comiso (2013), On the 2012 record low Arctic sea ice cover: Combined impact of preconditioning and an August storm, *Geophys. Res. Lett.*, *40*(7), 1356–1361.
- Partington, K., T. Flynn, D. Lamb, C. Bertioia, and K. Dedrick (2003), Late twentieth century Northern Hemisphere sea-ice record from US National Ice Center ice charts, *J. Geophys. Res.*, *108*(C11), 3343.
- Perkin, R., and E. Lewis (1984), Mixing in the West Spitsbergen current, *J. Phys. Ocean.*, *14*(8), 1315–1325.
- Perovich, D. K., B. Light, H. Eicken, K. F. Jones, K. Runciman, and S. V. Nghiem (2007), Increasing solar heating of the Arctic Ocean and adjacent seas, 1979–2005: Attribution and role in the ice-albedo feedback, *Geophys. Res. Lett.*, *34*(19), L19,505.

- Perovich, D. K., J. A. Richter-Menge, K. F. Jones, and B. Light (2008), Sunlight, water, and ice: Extreme Arctic sea ice melt during the summer of 2007, *Geophys. Res. Lett.*, *35*(11), L11,501.
- Peterson, A. K., I. Fer, M. G. McPhee, and A. Randelhoff (2017), Turbulent heat and momentum fluxes in the upper ocean under Arctic sea ice, *J. Geophys. Res.*, *122*(2), 1439–1456.
- Peterson, B. J., R. M. Holmes, J. W. McClelland, C. J. Vörösmarty, R. B. Lammers, A. I. Shiklomanov, I. A. Shiklomanov, and S. Rahmstorf (2002), Increasing river discharge to the Arctic Ocean, *Science*, *298*(5601), 2171–2173.
- Piechura, J., and W. Walczowski (2009), Warming of the West Spitsbergen Current and sea ice north of Svalbard, *Oceanologia*, *51*(2), 147–164.
- Polyakov, I., G. Alekseev, L. Timokhov, U. Bhatt, R. Colony, H. Simmons, D. Walsh, J. Walsh, and V. Zakharov (2004), Variability of the intermediate Atlantic water of the Arctic Ocean over the last 100 years, *J. Clim.*, *17*(23), 4485–4497.
- Polyakov, I. V., A. Y. Proshutinsky, and M. A. Johnson (1999), Seasonal cycles in two regimes of Arctic climate, *J. Geophys. Res.*, *104*(C11), 25,761–25,788.
- Polyakov, I. V., G. V. Alekseev, R. V. Bekryaev, U. S. Bhatt, R. Colony, M. A. Johnson, V. P. Karklin, D. Walsh, and A. V. Yulin (2003), Long-term ice variability in Arctic marginal seas, *J. Clim.*, *16*(12), 2078–2085.
- Polyakov, I. V., A. Beszczynska, E. C. Carmack, I. A. Dmitrenko, E. Fahrbach, I. E. Frolov, R. Gerdes, E. Hansen, J. Holfort, V. V. Ivanov, et al. (2005), One more step toward a warmer Arctic, *Geophys. Res. Lett.*, *32*(17), L17,605.
- Polyakov, I. V., L. A. Timokhov, V. A. Alexeev, S. Bacon, I. A. Dmitrenko, L. Fortier, I. E. Frolov, J.-C. Gascard, E. Hansen, V. V. Ivanov, et al. (2010), Arctic Ocean warming contributes to reduced polar ice cap, *J. Phys. Oceanogr.*, *40*(12), 2743–2756.
- Polyakov, I. V., A. V. Pnyushkov, and L. A. Timokhov (2012), Warming of the Intermediate Atlantic Water of the Arctic Ocean in the 2000s, *J. Clim.*, *25*(23), 8362–8370.
- Polyakov, I. V., A. V. Pnyushkov, M. B. Alkire, I. M. Ashik, T. M. Baumann, E. C. Carmack, I. Goszczko, J. Guthrie, V. V. Ivanov, T. Kanzow, et al. (2017), Greater role for Atlantic inflows on sea-ice loss in the Eurasian Basin of the Arctic Ocean, *Science*, *356*(6335), 285–291.
- Post, E., U. S. Bhatt, C. M. Bitz, J. F. Brodie, T. L. Fulton, M. Hebblewhite, J. Kerby, S. J. Kutz, I. Stirling, and D. A. Walker (2013), Ecological consequences of sea-ice decline, *Science*, *341*(6145), 519–524.
- Quadfasel, D., J.-C. Gascard, and K.-P. Koltermann (1987), Large-scale oceanography in Fram Strait during the 1984 Marginal Ice Zone Experiment, *J. Geophys. Res.*, *92*(C7), 6719–6728.
- Rampal, P., J. Weiss, and D. Marsan (2009), Positive trend in the mean speed and deformation rate of Arctic sea ice, 1979–2007, *J. Geophys. Res.*, *114*(C5), C05,013.

- Ricker, R., S. Hendricks, F. Girard-Arduin, L. Kaleschke, C. Lique, X. Tian-Kunze, M. Nicolaus, and T. Krumpfen (2017), Satellite-observed drop of Arctic sea ice growth in winter 2015–2016, *Geophys. Res. Lett.*, *44*(7), 3236–3245.
- Rigor, I. G., J. M. Wallace, and R. L. Colony (2002), Response of sea ice to the Arctic Oscillation, *J. Clim.*, *15*(18), 2648–2663.
- Rippeth, T. P., B. J. Lincoln, Y.-D. Lenn, J. M. Green, A. Sundfjord, and S. Bacon (2015), Tide-mediated warming of Arctic halocline by Atlantic heat fluxes over rough topography, *Nat. Geosci.*, *8*(3), 191.
- Rothrock, D. A., Y. Yu, and G. A. Maykut (1999), Thinning of the Arctic sea-ice cover, *Geophys. Res. Lett.*, *26*(23), 3469–3472.
- Rudels, B., E. Jones, L. Anderson, and G. Kattner (1994), On the intermediate depth waters of the Arctic Ocean, in *The Polar Oceans and Their Role in Shaping the Global Environment: The Nansen Centennial Volume*, pp. 33–46, edited by O. M. Johannessen, R. D. Muench, and J. E. Overland, AGU, Washington, D.C.
- Rudels, B., L. Anderson, and E. Jones (1996), Formation and evolution of the surface mixed layer and halocline of the Arctic Ocean, *J. Geophys. Res.*, *101*(C4), 8807–8821.
- Saloranta, T. M., and P. M. Haugan (2004), Northward cooling and freshening of the warm core of the West Spitsbergen Current, *Polar Res.*, *23*(1), 79–88.
- Schauer, U., E. Fahrbach, S. Osterhus, and G. Rohardt (2004), Arctic warming through the Fram Strait: Oceanic heat transport from 3 years of measurements, *J. Geophys. Res.*, *109*(C6), C06,026.
- Schauer, U., A. Beszczynska-Möller, W. Walczowski, E. Fahrbach, J. Piechura, E. Hansen, et al. (2008), *Variation of measured heat flow through the Fram Strait between 1997 and 2006*, chap. in *Arctic–Subarctic Ocean Fluxes: Defining the Role of the Northern Seas in Climate*, pp. 65–85, Springer, Dordrecht, Netherlands.
- Schlichtholz, P. (2011), Influence of oceanic heat variability on sea ice anomalies in the Nordic Seas, *Geophys. Res. Lett.*, *38*(5), L05,705.
- Schröder, D., D. L. Feltham, D. Flocco, and M. Tsamados (2014), September Arctic sea-ice minimum predicted by spring melt-pond fraction, *Nat. Clim. Change*, *4*(5), 353–357.
- Schrum, C., and J. O. Backhaus (1999), Sensitivity of atmosphere–ocean heat exchange and heat content in the North Sea and the Baltic Sea, *Tellus A*, *51*(4), 526–549.
- Schweiger, A., R. Lindsay, J. Zhang, M. Steele, H. Stern, and R. Kwok (2011), Uncertainty in modeled Arctic sea ice volume, *J. Geophys. Res.*, *116*(C8), C00D06.
- Screen, J. A. (2017), Simulated Atmospheric Response to Regional and Pan-Arctic Sea Ice Loss, *J. Clim.*, *30*, 3945–3962.
- Serreze, M. C., and R. G. Barry (2011), Processes and impacts of Arctic amplification: A research synthesis, *Global Planet. Change*, *77*(1), 85–96.

- Serreze, M. C., and J. Stroeve (2015), Arctic sea ice trends, variability and implications for seasonal ice forecasting, *Phil. Trans. R. Soc. A*, *373*(2045), 20140,159.
- Serreze, M. C., A. P. Barrett, A. G. Slater, R. A. Woodgate, K. Aagaard, R. B. Lammers, M. Steele, R. Moritz, M. Meredith, and C. M. Lee (2006), The large-scale freshwater cycle of the Arctic, *J. Geophys. Res.*, *111*(C11), C11,010.
- Serreze, M. C., M. M. Holland, and J. Stroeve (2007), Perspectives on the Arctic's shrinking sea-ice cover, *Science*, *315*(5818), 1533–1536.
- Serreze, M. C., A. D. Crawford, J. C. Stroeve, A. P. Barrett, and R. A. Woodgate (2016), Variability, trends, and predictability of seasonal sea ice retreat and advance in the Chukchi Sea, *J. Geophys. Res.*, *121*(10), 7308–7325.
- Sévellec, F., A. V. Fedorov, and W. Liu (2017), Arctic sea-ice decline weakens the Atlantic Meridional Overturning Circulation, *Nat. Clim. Change*, *7*(8), 604–610.
- Shimada, K., T. Kamoshida, M. Itoh, S. Nishino, E. Carmack, F. McLaughlin, S. Zimmermann, and A. Proshutinsky (2006), Pacific Ocean inflow: Influence on catastrophic reduction of sea ice cover in the Arctic Ocean, *Geophys. Res. Lett.*, *33*(8), L08,605.
- Sirevaag, A., and I. Fer (2009), Early spring oceanic heat fluxes and mixing observed from drift stations north of Svalbard, *J. Phys. Oceanogr.*, *39*(12), 3049–3069.
- Skagseth, Ø., T. Furevik, R. Ingvaldsen, H. Loeng, K. A. Mork, K. A. Orvik, and V. Ozhigin (2008), Volume and heat transports to the Arctic Ocean via the Norwegian and Barents Seas, in *Arctic–Subarctic Ocean Fluxes*, pp. 45–64, Springer.
- Smedsrud, L. H., I. Esau, R. B. Ingvaldsen, T. Eldevik, P. M. Haugan, C. Li, V. S. Lien, A. Olsen, A. M. Omar, O. H. Otterå, et al. (2013), The role of the Barents Sea in the Arctic climate system, *Rev. Geophys.*, *51*(3), 415–449.
- Smedsrud, L. H., M. H. Halvorsen, J. C. Stroeve, R. Zhang, and K. Kloster (2017), Fram Strait sea ice export variability and September Arctic sea ice extent over the last 80 years, *The Cryosphere*, *11*(1), 65–79.
- Smith, L. C., and S. R. Stephenson (2013), New Trans-Arctic shipping routes navigable by midcentury, *Proc. Nat. Acad. Sci.*, *110*(13), E1191–E1195.
- Sorokina, S. A., C. Li, J. J. Wettstein, and N. G. Kvamstø (2016), Observed atmospheric coupling between Barents Sea ice and the warm-Arctic cold-Siberian anomaly pattern, *J. Clim.*, *29*(2), 495–511.
- Spreen, G., R. Kwok, and D. Menemenlis (2011), Trends in Arctic sea ice drift and role of wind forcing: 1992–2009, *Geophys. Res. Lett.*, *38*(19), L19,501.
- Steele, M., and T. Boyd (1998), Retreat of the cold halocline layer in the Arctic Ocean, *J. Geophys. Res.*, *103*(C5), 10,419–10,435.
- Steele, M., and S. Dickinson (2016), The phenology of Arctic Ocean surface warming, *J. Geophys. Res.*, *121*(9), 6847–6861.

- Steele, M., W. Ermold, and J. Zhang (2008), Arctic Ocean surface warming trends over the past 100 years, *Geophys. Res. Lett.*, *35*(2), L02,614.
- Stroeve, J., M. M. Holland, W. Meier, T. Scambos, and M. Serreze (2007), Arctic sea ice decline: Faster than forecast, *Geophys. Res. Lett.*, *34*(9), L09,501.
- Stroeve, J., T. Markus, L. Boisvert, J. Miller, and A. Barrett (2014a), Changes in Arctic melt season and implications for sea ice loss, *Geophys. Res. Lett.*, *41*(4), 1216–1225.
- Stroeve, J., L. C. Hamilton, C. M. Bitz, and E. Blanchard-Wrigglesworth (2014b), Predicting September sea ice: Ensemble skill of the SEARCH Sea Ice Outlook 2008–2013, *Geophys. Res. Lett.*, *41*(7), 2411–2418.
- Stroeve, J. C., M. C. Serreze, M. M. Holland, J. E. Kay, J. Malanik, and A. P. Barrett (2012a), The Arctic’s rapidly shrinking sea ice cover: a research synthesis, *Clim. Change*, *110*(3), 1005–1027.
- Stroeve, J. C., V. Kattsov, A. Barrett, M. Serreze, T. Pavlova, M. Holland, and W. N. Meier (2012b), Trends in Arctic sea ice extent from CMIP5, CMIP3 and observations, *Geophys. Res. Lett.*, *39*(16), L16,502.
- Stroeve, J. C., J. R. Mioduszewski, A. Rennermalm, L. N. Boisvert, M. Tedesco, and D. Robinson (2017), Investigating the local scale influence of sea ice on Greenland surface melt, *The Cryosphere*, in press.
- Swart, N. C., J. C. Fyfe, E. Hawkins, J. E. Kay, and A. Jahn (2015), Influence of internal variability on Arctic sea-ice trends, *Nature Clim. Change*, *5*(2), 86–89.
- Taylor, K. E., R. J. Stouffer, and G. A. Meehl (2012), An overview of CMIP5 and the experiment design, *Bull. Amer. Meteor. Soc.*, *93*(4), 485–498.
- Thorndike, A., and R. Colony (1982), Sea ice motion in response to geostrophic winds, *J. Geophys. Res.*, *87*(C8), 5845–5852.
- Untersteiner, N. (1988), On the ice and heat balance in Fram Strait, *J. Geophys. Res.*, *93*(C1), 527–531.
- van Linschoten, J. (1601), Map of barentsz voyages, *Journal of Jan Huyghens van Linschoten*.
- Venegas, S. A., and L. A. Mysak (2000), Is there a dominant timescale of natural climate variability in the Arctic?, *J. Clim.*, *13*(19), 3412–3434.
- Vinje, T. (2001), Anomalies and trends of sea-ice extent and atmospheric circulation in the Nordic Seas during the period 1864–1998, *J. Clim.*, *14*(3), 255–267.
- Wadhams, P. (2000), *Ice in the Ocean*, Gordon and Breach Science Publishers, Cambridge.
- Walczowski, W., J. Piechura, R. Osinski, and P. Wiczorek (2005), The West Spitsbergen Current volume and heat transport from synoptic observations in summer, *Deep Sea Res.*, *52*(8), 1374–1391.

- Walsh, J. E., and C. M. Johnson (1979), An analysis of Arctic sea ice fluctuations, 1953–77, *J. Phys. Oceanogr.*, *9*(3), 580–591.
- Walsh, J. E., W. L. Chapman, and F. Fetterer (2015), Gridded Monthly Sea Ice Extent and Concentration, 1850 Onward, Version 1, Boulder, Colorado USA. NSIDC: National Snow and Ice Data Center. Digital media.
- Walsh, J. E., F. Fetterer, J. Scott Stewart, and W. L. Chapman (2017), A database for depicting Arctic sea ice variations back to 1850, *Geogr. Rev.*, *107*(1), 89–107.
- Woodgate, R. A., K. Aagaard, and T. J. Weingartner (2006), Interannual changes in the Bering Strait fluxes of volume, heat and freshwater between 1991 and 2004, *Geophys. Res. Lett.*, *33*(15), L15,609.
- Woodgate, R. A., T. Weingartner, and R. Lindsay (2010), The 2007 Bering Strait oceanic heat flux and anomalous Arctic sea-ice retreat, *Geophys. Res. Lett.*, *37*(1), L01,602.
- Yeager, S., and J. Robson (2017), Recent Progress in Understanding and Predicting Atlantic Decadal Climate Variability, *Curr. Clim. Change Rep.*, *3*(2), 112–127.
- Yeager, S. G., A. R. Karspeck, and G. Danabasoglu (2015), Predicted slowdown in the rate of Atlantic sea ice loss, *Geophys. Res. Lett.*, pp. 10,704–10,713.
- Zakharov, V. (1997), Sea ice in the climate system, *Tech. rep.*, World Climate Research Programme, Arctic Climate System Study, Geneva, Switzerland, wMO Tech. Doc. 782.
- Zhang, J., R. Lindsay, M. Steele, and A. Schweiger (2008), What drove the dramatic retreat of arctic sea ice during summer 2007?, *Geophys. Res. Lett.*, *35*(11), L11,505.
- Zhang, R. (2015), Mechanisms for low-frequency variability of summer Arctic sea ice extent, *Proc. Natl. Acad. Sci.*, *112*, 4570–4575.
- Zhang, X., and J. E. Walsh (2006), Toward a seasonally ice-covered Arctic Ocean: Scenarios from the IPCC AR4 model simulations, *J. Clim.*, *19*(9), 1730–1747.



## Paper I

### **Loss of sea ice during winter north of Svalbard**

Ingrid H. Onarheim, Lars H. Smedsrud, Randi B. Ingvaldsen, and Frank Nilsen  
*Tellus A*, 66, 23933 (2014)



# Loss of sea ice during winter north of Svalbard

By INGRID H. ONARHEIM<sup>1,2\*</sup>, LARS H. SMEDSRUD<sup>1,2,3</sup>, RANDI B. INGVALDSEN<sup>4</sup> and FRANK NILSEN<sup>3,1</sup>, <sup>1</sup>*Geophysical Institute, University of Bergen, Bergen, Norway*; <sup>2</sup>*Bjerknes Centre for Climate Research, Bergen, Norway*; <sup>3</sup>*University Centre in Svalbard, Longyearbyen, Norway*; <sup>4</sup>*Institute of Marine Research, Bergen, Norway*

(Manuscript received 29 January 2014; in final form 6 May 2014)

## ABSTRACT

Sea ice loss in the Arctic Ocean has up to now been strongest during summer. In contrast, the sea ice concentration north of Svalbard has experienced a larger decline during winter since 1979. The trend in winter ice area loss is close to 10% per decade, and concurrent with a 0.3°C per decade warming of the Atlantic Water entering the Arctic Ocean in this region. Simultaneously, there has been a 2°C per decade warming of winter mean surface air temperature north of Svalbard, which is 20–45% higher than observations on the west coast. Generally, the ice edge north of Svalbard has retreated towards the northeast, along the Atlantic Water pathway. By making reasonable assumptions about the Atlantic Water volume and associated heat transport, we show that the extra oceanic heat brought into the region is likely to have caused the sea ice loss. The reduced sea ice cover leads to more oceanic heat transferred to the atmosphere, suggesting that part of the atmospheric warming is driven by larger open water area. In contrast to significant trends in sea ice concentration, Atlantic Water temperature and air temperature, there is no significant temporal trend in the local winds. Thus, winds have not caused the long-term warming or sea ice loss. However, the dominant winds transport sea ice from the Arctic Ocean into the region north of Svalbard, and the local wind has influence on the year-to-year variability of the ice concentration, which correlates with surface air temperatures, ocean temperatures, as well as the local wind.

*Keywords:* Sea ice, Atlantic Water, Svalbard, heat transport, air–ice–sea interactions

## 1. Introduction

Loss of Arctic sea ice remains one of the most visible signs of present and future global warming. The ice loss is now visible for all months and in all regions, but varies substantially between regions and time of year. Within the Arctic Ocean, the ice area decline has been largest during summer (Comiso, 2012). Despite a small recovery during summer 2013, the current September trend stands at –13.7% per decade (NSIDC).

To understand the different forcings that contribute to the loss of Arctic sea ice, it is important to study loss of sea ice in different regions, because several factors likely have contributed differently in each region. Sea ice responds to changes in heating or cooling reaching the surface layer, both from above and below. Heat is transported towards the Arctic with the atmosphere and the ocean, and in general,

the Arctic air column is losing heat to space through outgoing longwave radiation.

Here we focus on the Whaler's Bay area north of Svalbard (black box in Fig. 1), the area where the warmest Atlantic Water (AW) inflow to the Arctic Ocean occurs. Aagaard et al. (1987), Saloranta and Haugan (2004), and Cokelet et al. (2008) estimated an ocean-to-air heat loss of 200–500 W/m<sup>2</sup> in this region, and stated that mixing between AW and colder ambient waters has provided sufficient oceanic heat to keep Whaler's Bay ice-free. Whaler's Bay is a prominent year-round polynya, and the AW heat may both prevent ice freezing during winter and melt the ice cover from below. Intense heat loss from the open ocean north of Svalbard modifies some of the AW by transforming it into Arctic intermediate water (Aagaard et al., 1987). How far into the Arctic Ocean the AW loses heat to the air, and how efficient the vertical mixing in this area is, are presently under discussion.

In this study we discuss the sea ice variability north of Svalbard and suggest possible drivers of the observed local ice area loss since 1979. The results indicate the

\*Corresponding author.  
email: Ingrid.Onarheim@gfi.uib.no

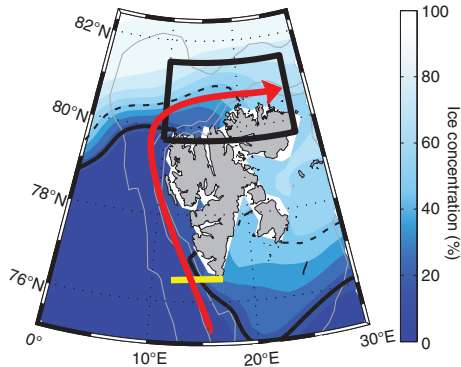


*Fig. 1.* Mean ice concentration field from 1979 to 2012, including the ice edge (15% ice concentration, solid black) and the mean ice concentration in the study region (48%, dashed black). The black box shows the study region north of Svalbard. The position of the West Spitsbergen Current (WSC) temperature measurements at Sørkapp is indicated in yellow, while the red arrow indicates the pathway of the Svalbard Branch of the WSC. The bathymetry is drawn as thin grey lines.

AW warming as the main driver of the ice loss and as an important contributor to the atmospheric warming in the region. A sketch of the main processes occurring as the inflowing AW cools and meets the ice, driven in the opposite direction by winds, is shown in Fig. 2. In general, the winds bring along atmospheric air masses, so a wind from the north transports colder air towards Svalbard. Northerly winds also advect more ice from the transpolar drift stream into the region north of Svalbard. Presence of sea ice isolates the colder air, and contributes to colder air temperatures. Further, the wind could drive upwelling of AW along the Svalbard coast (Lind and Ingvaldsen, 2012). However, enhanced ice melt due to warmer AW creates a more stable freshwater layer underneath the ice, reducing further ice melt. According to Untersteiner (1988), the AW heat loss is sufficient to melt the advancing ice, maintaining the mean annual ice boundary at about 80°N.

## 2. Data and methods

In this work, we focus on the AW inflow region, so the datasets are bounded to the south by 79.7°N, to the north by 81.5°N, and lie within the zonal band 10–27°E ( $\sim 60\,000\text{ km}^2$ ) (Fig. 1). The datasets cover the years 1979–2012. Winter [December–March (DJFM)] and summer [June–September (JJAS)] means are calculated to describe the variability. Trends are estimated using linear least-squares regression, while two-sided *t*-tests are used to find significant levels for

trends and correlations. Long-term trends in the datasets can increase the correlation coefficients, and moreover reduce the degrees of freedom. Quenouille (1952) defined the effective number of observations as:

$$n_{\text{eff}} = \frac{n}{1 + 2(r_1 r'_1 + r_2 r'_2 + \dots + r_n r'_n)}, \quad (1)$$

where  $n$  is the sample size,  $r_1$  and  $r'_1$  are the lag-1 autocorrelations of the two time series,  $r_2$  and  $r'_2$  are the lag-2 autocorrelations, and so on. To account for trends, we use the effective number of observations when estimating significant levels.

### 2.1. Sea ice

Daily averaged sea ice concentrations (percentage of ocean area covered by sea ice) are derived from passive microwave remote sensing data, using the NASA Team algorithm, from the Nimbus-7 Scanning Multichannel Microwave Radiometer (SMMR) and the Defense Meteorological Satellite Program (DMSP) Special Sensor Microwave/Imager (SSM/I), provided by the National Snow and Ice Data Center (NSIDC). Cavalieri et al. (1996) and references therein described the methods used to generate a consistent dataset from brightness temperature from the sensors. The dataset, with a resolution of  $25\text{ km} \times 25\text{ km}$ , is spatially averaged over the study region north of Svalbard.

### 2.2. Atmospheric data

Daily atmospheric data are obtained from ERA-Interim reanalysis produced by the European Centre for Medium-Range Weather Forecasts (ECMWF). See Dee et al. (2011) and references therein for a detailed description of the reanalysis. Data of air temperature at 2 m height and wind at 10 m height are obtained at 12:00 UTC. The datasets have a spatial resolution of  $0.75^\circ \times 0.75^\circ$  and are spatially averaged over the region north of Svalbard. Moreover, surface latent heat flux, surface sensible heat flux and surface net thermal radiation in the study region north of Svalbard and in an area west of Svalbard (5–15°E, 76–80°N) are reviewed.

### 2.3. AW temperature

AW temperature of the West Spitsbergen Current (WSC) westward from Sørkapp (Fig. 1) has been measured annually since 1977 by the Norwegian Institute of Marine Research. The results are based on data from the upper 50–200 m of a hydrographic section observed in autumn season (August–October). See Lind and Ingvaldsen (2012) for a more detailed description of the dataset. Missing data in 2003 and 2011 are linearly interpolated.

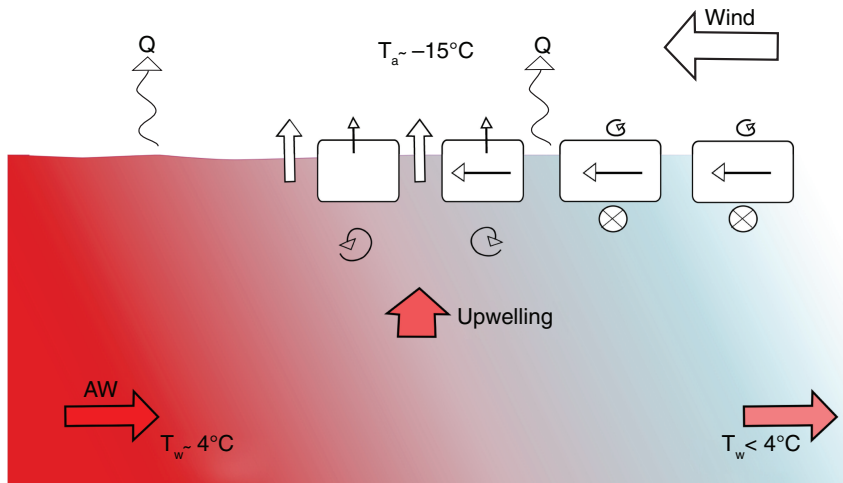


Fig. 2. Schematic of air-ice-sea interactions north of Svalbard. Northerly winds transport sea ice from the Arctic Ocean (slightly deflected to the right) and bring cold air masses, facilitating larger ice cover. Upwelling of warm Atlantic Water (AW, reddish) melts the approaching sea ice, and a fresh, cold layer forms below the ice (bluish). Depending on the vertical mixing below the ice, the freshwater layer reduces further ice melt. The large ocean-to-atmosphere heat flux,  $Q$ , is strongly reduced by the presence of sea ice. In winter,  $Q$  is the sum of net longwave radiation, latent heat and sensible heat. Excess heat is lost to space through longwave radiation.  $T_a$ : air temperature, and  $T_w$ : water temperature.

The AW temperature observations at Sørkapp are about 500 km upstream of our study region north of Svalbard (Fig. 1). Hence, the temperature observations are independent of the sea ice cover, wind and air temperature variability north of Svalbard. With a mean speed of  $10 \text{ cm s}^{-1}$ , the water at Sørkapp needs near two months to reach the study region, delaying the influence from the AW. Saloranta and Haugan (2001) showed coherent variations at 100–300 m depth near  $76^\circ\text{N}$  and  $80^\circ\text{N}$  during the 1980s and 1990s. For the analyses, AW temperature at Sørkapp in autumn is related to ice concentration north of Svalbard the following winter (i.e. AW temperature in autumn 1999 is compared to the ice concentration mean from December 1999 through March 2000). Hence ice concentration, wind and air temperature are lagging AW temperature by a few months for all analyses.

### 3. Results

The study region north of Svalbard (black box in Fig. 1) has an annual mean ice concentration of 48% between 1979 and 2012. Ice is present in all months with minimum ice concentration in September (Fig. 3). Largest ice cover is generally reached in April. The mean ice con-

centration field around Svalbard indicates the ice edge (15% ice concentration) near  $80^\circ\text{N}$  west of Svalbard (Fig. 1).

During the last three decades, the sea ice concentration has decreased north of Svalbard (Fig. 4), with record low annual minimum in 2012 (not shown). All months experience an ice loss, with largest negative trends in December, February and January, respectively (Fig. 3). The resulting winter (DJFM) ice loss is 10% per decade. August and September demonstrate the smallest reductions. The summer ice cover (JJAS) experiences an ice loss of 6% per decade and increased interannual variability since 1995 (Fig. 4b).

The spatial winter ice loss north of Svalbard since the 1980s illustrates an ice retreat above the pathway of the AW (Fig. 5). Lower ice concentrations are gradually moving northeastward along Svalbard's northern coast. In 2012, the winter averaged 40% ice concentration contour line reaches almost  $82^\circ\text{N}$  east of our study region, reflecting the second lowest winter ice minimum. Also the winter ice edge (15% ice concentration) has gradually shifted northeastward, retreating about  $5^\circ$  eastward and  $0.5^\circ$  northward since 1979 (not shown).

Time series of winter mean ice concentration, AW temperature, air temperature, north-south wind and east-west wind from 1979 to 2012 are shown in Fig. 6. Concurrent with

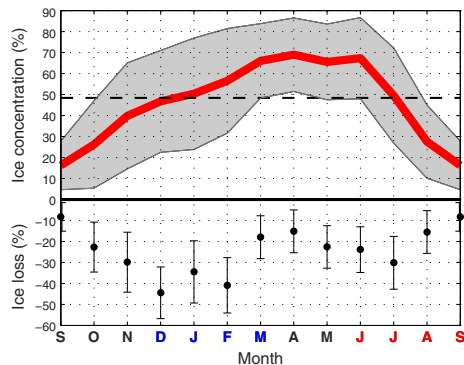


Fig. 3. Upper: Monthly averaged satellite-observed sea ice concentration (red line, September to September) including the standard deviation (grey region). The dashed line shows the annual mean ice concentration. Lower: The total 1979–2012 ice concentration reduction for each month is shown as black dots, with error bars indicating the 95% confidence intervals.

reduced ice concentrations, Fig. 6b indicates an overall AW warming of  $1.1^{\circ}\text{C}$  since 1979. Moreover, the winter mean air temperature is rising by  $6.9^{\circ}\text{C}$  during the last 34 yr (Fig. 6c). These trends are significant on the 95% level. The air temperature shows large interannual variability concurrent with the variations in ice concentration. Easterly–northeasterly winds dominate north of Svalbard, however, with strong year-to-year variations (Fig. 6d and e). Slightly stronger northerly winds have apparently been simulated since 1979; however, the trends in winds are too small to be significant.

In order to find the main drivers of the winter sea ice variability, multivariate regression analyses were performed by analysing detrended and standardised AW temperature and north–south wind. Air temperature was not used due to the strong coupling between air temperature and ice concentration. Higher air temperatures cause less ice freezing, while presence of ice cover has a strong impact on air temperatures. Hence, we cannot differentiate between the predictor and the responder. The ice concentration regression based on AW temperature and north–south wind explains 32% of the variability in the satellite-derived ice concentration, suggesting that winter ice concentration variability on annual time scales is partly driven by variations in AW temperature and north–south wind. The east–west wind component was also tested, but did not increase the overall fit. EOF analyses of detrended and standardised values indicate that 58% of the combined variability (EOF1) is associated with high AW temperatures, high air temperatures, wind from the south and low ice concentrations (not shown).

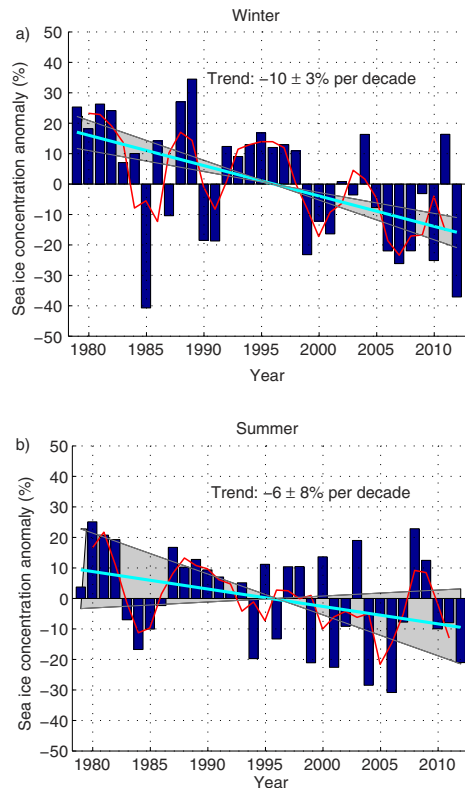


Fig. 4. Satellite-derived sea ice concentration anomalies north of Svalbard, 1979–2012. Dark blue is winter (a) and summer (b) means; and red shows the 3 yr running mean. The zero line represents the winter (56%) and summer (40%) 1979–2012 average. Linear trends are shown in light blue, and the shaded areas indicate the 95% confidence interval for the trend estimates.

#### 4. Discussion

Concurrent with reduced ice concentrations in the area north of Svalbard, the AW and atmosphere have warmed over the last three decades. Despite the large air temperature rise of  $6.9^{\circ}\text{C}$  (Fig. 6c), the air temperature remains well below freezing during winter. Thus, higher air temperatures will have caused reduced ice freezing rather than enhanced ice melt. With wind-driven ice transport from the Arctic Ocean and strong direct interactions between AW and sea ice north of Svalbard, the early winter sea ice concentration can be described in terms of ocean temperature and north–south wind ( $r = 0.56$ ). Combinations of warm AW, high air

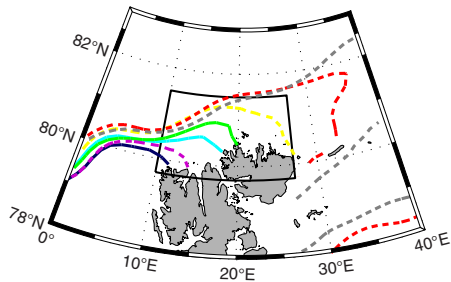


Fig. 5. Contour lines of the 40% winter (DJFM) ice concentration north of Svalbard during the 1980s (dark blue), 1990s (light blue), and 2000s (green). The most recent winters are also included with dashed lines (2010: yellow, 2011: purple, and 2012: red). In addition, February 2012 is shown in grey (dashed) to indicate a period with especially low ice concentrations, and ice-free areas extending towards Franz Josef Land. The black box indicates the study region.

temperatures and wind from the south are associated with reduced ice concentration north of Svalbard. The opposite is also true, cold AW and air temperatures, and stronger winds from the north, tend to increase the ice concentration. Onwards we discuss the influence of AW temperature, air temperature and wind on the reduced ice cover north of Svalbard, with the aim to explain the changes that have occurred.

Detrended winter ice concentration correlates significantly with north–south wind and air temperature (Table 1), suggesting large atmospheric influence on interannual variations in ice concentration. Northerly winds increase the ice concentration directly by transporting ice from the Arctic Ocean towards Svalbard, and indirectly by bringing colder air masses, enhancing ice freezing. Table 1 also shows significant correlation between detrended north–south wind and air temperature ( $r = 0.51$ ), suggesting that atmospheric circulation affects variations in winter air temperature on an interannual basis.

When it comes to the atmospheric trends, there is no statistically significant trend in the winds. Thus the significant negative trend in ice concentration since 1979 cannot be driven by the winds. The strong air temperature rise of  $6.9^{\circ}\text{C}$  over the 34-yr study period corresponds to a linear temperature trend of  $2^{\circ}\text{C}$  per decade. This trend is 20–45% larger than the trends observed for almost the same time span (1975–2011) at comparable sites further south [Ny-Ålesund  $1.36^{\circ}\text{C}$  per decade, and Svalbard Airport  $1.66^{\circ}\text{C}$  per decade (Førland et al., 2011)]. Because surface air temperature is closely coupled to the ice cover, we proceed to the other possible driver of the changes in ice concentration, the AW.

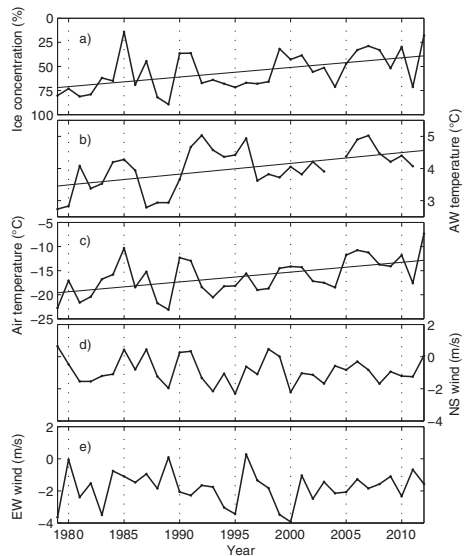


Fig. 6. Winter (DJFM) averaged sea ice concentration (a), AW temperature (b), air temperature (c), north–south wind component (positive from the south) (d), and east–west wind component (positive from the west) (e), 1979–2012. Note that the ice concentration (a) is inverted. Statistical significant linear trends (95%) are indicated by straight lines.

Increased heat transport by the WSC to our region increases the reservoir of heat below the sea ice, and given that vertical mixing is not a limiting factor, the ice cover experiences enhanced bottom melt and reduced ice formation. Increased AW heat transport in recent years with both warmer water and stronger flow, was discussed by Beszczynska-Möller et al. (2012), Piechura and Walczowski (2009) and Polyakov et al. (2012a). Model studies of the AW heat transport and bottom melting in the Arctic Ocean suggest that periods of increased heat transport lead to enhanced bottom melting (Alexeev et al., 2013; Sandø et al., 2014). Here, we only consider AW temperature, because there is no available current meter record before the 1990s.

AW temperature and ice concentration correlate with  $r = -0.20$  when the trends are removed. However, if the trends are maintained, the correlation increases to  $r = -0.41$  (Table 1). This may imply slow oscillations in AW temperature that last longer than the 34-yr long time series, or just a general linear warming. Such long-term oscillations in AW transport are documented in the Barents Sea where time series longer than 100 yr are available (Smedsrud et al., 2013). How much of an impact could a  $\sim 1^{\circ}\text{C}$  ocean warming have on the sea ice cover and the

Table 1. Correlations between winter (DJFM) means

	Ice	v	AW	T <sub>a</sub>	u
Ice	—	<b>-0.50</b>	-0.20	<b>-0.90</b>	0.11
v	<i>-0.37</i>	—	-0.13	<b>0.51</b>	0.06
AW	<i>-0.41</i>	<i>-0.17</i>	—	0.27	-0.05
T <sub>a</sub>	<b>-0.92</b>	<b>0.36</b>	<b>0.47</b>	—	0.03
u	<i>0.09</i>	<i>0.05</i>	<i>-0.03</i>	<i>0.04</i>	—

The upper right triangle (roman) represents correlations between detrended time series, while the lower left triangle (italic) shows correlations including trends. Significant correlations within a 95% confidence level are marked with boldface. Ice: ice concentration, v: north-south wind, AW: Atlantic Water temperature, T<sub>a</sub>: air temperature, u: east-west wind.

atmosphere above? To answer that question we estimate some related heat budgets, and find that although AW temperature may not have a strong impact on interannual variations in ice concentration, the AW warming could drive the ice loss as well as the atmospheric warming in our region.

The heat capacity of the ocean is much larger than that of the air. To compare the two observed temperature trends, we first calculate the change in heat content of a column of water or air:

$$\Delta Q = cm\Delta T, \quad (2)$$

where  $\Delta Q$  is a change in heat content ( $\text{J m}^{-2}$ ),  $c$  is heat capacity ( $\text{J kg}^{-1} \text{K}^{-1}$ ),  $m$  is mass ( $\text{kg m}^{-2}$ ) and  $\Delta T$  is a change in temperature. Assuming an atmospheric boundary layer height of 800 m, the atmospheric warming of  $6.9^\circ\text{C}$  increases the atmospheric heat content by  $7.7 \times 10^6 \text{ J m}^{-2}$ . A similar increase in heat content in the ocean can be achieved by an AW warming of  $0.03^\circ\text{C}$  in the upper 50 m of the ocean. Hence, an ocean warming of  $1^\circ\text{C}$  contains several orders of magnitude more heat ( $\text{J m}^{-2}$ ) than the observed atmospheric warming.

Assuming a steady AW transport of 3 Sv ( $\text{Sv} \equiv 1 \times 10^6 \text{ m}^3 \text{ s}^{-1}$ ) (Beszczynska-Möller et al., 2012), the inflowing and exiting temperatures of the AW determine the heat transport. The time series in Fig. 6b shows the observed changes in inflow temperature, and we first use a representative AW temperature for around 1980 of  $3.0^\circ\text{C}$ . The AW temperature decreases along the WSC, and at 800 km downflow, at the eastern end of our area, the temperature has decreased to about  $1.5^\circ\text{C}$  (Cokelet et al., 2008). Based on the heat conservation equation at stationary conditions,

$$Q = c\rho V\Delta T, \quad (3)$$

where  $Q$  is the heat (W),  $\rho$  is the density of seawater ( $\text{kg m}^{-3}$ ) and  $V$  is the volume transport (Sv), the estimated current in 1980 would result in a heat transport of 36 TW at Sørkapp. Assuming an outflow temperature of  $1.5^\circ\text{C}$  (following Cokelet et al. [2008]), 50% of the heat would continue further into the Arctic Ocean. Unknown portions would go directly to the air before the AW reaches the ice-covered areas, to lateral mixing, and to melting of sea ice in

our area. The winter mean ice concentration at the time was 75% (Fig. 6) and the atmospheric temperature was  $-20^\circ\text{C}$ , implying a mean surface outgoing longwave radiation flux of  $232 \text{ W m}^{-2}$  during winter.

In contrast to the situation in 1980, we know that the AW inflow temperature has increased with  $1.0^\circ\text{C}$  up to 2010, and that the ice concentration dropped to about 40%. A  $1^\circ\text{C}$  warming at Sørkapp implies an enhanced northward heat transport of 12 TW, assuming a constant AW flow. Unfortunately, there are no long-term observations of changes in outflow AW temperature. However, by comparing 1990–1995 observations with Russian climatologies, Grotedefndt et al. (1998) described a  $\sim 0.5^\circ\text{C}$  warming of the AW temperature at 500 m depth east of our area. Therefore, we assume that half of the extra heat due to the AW warming at Sørkapp carries on with the AW flow inside the Arctic Ocean, while 25% (3 TW) is available for melting sea ice, and the last 25% warm the air directly. This is consistent with assuming a change in outflow temperature from  $1.5^\circ\text{C}$  in 1980, to  $2.0^\circ\text{C}$  in 2010. During winter, a mean surface outgoing longwave radiation flux from the  $-13^\circ\text{C}$  surface would be  $259 \text{ W m}^{-2}$ , that is,  $27 \text{ W m}^{-2}$  larger than in 1980. This compares to 1.6 TW over our area ( $\sim 60000 \text{ km}^2$ ), stating that a substantial part of the overall available extra heat, but not all, has reached the atmospheric boundary layer.

A rough estimate of atmospheric heat fluxes supports our assumptions concerning the heat budgets. ERA-Interim reanalysis indicates a slight increase in surface sensible heat flux, surface latent heat flux and surface net longwave radiation (outgoing fluxes) in the area north of Svalbard between 1979 and 2012 (not shown). Increased upward heat fluxes are also found above the WSC west of Spitsbergen ( $5\text{--}15^\circ\text{E}$ ,  $76\text{--}80^\circ\text{N}$ ) (not shown). The reanalysis shows an increased upward heat flux of about 2 TW over the 1979–2012 period between Sørkapp and the outflow of our study region. This indicates that some heat is lost to the atmosphere, while most of the extra heat likely has contributed to melting of sea ice and warming of ambient waters.

Most of the ice reduction in the area around Svalbard has occurred in the study region north of Svalbard (Fig. 5).

In our region, the ice cover has been reduced by 15 000 km<sup>2</sup> since 1979. An estimate of the heat needed to melt  $H$  meters of sea ice can be calculated using:

$$Q = H\rho_i L, \quad (4)$$

where  $Q$  is the energy needed (J m<sup>-2</sup>),  $\rho_i$  is ice density (kg m<sup>-3</sup>) and  $L$  is latent heat of fusion (J kg<sup>-1</sup>). Assuming that the extra available AW heat of 3 TW reaches the ice and is equally distributed over the study region, 2 m thick ice would melt in about four and a half months. However, with a winter mean ice concentration of 56%, ice-free waters may be reached faster.

The estimated available AW heat is thus clearly enough to cause the observed sea ice loss north of Svalbard, and the main winter ice loss above the core of the AW north of Svalbard suggests that the warm AW has reached the sea ice. Although increasing ice melt creates a more stable freshwater layer between the salty AW ( $S \sim 35$ ) and the fresh sea ice melt, local wind mixing can provide energy for transfer of heat from the AW to the upper layer and consequently to ice melt and to the atmosphere (Rudels, 2012). The monthly mean sea ice advection speed during winter in our area is 2–6 cm/s (<ftp://sidads.colorado.edu/pub/DATASETS/nsidc0116icemotionvectorsv2/browse/north/months/>), suggesting a transit time of about 1–4 months. This means that the thickness of the entering sea ice is important, and may suggest that residence time above the AW is a more limiting factor than the available heat.

As the AW temperature is measured at Sørkapp, ~500 km upstream, it is independent of the air temperature rise and ice concentration loss north of Svalbard. An ocean-driven ice loss north of Svalbard would, however, result in stronger ocean-to-atmosphere heat fluxes locally. This is consistent with Polyakov et al. (2012b) who stated that local atmospheric warming over areas of ice loss is a response to, rather than a driver of, the declining ice cover. Our results indicate that part of the air temperature increase has been caused locally by the ice loss. Assuming an ocean-to-atmosphere open water mean winter heat flux of 200 W m<sup>-2</sup> (Smedsrud et al., 2013), the increased heat flux to the atmosphere caused by the extra 15 000 km<sup>2</sup> of open water (ice loss), would give an extra heating of 3 TW. This suggests that ~50% of the heat lost to the atmospheric boundary layer is lost through longwave radiation as calculated above (1.6 TW), and that the other half has been transported out of the region by atmospheric circulation. The ice loss above the AW pathway is therefore likely a driver of the atmospheric warming, and not vice versa. Climate projections indicate a substantial air temperature warming northeast of Svalbard due to reduced sea ice coverage (Førland et al., 2009).

Another indication of warm water as a major contributor to the ice loss is the large winter ice reduction, in contrast to

the Arctic Ocean summer ice loss. With winter air temperatures well below freezing, the AW is the only heat source in the area north of Svalbard (Rudels, 2010), and largest AW influence is expected during winter. During summer other factors probably contribute more to the observed ice loss.

Warmer surface waters cause delayed ice formation and consequently lower ice concentrations in early winter. Our results agree with findings by Årthun et al. (2012) who compared observations and simulations for reductions in the Barents Sea winter ice cover due to increased AW heat transport. According to Årthun et al. (2012), an increase in AW heat transport to the Barents Sea of 10 TW has resulted in an ice reduction of 70 000 km<sup>2</sup>. Based on these values the estimated extra oceanic heat transport to our area (3 TW) would potentially cause an ice reduction of 21 000 km<sup>2</sup>. This is 40% larger than the observed loss in our area. The ice would be thicker in our area, and more ice would be formed elsewhere and transported in, so this could explain the different response. Ivanov et al. (2012) described a winter ice loss in the Western Nansen Basin, and observed a thinner and less extensive ice cover above the pathway of the AW there. They thus suggested an influence from the warmer AW on the winter ice reduction in that region, consistent with our results.

As the Arctic and the rest of the globe continue to warm, and the ice cover continues to decrease, a number of key elements remain almost unobserved. We have documented the warming in both the atmosphere and the ocean, and the decline in ice concentration since 1979, but we are lacking comparable time series for changes in AW volume transport, sea ice thickness and vertical mixing. Clearly the sea ice is probably thinner north of Svalbard now than in the 1980s, but the longest observational record of ice thickness started first in 1990 (Hansen et al., 2013), and covers the western side of Fram Strait. A response in sea ice concentration will only occur when the sea ice has thinned considerably, and might explain parts of the 'missing response' to the initial rise in AW temperature around 1990 (Fig. 6b).

Proper observations of ocean volume transport started in 1997 (Schauer and Beszczynska-Möller, 2009). Variations in volume transport before this time, and also how the total transport is distributed within the Arctic Ocean, remain unknown. The peak in total heat transport in 2004 seems to lead that of the temperature maximum occurring in 2006 (Schauer and Beszczynska-Möller, 2009). For ocean mixing in the Arctic, only snapshots in temporal and spatial coverage are available (Rainville and Winsor, 2008; Sirevaag and Fer, 2009). Any long-term changes, as well as a reasonable climatic annual mean for the region north of Svalbard, are not available.

The long-term prospects for Arctic sea ice are bad, especially for the summer ice. The large loss of the winter ice north of Svalbard is not typical for other regions inside

the Arctic Ocean, but more in line with the ongoing changes in the Barents Sea over the last decades (Årthun et al., 2012). Now that the AW heat transport seems to have reached an all-time high value in 2004, a recovery of the winter ice could actually be expected over the next 10 yr. On the other hand, the sea ice is thinner, and vertical mixing could increase due to the reduced ice cover. It thus appears more difficult than ever to come up with future predictions.

## 5. Summary

Satellite observations north of Svalbard demonstrate reduced ice concentrations between 1979 and 2012. In contrast to other areas of the Arctic Ocean, the largest ice loss has occurred during winter with  $\sim 10\%$  loss per decade. The summer ice loss trend is about half of the winter trend. Over the same period, the AW temperature has increased  $\sim 1^\circ\text{C}$  and the regional winter air temperature has increased  $\sim 7^\circ\text{C}$ , but there is no significant trend in the local wind.

Year-to-year ice variability is substantial, with winter means ranging between 15% and 90%. Although the winds apparently do not have impact on the trends, they have significant impact on the year-to-year variability. Low anomalies in sea ice concentration are consistently associated with winds from the south (less wind from the north), warmer air and higher AW temperatures.

The shrinking winter ice cover above the core of the AW indicates a direct influence from the AW on the ice conditions. Analytical estimates assuming constant volume flow and that  $\sim 25\%$  of the heat transport reaches the ice-covered surface, indicate that the warmer AW has been a major driver of the ice reduction. Temporal changes in the vertical mixing of AW heat towards the ice, and long-term changes in sea ice thickness remain unknown, but may have played a significant role in the observed changes.

The decadal air temperature trend in our region is 20–45% higher than further south. This indicates that the local warming is forced by the increased oceanic heat transport, which has caused more open water and larger ocean-to-atmosphere heat fluxes. Because winter mean atmospheric temperature is still  $\sim -10^\circ\text{C}$ , the atmospheric warming would not lead to ice melting, but to reduced local ice growth.

## 6. Acknowledgements

This work was funded by the Centre for Climate Dynamics at the Bjerknes Centre through the Fast-Track Initiative grant. We thank Igor Polyakov and Asgeir Sorteberg for constructive and helpful comments that improved our manuscript.

## References

- Aagaard, K., Foldvik, A. and Hillman, S. R. 1987. The West Spitsbergen Current: disposition and water mass transformation. *J. Geophys. Res.* **92**, 3778–3784.
- Alexeev, V. A., Ivanov, V. V., Kwok, R. and Smedsrud, L. H. 2013. North Atlantic warming and declining volume of Arctic sea ice. *The Cryosphere Discuss.* **7**, 245–265.
- Årthun, M., Eldevik, T., Smedsrud, L. H., Skagseth, Ø. and Ingvaldsen, R. B. 2012. Quantifying the influence of Atlantic heat on Barents Sea ice variability and retreat. *J. Climate.* **25**, 4736–4743.
- Beszczyńska-Möller, A., Fahrback, E., Schauer, U. and Hansen, E. 2012. Variability in Atlantic water temperature and transport at the entrance to the Arctic Ocean, 1997–2010. *ICES J. Mar. Sci.* **69**, 852–863.
- Cavaleri, D., Parkinson, C., Gloersen, P. and Zwally, H. J. 1996. *Sea Ice Concentrations from Nimbus-7 SMMR and DMSP SSM/I Passive Microwave Data*. Digital media, Boulder, Colorado USA: National Snow and Ice Data Center. Online at: <http://nsidc.org/data/nsidc-0051.html>
- Cokelet, E., Tervalon, N. and Bellingham, J. 2008. Hydrography of the West Spitsbergen Current, Svalbard Branch: Autumn 2001. *J. Geophys. Res.* **113**, C01006.
- Comiso, J. C. 2012. Large decadal decline of the Arctic multiyear ice cover. *J. Climate.* **25**, 1176–1193.
- Dee, D. P., Uppala, S. M., Simmons, A. J., Berrisford, P., Poli, P. and co-authors. 2011. The ERA-Interim reanalysis: configuration and performance of the data assimilation system. *Q.J.R. Meteorol. Soc.* **137**, 553–597.
- Førland, E. J., Benestad, R. E., Flatoy, F., Hanssen-Bauer, I., Haugen, J. E. and co-authors. 2009. *Climate development in North Norway and the Svalbard region during 1900–2100. Technical Report*, Norwegian Polar Institute, Tromsø.
- Førland, E. J., Benestad, R., Hanssen-Bauer, I., Haugen, J. E. and Skaugen, T. E. 2011. Temperature and precipitation development at Svalbard 1900–2100. *Adv. Meteorol.* **2011**, 14 pp.
- Grotefendt, K., Logemann, K., Quadfasel, D. and Ronski, S. 1998. Is the Arctic Ocean warming? *J. Geophys. Res.* **103**, 27679–27687.
- Hansen, E., Gerland, S., Granskog, M. A., Pavlova, O., Renner, A. H. H. and co-authors. 2013. Thinning of Arctic sea ice observed in Fram Strait: 1990–2011. *J. Geophys. Res.* **118**, 5202–5221.
- Ivanov, V. V., Alexeev, V. A., Repina, I., Koldunov, N. V. and Smirnov, A. 2012. Tracing Atlantic Water signature in the Arctic sea ice cover east of Svalbard. *Adv. Meteorol.* **2012**, 11.
- Lind, S. and Ingvaldsen, R. B. 2012. Variability and impacts of Atlantic water entering the Barents Sea from the north. *Deep Sea Res. Part I.* **62**, 70–88.
- NSIDC (2013, October). A better year for the cryosphere. Beitler, J. Online at: <http://nsidc.org/arcticseaicenews/2013/10/a-better-year-for-the-cryosphere/>
- Piechura, J. and Walczowski, W. 2009. Warming of the West Spitsbergen Current and sea ice north of Svalbard. *Oceanologia.* **51**, 147–164.
- Polyakov, I. V., Pnyshkov, A. V. and Timokhov, L. A. 2012a. Warming of the Intermediate Atlantic Water of the Arctic Ocean in the 2000s. *J. Climate.* **25**, 8362–8370.

- Polyakov, I. V., Walsh, J. E. and Kwok, R. 2012b. Recent changes of Arctic multiyear sea ice coverage and the likely causes. *Bull. Amer. Meteor. Soc.* **93**, 145–151.
- Quenouille, M. H. 1952. *Associated Measurements*. Butterworths Scientific, London, UK, 242 pp.
- Rainville, L. and Winsor, P. 2008. Mixing across the Arctic Ocean: microstructure observations during the Beringia 2005 expedition. *Geophys. Res. Lett.* **35**, L08606.
- Rudels, B. 2010. Constraints on exchanges in the Arctic Mediterranean – do they exist and can they be of use? *Tellus A.* **62**, 109–122.
- Rudels, B. 2012. Arctic Ocean circulation and variability – advection and external forcing encounter constraints and local processes. *Ocean Sci.* **8**, 261–286.
- Saloranta, T. M. and Haugan, P. M. 2001. Interannual variability in the hydrography of Atlantic water northwest of Svalbard. *J. Geophys. Res.* **106**, 13931–13943.
- Saloranta, T. M. and Haugan, P. M. 2004. Northward cooling and freshening of the warm core of the West Spitsbergen Current. *Polar Res.* **23**, 79–88.
- Sando, A. B., Gao, Y. and Langehaug, H. R. 2014. Poleward ocean heat transports, sea ice processes, and Arctic sea ice variability in NorESM1-M simulations. *J. Geophys. Res.* **119**, 2095–2108.
- Schauer, U. and Beszczynska-Möller, A. 2009. Problems with estimation and interpretation of oceanic heat transport – conceptual remarks for the case of Fram Strait in the Arctic Ocean. *Ocean Sci.* **5**, 487–494.
- Sirevaag, A. and Fer, I. 2009. Early spring oceanic heat fluxes and mixing observed from drift stations north of Svalbard. *J. Phys. Oceanogr.* **39**, 3049–3069.
- Smedsrud, L. H., Esau, I., Ingvaldsen, R. B., Eldevik, T., Haugan, P. M. and co-authors. 2013. The role of the Barents Sea in the Arctic climate system. *Rev. Geophys.* **51**, 415–449.
- Untersteiner, N. 1988. On the ice and heat balance in Fram Strait. *J. Geophys. Res.* **93**, 527–531.



# Paper II

## Skillful prediction of Barents Sea ice cover

Ingrid H. Onarheim, Tor Eldevik, Marius Årthun, Randi B. Ingvaldsen, and Lars H. Smedsrud

*Geophysical Research Letters*, 42, 5364–5371 (2015)

II





## RESEARCH LETTER

10.1002/2015GL064359

## Skillful prediction of Barents Sea ice cover

Ingrid H. Onarheim<sup>1</sup>, Tor Eldevik<sup>1</sup>, Marius Årthun<sup>1</sup>, Randi B. Ingvaldsen<sup>2</sup>, and Lars H. Smedsrud<sup>1</sup><sup>1</sup>Geophysical Institute, University of Bergen and Bjerknes Centre for Climate Research, Bergen, Norway, <sup>2</sup>Institute of Marine Research, Bergen, Norway

## Key Points:

- Propose and evaluate a framework that predicts Barents Sea ice cover
- Demonstrate skillful predictions from recent available observations
- Model imperfections can largely be diagnosed from simultaneous meridional winds

## Correspondence to:

I. H. Onarheim,  
ingrid.onarheim@uib.no

## Citation:

Onarheim, I. H., T. Eldevik, M. Årthun, R. B. Ingvaldsen, and L. H. Smedsrud (2015), Skillful prediction of Barents Sea ice cover, *Geophys. Res. Lett.*, 42, 5364–5371, doi:10.1002/2015GL064359.

Received 24 APR 2015

Accepted 12 JUN 2015

Accepted article online 18 JUN 2015

Published online 8 JUL 2015

©2015. The Authors.

This is an open access article under the terms of the Creative Commons Attribution-NonCommercial-NoDerivs License, which permits use and distribution in any medium, provided the original work is properly cited, the use is non-commercial and no modifications or adaptations are made.

**Abstract** A main concern of present climate change is the Arctic sea ice cover. In wintertime, its observed variability is largely carried by the Barents Sea. Here we propose and evaluate a simple quantitative and prognostic framework based on first principles and rooted in observations to predict the annual mean Barents Sea ice cover, which variance is carried by the winter ice (96%). By using observed ocean heat transport and sea ice area, the proposed framework appears skillful and explains 50% of the observed sea ice variance up to 2 years in advance. The qualitative prediction of increase versus decrease in ice cover is correct 88% of the time. Model imperfections can largely be diagnosed from simultaneous meridional winds. The framework and skill are supported by a 60 year simulation from a regional ice-ocean model. We particularly predict that the winter sea ice cover for 2016 will be slightly less than 2015.

## 1. Introduction

The Arctic sea ice cover is a well-observed and sensitive indicator of climate variability and change [Serreze *et al.*, 2007]. Negative sea ice area trends are observed in all seasons and all regions, but with large seasonal and interannual variability [Cavalieri and Parkinson, 2012; Simmonds, 2015]. The rapid changes in Arctic sea ice cover have led to an increase in demand for realistic local and regional sea ice forecast systems [Eicken, 2013]. Skillful sea ice predictions provide important information for end users interested in marine access, fisheries, and resource extraction, and are also of interest due to the suggested impacts of the Arctic sea ice cover on weather conditions and climate [e.g., Honda *et al.*, 2009; Inoue *et al.*, 2012], although debated [e.g., Screen and Simmonds, 2013; Perlwitz *et al.*, 2014]. The growing effort in producing seasonal to decadal Arctic sea ice forecasts has been especially large for the September minimum sea ice cover [e.g., Schröder *et al.*, 2014; Kapsch *et al.*, 2014; Stroeve *et al.*, 2014]. Predictions of the Arctic winter sea ice variability have on the other hand been limited.

During winter the Arctic Ocean sea ice variability largely reflects variations in the Barents Sea ice cover (Figure 1). An intimate relation between the Barents Sea ice conditions and ocean heat has been understood for more than a century [Helland-Hansen and Nansen, 1909] and was recently quantified by Årthun *et al.* [2012]. Ocean heat anomalies can be generated locally [Schlichtholz, 2011] or be advected from the Norwegian Sea [Vinje, 2001; Kauker *et al.*, 2003; Francis and Hunter, 2007], providing predictive potential for the Barents Sea ice cover. Based on reanalysis data, Nakanowatari *et al.* [2014] found that subsurface temperature has predictive skill for early winter sea ice cover. The influence of the atmosphere on the Barents Sea ice cover has also been highlighted in recent years. Winds affect the Barents Sea climate variability through transport and redistribution of sea ice [Hilmer *et al.*, 1998; Koenigk *et al.*, 2009; Kwok, 2009], advection of air masses and Atlantic heat into the Barents Sea [Ingvaldsen *et al.*, 2004a; Kvingedal, 2005], and by increasing turbulent surface heat fluxes. The largest influence of northerly winds is often found during winter due to stronger winds [Pavlova *et al.*, 2013]. Processes related to large-scale atmospheric circulation [Maslanik *et al.*, 2007; Deser and Teng, 2008; Zhang *et al.*, 2008], cyclone activity [Sorteberg and Kvingedal, 2006; Simmonds and Keay, 2009], the length of the freezing season, and the amount of ice that remains after the summer melt season may also be of large importance for the sea ice variability.

The aim of this study is to understand and assess the predictability of the annual mean, and, in particular, the winter Barents Sea ice cover (Figure 1). We develop a prognostic framework from first principles and, based on direct observations and a 60 year simulation, assess the role of the Atlantic inflow as a main source of Barents Sea ice predictability 1–2 years in advance. Moreover, the influence and predictive potential of meridional winds on the interannual sea ice variability are investigated.

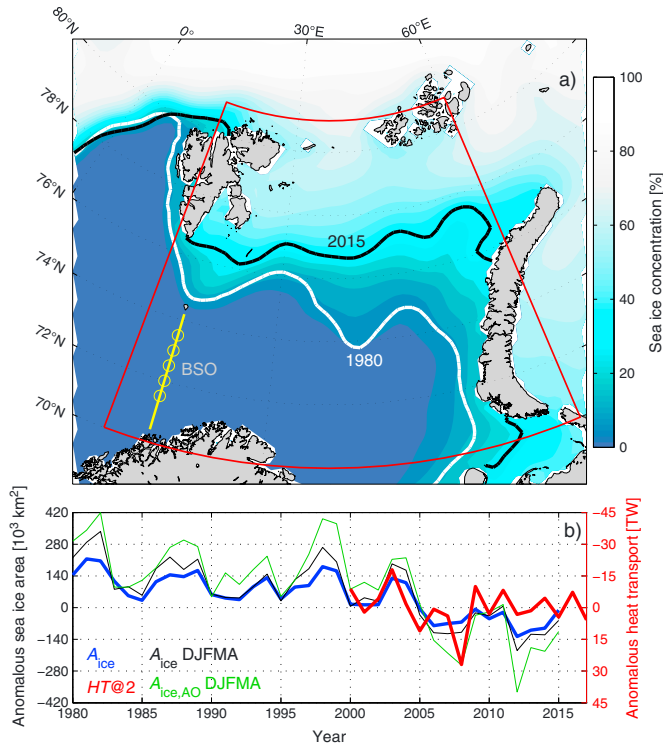


**Figure 1.** (a) Satellite-derived (National Snow and Ice Data Center, NSIDC) mean sea ice concentration between 1980 and 2015. The ice edge (15% ice concentration) is indicated for 1980 (white line) and 2015 (black line). We confine the Barents Sea by the red line. The mooring array across the Barents Sea Opening (BSO, yellow line) is indicated by yellow circles. (b) Time series of interannual sea ice area. Annual (July–June, blue) sea ice variability is dominated by changes in winter (December–April, black) sea ice area. During winter variations in the anomalous Arctic Ocean (interior basins and surrounding shelf seas) sea ice area (green) mainly reflect the Barents Sea ice variability; the correlation between the winter sea ice area in the Barents Sea and the Arctic Ocean is 0.96, and the standard deviations are  $131 \cdot 10^3 \text{ km}^2$  and  $191 \cdot 10^3 \text{ km}^2$ , respectively. Observed annual mean heat transport (red) shifted to the ice cover by 2 years is also shown (note reversed axis).

## 2. Data and Methods

We confine the Barents Sea to the area between  $70\text{--}81^\circ\text{N}$ ,  $15\text{--}60^\circ\text{E}$  (Figure 1; following *Årthun et al.* [2012]). The Barents Sea ice cover is characterized by a strong seasonal cycle where almost all ice melts in summer. The majority of sea ice is formed locally during winter [e.g., *Vinje*, 2001], although in some winters sea ice import from the Arctic Ocean is substantial [*Kwok et al.*, 2005]. We thus consider winter-centered annual means (July–June) for all variables, i.e., the indicated year denotes the winter-centered mean that ends in the respective year (e.g., 2015 represents July 2014 to June 2015). As the summer is practically ice free, winter (December–April) explains 96% of the annual mean variance.

### 2.1. Observations

Monthly sea ice area from 1979 to 2015 is obtained from the National Snow and Ice Data Center (NSIDC) [*Cavalieri et al.*, 1996], with a spatial resolution of  $25 \text{ km} \times 25 \text{ km}$ . The sea ice algorithms and the method used to derive a consistent data set are described in *Cavalieri et al.* [1999, and references therein].

To test the Atlantic heat transport as a potential predictor of the Barents Sea ice cover, we use the Atlantic water ( $T > 3^{\circ}\text{C}$ ) [Ingvaldsen *et al.*, 2004b] inflow through the Barents Sea Opening (BSO,  $71.5\text{--}73.5^{\circ}\text{N}$ ,  $20^{\circ}\text{E}$ ), measured by the Institute of Marine Research, Norway since September 1997. Current meter moorings deployed every 30 nm (= 56 km) in the BSO sample temperature and velocity at 50 m depth and 15 m above bottom (the current is mostly barotropic, driven by sea level changes [Ingvaldsen *et al.*, 2004a]), allowing for calculation of heat transport. July and August 1997, and May and June 2015 are estimated from climatological (1998–2014) values in order to get winter-centered annual mean values for 1998 and 2015, respectively. Note that the near-real-time data from April 2014 to April 2015 was postprocessed in the field after recovering the moorings. The 2015 value used herein is therefore a present best estimate of recent heat transport.

The influence from regional winds on the sea ice variability is investigated using monthly reanalysis data of the meridional wind component from the National Centers for Environmental Prediction (NCEP)-National Centers for Atmospheric Research (NCAR) [Kalnay *et al.*, 1996] on a  $2.5^{\circ} \times 2.5^{\circ}$  grid. The reanalysis data are comparable to observed surface wind speeds over the Barents Sea [Kolstad, 2008] and capture synoptic changes in sea level pressure distribution and associated changes in geostrophic winds [e.g., Deser and Teng, 2008].

### 2.2. Model Simulation

To complement the relatively short observational record, we use the 60 year (1948–2007) model simulation of *Arthun et al.* [2011]. The model used is the regional coupled ice-ocean model Hamburg Shelf Ocean Model (HAMSOM) [Schrum and Backhaus, 1999]. HAMSOM has a horizontal resolution of  $7\text{km} \times 7\text{km}$  and is forced with NCEP/NCAR reanalysis data. The model shows good agreement with observations, in general, and in particular with the Barents Sea ice area [Arthun *et al.*, 2012]; the simulated sea ice area is essentially the observed. The hydrographic structure of the Barents Sea is also captured by the model, and the interannual variability is realistic. Accordingly, the HAMSOM simulation seems appropriate to examine the predictability of the Barents Sea ice cover.

### 2.3. Prediction Evaluation

Prediction skill is assessed by variance explained ( $r^2$ ), and root-mean-square error,  $\text{RMSE} = \left[ \sum_{i=1}^N (x_i - y_i)^2 / N \right]^{1/2}$ , where  $N$  is the length of the time series and  $x$  and  $y$  are the observed and predicted time series, respectively. A common definition of skill is for a prediction framework to beat persistence [e.g., Kapsch *et al.*, 2014]. The persistence forecast is simply constructed by assuming that the present rate of change in sea ice area persists. Predicted change is quantified with respect to the presently observed sea ice area. They are both scored against the sign of change subsequently observed. The proposed framework is also evaluated against linear trend predictions, which are constructed by extrapolating the observed linear trend in sea ice cover. The term skillful herein describes a prediction that beats the skill both of persistence and of linear trend prediction.

## 3. Prognostic Framework

The Barents Sea is a confined, relatively shallow basin where the oceanic heat is essentially provided through the BSO [e.g., Smedsrud *et al.*, 2013], and effectively lost to the atmosphere in the southern ice-free part [Häkkinen and Cavalieri, 1989; Arthun and Schrum, 2010; Smedsrud *et al.*, 2010]. Consequently, there is little heat leaving the Barents Sea to the Arctic Ocean [Gammelsrød *et al.*, 2009]. Both the recent trend and the sea ice variability are largely related to the inflowing Atlantic water through the BSO [Arthun *et al.*, 2012]. We now outline a predictive and explicit framework linking ocean heat transport to the Barents Sea ice cover.

The integrated heat budget of the Barents Sea is

$$\frac{dHC}{dt} = -HF + HT, \tag{1}$$

with  $HC$  being the ocean heat content,  $HF$  the net surface heat flux (the sum of shortwave, longwave, sensible, and latent heat fluxes at the ocean surface), and  $HT$  the ocean heat transport through the BSO. The quantities will be understood as anomalies for the present application. An increase in heat transport through the BSO results in warmer ocean conditions, larger heat loss to the atmosphere, and hence reduced sea ice freezing and smaller sea ice cover. Arthun *et al.* [2012] found that the regional ocean heat content and heat loss to the atmosphere reflect the annual mean extent of ice-free ocean. Hence, we model the anomalous ocean heat content and heat loss to the atmosphere to scale with the anomalous sea ice area,  $A_{\text{ice}}$ :

$$HC = -hc_0 A_{\text{ice}}, \quad HF = -q_0 A_{\text{ice}}, \tag{2}$$

where  $hc_0$  and  $q_0$  are scaling factors representing the heat content and heat loss per area of an anomalous ice-free sea surface (see Appendix A for details). Inserting the scaling into the conservation of heat results in a simple prognostic relation for the anomalous sea ice area, where heat loss to the atmosphere acts as a relaxation toward no anomalous sea ice area, and ocean heat transport drives changes in sea ice area:

$$\frac{dA_{ice}}{dt} = -\frac{q_0}{hc_0}A_{ice} - \frac{1}{hc_0}HT. \quad (3)$$

The relation constitutes a quantification of changes in the sea ice area from ocean heat transport and sea ice area. In its simplest form, the right-hand side represents a qualitative prediction for the sign of change from which is the most dominant predictor, ice cover versus heat transport. Hence, the framework predicts the Barents Sea ice area based on observed sea ice area and heat transport through the BSO.

Solving equation (3) analytically results in an explicit expression of the anomalous sea ice area:

$$A_{ice}(t) = \left( A_0 - \frac{1}{q_0\tau} \int_0^t HT(t)e^{-\frac{t}{\tau}} dt \right) e^{-\frac{t}{\tau}}, \quad (4)$$

where  $A_0$  is the initial sea ice anomaly and  $\tau = hc_0/q_0$  is the characteristic time scale for heat balance indicating the flushing time of the Barents Sea. The anomalous sea ice area at a given time is thus set by the initial sea ice area and the integrated heat input through the BSO. The weight of the past decreases exponentially with time scale  $\tau$ . Both the observational record and the HAMSOM data indicate a memory (heat balance) of the Barents Sea of approximately 3 years (Appendix A). This compares well with the flushing time of the Barents Sea which is less than 5 years based on a throughflow of 2 Sv ( $1\text{ Sv} = 10^6 \text{ m}^3 \text{ s}^{-1}$ ) and a basin volume of  $3 \cdot 10^{14} \text{ m}^3$  and is also consistent with the lagged sea ice response to a variable Atlantic inflow, as suggested by *Arthun et al.* [2012].

Forward discretization of equation (3) gives a prognostic relation linking the anomalous sea ice area to the anomalous ice area and heat transport the previous year:

$$A_{ice}^{n+1} = -\left( \frac{q_0}{hc_0}A_{ice}^n + \frac{1}{hc_0}HT^n \right) \Delta t + A_{ice}^n, \quad (5)$$

where  $n$  indicates time and  $\Delta t$  is the time step of 1 year. Note that equation (5) predicts year  $n + 1$  based on the true sea ice area and heat transport for year  $n$ , i.e., a simplest form of data assimilation. Equation (4) integrates the heat transport over time only considering the initial sea ice anomaly. Hence, the analytical solution in equation (4) potentially accumulates model imperfections (related to equation (2)) with time. Predictions based on the discretized equation (5) can therefore maybe be expected to be more skillful, and to be more appropriate for practical use.

#### 4. Predictions of the Barents Sea Ice Cover

To evaluate the proposed framework predicting the Barents Sea ice cover, we first use direct observations and thereafter the 60 year model simulation. Using the observation-based scaling parameters (cf. Appendix A) in equations (4) and (5) allows for predictions of the Barents Sea ice cover based on available observations. The analytical estimate using direct observations as input shows good agreement to the observed sea ice cover (Figure 2a). Using equation (5), 50% of the variance is explained, and the RMSE is relatively small (roughly half of a standard deviation of  $91 \cdot 10^3 \text{ km}^2$ ; Table 1). There is, however, the expected underestimation of magnitude due to variance not explained (cf. Appendix A). This suggests that the proposed framework linking observed Barents Sea ice cover and heat transport through the BSO is useful for predicting the Barents Sea ice cover 1 year in advance. It is in particular predicted that the sea ice area in 2016 will be  $12 \cdot 10^3 \text{ km}^2$  smaller than that of 2015. The predicted sea ice area for 2016 is near the mean over the last 20 years, but still corresponds to the eighth lowest sea ice area since 1979. The results are supported by HAMSOM data (Figure 2b). Based on equation (4), the analytical estimate using HAMSOM data as input explains 63% of the variance in sea ice cover, and the RMSE is relatively small ( $43 \cdot 10^3 \text{ km}^2$  compared to the standard deviation of  $69 \cdot 10^3 \text{ km}^2$ ). For HAMSOM the prediction from the integral equation (4) is slightly better than the prediction based on equation (5), with  $r^2 = 55\%$  and  $\text{RMSE} = 46 \cdot 10^3 \text{ km}^2$ . This corroborates that ocean heat transport is a dominant driver of the HAMSOM simulated sea ice cover.

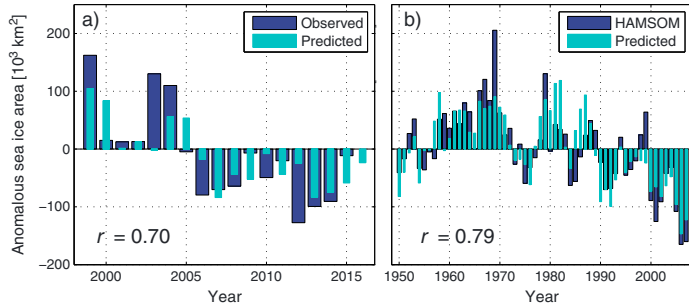


**Figure 2.** (a) Annual (July–June) observed and predicted anomalous Barents Sea ice area between 1999 and 2016. Anomalies are relative to the mean sea ice area of  $238 \cdot 10^3 \text{ km}^2$  for the 1998–2015 period. The prediction is based on the sea ice area and heat transport through the Barents Sea Opening the previous year (equation (5)). (b) Annual (July–June) modeled (HAMSOM) and predicted anomalous Barents Sea ice area between 1950 and 2007. Anomalies are relative to the mean sea ice area of  $377 \cdot 10^3 \text{ km}^2$  for the 1949–2007 period. The prediction is based on the integrated heat transport through the Barents Sea Opening and the initial sea ice area (equation (4)).

### 5. Evaluation of Predictability

As our prediction of the Barents Sea ice cover compares well with observed sea ice variability, we now assess the skill (cf. section 2) of the proposed framework. The qualitative prediction of an increase/decrease in sea ice cover is correct in 15 years out of the 17 available years, i.e., 88% of the time considering the observations retrospectively (Figure 3 and Appendix A). The proposed method to predict changes in sea ice cover thus beats persistence (correct 88% of the time compared to 63% for persistence). Our physically based framework also beats linear trend predictions. By considering the trend over the period of observed heat transport, the linear trend prediction gives a RMSE of  $87 \cdot 10^3 \text{ km}^2$ , compared with  $56 \cdot 10^3 \text{ km}^2$  from equation (5) (Table 1). The RMSE is slightly reduced ( $73 \cdot 10^3 \text{ km}^2$ ) when basing extrapolation on the full satellite observed sea ice record. We thus find the proposed framework to be skillful.

To further evaluate the framework, we account for the memory of the Barents Sea (3 years; Appendix A), and evaluate the prediction with up to 3 years time lag between heat transport and sea ice cover. Accordingly the forecast horizon of the framework may possibly be extended. Results from linear regression (cf. equation (A1)) show that the observational based prediction is slightly improved using a 2 year leading heat transport (Table 1). The heat transport leading the ice cover by 3 years has only a minor influence on the sea ice cover. The forecast horizon can thus be considered to be to 2 years from the point of view of ocean heat transport.

**Table 1.** Evaluation Statistics for the Predictions<sup>a</sup>

Method	Observations		HAMSOM	
	$r^2$	RMSE	$r^2$	RMSE
Based on equation (5)				
$A_{ice@1, HT@1}$	50	56	55	46
$A_{ice@1, HT@2}$	50	49	41	53
$A_{ice@1, HT@1, v@1}$	52	55	63	42
$A_{ice@1, HT@1, v@0}$	78	38	66	40
Based on equation (4)				
	42	69	63	43

<sup>a</sup>Explained variance,  $r^2$  (%); root-mean-square error, RMSE ( $\times 10^3 \text{ km}^2$ ); and time lag, @ (year).  $A_{ice}$ , sea ice area;  $HT$ , ocean heat transport; and  $v$ , meridional wind; all are anomalies.

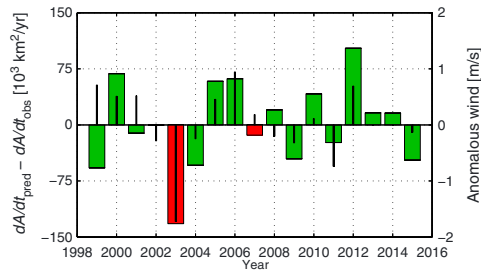


**Figure 3.** Difference between predicted and observed rate of change in the Barents Sea ice cover from one year to the next (thick bars). Green indicates that the correct sign of change is predicted and red the opposite. Thin bars show anomalous wind (meridional wind component averaged over the Barents Sea), where positive values indicate wind from the south.

Our suggested framework has so far not considered wind explicitly. Winds may have a large impact on interannual sea ice variability [e.g., Kwok, 2009] and was suggested as a possible predictor by Nakanowatari et al. [2014]. Our large underestimation of sea ice in 2003 corresponds to anomalous winds from the north (Figure 3). According to Kwok et al. [2005] winds caused an unusually high import of sea ice to the Barents Sea during winter 2003. Due to the potential influence of winds, we examine meridional wind at different time lags as predictor. Using linear regression analysis (cf. equation (A1)), we find that the prediction performance is not largely improved by accounting for wind with a time lag, while simultaneous wind adds variance explained (Table 1), consistent with the findings of Nakanowatari et al. [2014]. The effect from simultaneous wind is demonstrated in Figure 3, showing that mismatch between observed and predicted changes in the ice cover can be reconciled also considering anomalous wind conditions. By combining the predictive equation (5) with simultaneous winds (in the form of equation (A1)), 78% of the sea ice variance is explained (Table 1). A more elaborate evaluation of wind influence, by investigating more regional winds, indicates that the results are robust. This corroborates that ocean heat conditions and winds appear as main drivers of the Barents Sea ice cover. Still, the proposed framework (equation (4) or (5)) captures most of the sea ice variance and qualitatively predicts an increase/decrease in ice cover skillfully.

### 6. Discussion and Conclusion

Using direct observations, a regional ice-ocean model and a simple prognostic heat budget (equations (1)–(5)), we have shown that sea ice anomalies in the Barents Sea can be skillfully predicted from recent sea ice area and ocean heat transport. Overall the proposed framework skillfully predicts the observed sea ice cover both quantitatively (Figure 2) and qualitatively (Figure 3) predicting an increase versus decrease in ice cover. By accounting for simultaneous meridional winds, 78% of the sea ice variance is explained. Preceding ocean heat transport and sea ice area combined with these winds are thus all important to explain recent sea ice variability (Table 1).

As ocean heat transport and sea ice cover provide significant predictive skill for the Barents Sea ice cover, this work corroborates the strong link between Atlantic water inflow and the Barents Sea ice cover [e.g., Schlichtholz, 2011; Årthun et al., 2012]. Parkinson et al. [2006] found that many climate models simulate more sea ice in the Barents Sea than what is observed and hypothesized that the models underestimate the ocean heat transport. It thus appears essential for ocean and earth system models to adequately resolve the variable Atlantic heat transport through the Nordic Seas into the Barents Sea and Arctic Ocean, in order to simulate Arctic sea ice variability well.

The proposed framework offers a novel approach to predict winter Arctic sea ice cover, where the Barents Sea at present essentially explains the winter variance (92%, cf. Figure 1b). Related to this, Zhang [2015] suggested a relation between the Barents Sea ice cover and also summer Arctic sea ice extent via Atlantic heat. Skillful predictions of Barents Sea ice may therefore have the potential to improve predictions of the Arctic Ocean sea ice cover in general. In the future the processes driving today's Barents Sea winter ice cover may become even more relevant as first-year ice is likely to dominate the Arctic Ocean.

Our results highlight the potential for skillful physical-based prediction models of the Arctic sea ice cover. We demonstrate that the Barents Sea ice cover is skillfully predictable 1–2 years ahead (Figure 2). Due to relatively small 2015 anomalies in sea ice and heat, but with a relative dominance of anomalous Atlantic heat input, it is in particular predicted (cf. equation (5)) that the Barents Sea ice cover in 2016 will be smaller than that of 2015 (Figure 2a).

### Appendix A: Scaling Parameters

Our suggested framework (equation (5)) can be considered a special case of the regressional relation

$$\frac{A_{ice}^{n+1} - A_{ice}^n}{\Delta t} = aA_{ice}^{n-k} + bHT^{n-l} + cV^{n-m}, \tag{A1}$$

where  $a$ ,  $b$ , and  $c$  are regression coefficients for the ice cover, heat transport, and meridional wind,  $v$ , respectively, and  $k$ ,  $l$ ,  $m$  are any additional time lags. In the case of equation (5),  $c = k = l = 0$ , i.e., neither the direct influence of wind nor any time lag beyond the present are considered, and  $a = -q_0/hc_0$ ,  $b = -1/hc_0$ . Simplest estimates of the scaling factors,  $q_0$  and  $hc_0$ , would be  $hc_0 = \text{std}(HC)/\text{std}(A_{ice})$  and  $q_0 = \text{std}(HF)/\text{std}(A_{ice})$ , where  $\text{std}(X)$  is the standard deviation of the annual time series  $X$ , and assuming the model assumption (equation (2)) to be perfect. Unfortunately, observational time series of ocean heat content and heat flux to the atmosphere are not available. By considering the full observational record, linear regression (equation (A1)) gives  $a = -0.403 \text{ yr}^{-1}$ , and  $b = -0.001 \text{ m}^2 \text{ J}^{-1}$  for the observational record. For HAMSOM data the regression coefficients become  $a = -0.617 \text{ yr}^{-1}$  and  $b = -0.003 \text{ m}^2 \text{ J}^{-1}$ , which compare well with scaling parameters calculated from standard deviations ( $a = -0.616 \text{ yr}^{-1}$  and  $b = -0.005 \text{ m}^2 \text{ J}^{-1}$ ). The observed and modeled parameters differ partly because the scaling parameters may change over time but also simply because HAMSOM is a model. The robustness of the scaling parameters was therefore tested by the random subsampling of  $N$  data points for the regressional relationship (equation (A1));  $N \leq 30$  for HAMSOM;  $N \leq 12$  for observations). The procedure was repeated 1000 times for each  $N$ . The scaling parameters converged to their respective values in about 15 years, implying the HAMSOM estimates to be robust, but that one would probably still benefit from a longer observational series. We finally note that prediction based on regression generically underestimates the variance of a predictand unless there is perfect covariance between predictor(s) and the predictand (cf. Figure 2).

#### Acknowledgments

The data sets for this paper are properly cited and referred to in the reference list. This work was supported by the Centre for Climate Dynamics (SKD) at the Bjerknes Centre and by the Research Council of Norway through the projects NORTH and EPOCASA. We thank two anonymous reviewers for constructive suggestions that improved the manuscript.

The Editor thanks two anonymous reviewers for their assistance in evaluating this paper.

#### References

- Årthun, M., and C. Schrum (2010), Ocean surface heat flux variability in the Barents Sea, *J. Mar. Syst.*, *83*, 88–98, doi:10.1016/j.jmarsys.2010.07.003.
- Årthun, M., R. Ingvaldsen, L. H. Smedsrud, and C. Schrum (2011), Dense water formation and circulation in the Barents Sea, *Deep Sea Res.*, *58*(8), 801–817, doi:10.1016/j.dsr.2011.06.001.
- Årthun, M., T. Eldevik, L. H. Smedsrud, Ø. Skagseth, and R. B. Ingvaldsen (2012), Quantifying the influence of Atlantic heat on Barents Sea ice variability and retreat, *J. Clim.*, *25*, 4736–4743, doi:10.1175/JCLI-D-11-00466.1.
- Cavalleri, D. J., and C. L. Parkinson (2012), Arctic sea ice variability and trends, 1979–2010, *Cryosphere*, *6*(4), 881–889, doi:10.5194/tc-6-881-2012.
- Cavalleri, D. J., C. L. Parkinson, P. Gloersen, and H. Zwally (1996), *Sea Ice Concentrations From Nimbus-7 SMMR and DMSP SSM/I Passive Microwave Data*, Digital Media, Natl. Snow and Ice Data Cent., Boulder, Colo.
- Cavalleri, D. J., C. L. Parkinson, P. Gloersen, J. C. Comiso, and H. J. Zwally (1999), Deriving long-term time series of sea ice cover from satellite passive-microwave multisensor data sets, *J. Geophys. Res.*, *104*(C7), 15,803–15,814, doi:10.1029/1999JC900081.
- Deser, C., and H. Teng (2008), Evolution of Arctic sea ice concentration trends and the role of atmospheric circulation forcing, 1979–2007, *Geophys. Res. Lett.*, *35*, L02504, doi:10.1029/2007GL032023.
- Eicken, H. (2013), Ocean science: Arctic sea ice needs better forecasts, *Nature*, *497*(7450), 431–433, doi:10.1038/497431a.
- Francis, J. A., and E. Hunter (2007), Drivers of declining sea ice in the Arctic winter: A tale of two seas, *Geophys. Res. Lett.*, *34*, L17503, doi:10.1029/2007GL030995.
- Gammelsrød, T., Ø. Leikvin, V. Lien, W. P. Budgell, H. Loeng, and W. Maslowski (2009), Mass and heat transports in the NE Barents Sea: Observations and models, *J. Mar. Syst.*, *75*(1), 56–69, doi:10.1016/j.jmarsys.2008.07.010.
- Häkkinen, S., and D. J. Cavalieri (1989), A study of oceanic surface heat fluxes in the Greenland, Norwegian, and Barents Seas, *J. Geophys. Res.*, *94*(C5), 6145–6157, doi:10.1029/JC094iC05p06145.
- Helland-Hansen, B., and F. Nansen (1909), The Norwegian Sea, *Fiskdir. Skr. Ser. Havunders.*, *2*(2), 1–360.
- Hilmer, M., M. Harder, and P. Lemke (1998), Sea ice transport: A highly variable link between Arctic and North Atlantic, *Geophys. Res. Lett.*, *25*(17), 3359–3362, doi:10.1029/98GL52360.
- Honda, M., J. Inoue, and S. Yamane (2009), Influence of low Arctic sea-ice minima on anomalously cold Eurasian winters, *Geophys. Res. Lett.*, *36*, L08707, doi:10.1029/2008GL037079.
- Ingvaldsen, R. B., L. Asplin, and H. Loeng (2004a), Velocity field of the western entrance to the Barents Sea, *J. Geophys. Res.*, *109*, C03021, doi:10.1029/2003JC001811.
- Ingvaldsen, R. B., L. Asplin, and H. Loeng (2004b), The seasonal cycle in the Atlantic transport to the Barents Sea during the years 1997–2001, *Cont. Shelf Res.*, *24*(9), 1015–1032, doi:10.1016/j.csr.2004.02.011.

- Inoue, J., M. E. Hori, and K. Takaya (2012), The role of Barents Sea ice in the wintertime cyclone track and emergence of a warm-Arctic cold-Siberian anomaly, *J. Clim.*, *25*(7), 2561–2568, doi:10.1175/JCLI-D-11-00449.1.
- Kalnay, E., et al. (1996), The NCEP/NCAR 40-year reanalysis project, *Bull. Am. Meteorol. Soc.*, *77*(3), 437–471, doi:10.1175/1520-0477(1996)077<0437:TNYP>2.0.CO;2.
- Kapsch, M.-L., R. G. Graversen, T. Economou, and M. Tjernström (2014), The importance of spring atmospheric conditions for predictions of the Arctic summer sea ice extent, *Geophys. Res. Lett.*, *41*, 5288–5296, doi:10.1002/2014GL060826.
- Kauker, F., R. Gerdes, M. Karcher, C. Köberle, and J. L. Lieser (2003), Variability of Arctic and North Atlantic sea ice: A combined analysis of model results and observations from 1978 to 2001, *J. Geophys. Res.*, *108*(C6), 3182, doi:10.1029/2002JC001573.
- Koenigk, T., U. Mikolajewicz, J. H. Jungclauss, and A. Kroll (2009), Sea ice in the Barents Sea: Seasonal to interannual variability and climate feedbacks in a global coupled model, *Clim. Dyn.*, *32*(7–8), 1119–1138, doi:10.1007/s00382-008-0450-2.
- Kolstad, E. (2008), A QuikSCAT climatology of ocean surface winds in the Nordic seas: Identification of features and comparison with the NCEP/NCAR reanalysis, *J. Geophys. Res.*, *113*, D11106, doi:10.1029/2007JD008918.
- Kvingedal, B. (2005), Sea-ice extent and variability in the Nordic Seas, 1967–2002, in *The Nordic Seas: An Integrated Perspective*, vol. 158, edited by B. Kvingedal, pp. 137–156, AGU, Washington, D. C., doi:10.1029/158GM04.
- Kwok, R. (2009), Outflow of Arctic Ocean sea ice into the Greenland and Barents Seas: 1979–2007, *J. Clim.*, *22*(9), 2438–2457, doi:10.1175/2008JCLI2819.1.
- Kwok, R., W. Maslowski, and S. W. Laxon (2005), On large outflows of Arctic sea ice into the Barents Sea, *Geophys. Res. Lett.*, *32*, L22503, doi:10.1029/2005GL024485.
- Maslanik, J., S. Drobot, C. Fowler, W. Emery, and R. Barry (2007), On the Arctic climate paradox and the continuing role of atmospheric circulation in affecting sea ice conditions, *Geophys. Res. Lett.*, *34*, L03711, doi:10.1029/2006GL028269.
- Nakanowatari, T., K. Sato, and J. Inoue (2014), Predictability of the Barents Sea ice in early winter: Remote effects of oceanic and atmospheric thermal conditions from the North Atlantic, *J. Clim.*, *27*(23), 8884–8901, doi:10.1175/JCLI-D-14-00125.1.
- Parkinson, C. L., K. Y. Vinnikov, and D. J. Cavalieri (2006), Evaluation of the simulation of the annual cycle of Arctic and Antarctic sea ice coverages by 11 major global climate models, *J. Geophys. Res.*, *111*, C07012, doi:10.1029/2005JC003408.
- Pavlova, O., V. Pavlov, and S. Gerland (2013), The impact of winds and sea surface temperatures on the Barents Sea ice extent, a statistical approach, *J. Mar. Syst.*, *130*, 248–255, doi:10.1016/j.jmarsys.2013.02.011.
- Perlwitz, J., M. Hoerling, and R. Dole (2014), Arctic tropospheric warming: Causes and linkages to lower latitudes, *J. Clim.*, *28*, 2154–2167, doi:10.1175/JCLI-D-14-00095.1.
- Schlichtholz, P. (2011), Influence of oceanic heat variability on sea ice anomalies in the Nordic Seas, *Geophys. Res. Lett.*, *38*, L05705, doi:10.1029/2010GL045894.
- Schröder, D., D. L. Feltham, D. Flocco, and M. Tsamados (2014), September Arctic sea-ice minimum predicted by spring melt-pond fraction, *Nat. Clim. Change*, *4*(5), 353–357, doi:10.1038/nclimate2203.
- Schrum, C., and J. O. Backhaus (1999), Sensitivity of atmosphere-ocean heat exchange and heat content in the North Sea and the Baltic Sea, *Tellus A*, *51*(4), 526–549, doi:10.1034/j.1600-0870.1992.00006.x.
- Screen, J. A., and I. Simmonds (2013), Exploring links between Arctic amplification and mid-latitude weather, *Geophys. Res. Lett.*, *40*, 959–964, doi:10.1002/grl.50174.
- Serreze, M. C., M. M. Holland, and J. Stroeve (2007), Perspectives on the Arctic's shrinking sea-ice cover, *Science*, *315*(5818), 1533–1536, doi:10.1126/science.1139426.
- Simmonds, I. (2015), Comparing and contrasting the behaviour of Arctic and Antarctic sea ice over the 35 year period 1979–2013, *Ann. Glaciol.*, *56*, 18–28, doi:10.3189/2015AoG69A909.
- Simmonds, I., and K. Keay (2009), Extraordinary September Arctic sea ice reductions and their relationships with storm behavior over 1979–2008, *Geophys. Res. Lett.*, *36*, L19715, doi:10.1029/2009GL039810.
- Smedsrud, L. H., R. Ingvaldsen, J. E. Ø. Nilsen, and Ø. Skagseth (2010), Heat in the Barents Sea: Transport, storage, and surface fluxes, *Ocean Sci.*, *6*, 219–234, doi:10.5194/os-6-219-2010.
- Smedsrud, L. H., et al. (2013), The role of the Barents Sea in the Arctic climate system, *Rev. Geophys.*, *51*, 415–449, doi:10.1002/rog.20017.
- Sorteberg, A., and B. Kvingedal (2006), Atmospheric forcing on the Barents Sea winter ice extent, *J. Clim.*, *19*(19), 4772–4784, doi:10.1175/JCLI3885.1.
- Stroeve, J., L. C. Hamilton, C. M. Bitz, and E. Blanchard-Wrigglesworth (2014), Predicting September sea ice: Ensemble skill of the SEARCH Sea Ice Outlook 2008–2013, *Geophys. Res. Lett.*, *41*, 2411–2418, doi:10.1002/2014GL059388.
- Vinje, T. (2001), Anomalies and trends of sea-ice extent and atmospheric circulation in the Nordic Seas during the period 1864–1998, *J. Clim.*, *14*(3), 255–267, doi:10.1175/1520-0442(2001)014<0255:AATOSI>2.0.CO;2.
- Zhang, R. (2015), Mechanisms for low-frequency variability of summer Arctic sea ice extent, *Proc. Natl. Acad. Sci.*, *112*, 4570–4575, doi:10.1073/pnas.1422296112.
- Zhang, X., A. Sorteberg, J. Zhang, R. Gerdes, and J. C. Comiso (2008), Recent radical shifts of atmospheric circulations and rapid changes in Arctic climate system, *Geophys. Res. Lett.*, *35*, L22701, doi:10.1029/2008GL035607.

# Paper III

## Toward an ice-free Barents Sea

Ingrid H. Onarheim and Marius Årthun  
*Geophysical Research Letters*, 44, 8387–8395 (2017)



III





## RESEARCH LETTER

10.1002/2017GL074304

## Key Points:

- Record low sea ice extent in the Barents Sea in recent winters
- The current observed trend appears as an uncommon feature in observations and climate models
- Large spread in model projections of ice-free conditions due to large internal variability

## Correspondence to:

I. H. Onarheim,  
ingrid.onarheim@uib.no

## Citation:

Onarheim, I. H., and M. Årthun (2017), Toward an ice-free Barents Sea, *Geophys. Res. Lett.*, 44, 8387–8395, doi:10.1002/2017GL074304.

Received 1 JUN 2017

Accepted 31 JUL 2017

Accepted article online 3 AUG 2017

Published online 25 AUG 2017

©2017. The Authors.

This is an open access article under the terms of the Creative Commons Attribution-NonCommercial-NoDerivs License, which permits use and distribution in any medium, provided the original work is properly cited, the use is non-commercial and no modifications or adaptations are made.

## Toward an ice-free Barents Sea

Ingrid H. Onarheim<sup>1</sup> and Marius Årthun<sup>1</sup><sup>1</sup>Geophysical Institute, University of Bergen and Bjerknes Centre for Climate Research, Bergen, Norway

**Abstract** Arctic winter sea ice loss is most pronounced in the Barents Sea. Here we combine observations since 1850 with climate model simulations to examine the recent record low winter Barents Sea ice extent. We find that the present observed winter Barents Sea ice extent has been reduced to less than one third of the pre-satellite mean and is lower than the minimum sea ice extent in all multicentury climate model control simulations assessed here. The current observed sea ice loss is furthermore unprecedented in the observational record and appears as an uncommon trend in the long control simulations. In a warming climate, projections from the large ensemble simulation with the Community Earth System Model show a winter ice-free Barents Sea for the first time within the time period 2061–2088. The large spread in projections of ice-free conditions highlights the importance of internal variability in driving recent and future sea ice loss.

## 1. Introduction

The loss of Arctic summer sea ice in recent decades is well documented and one of the most visible manifestations of ongoing climate change [Serreze *et al.*, 2007]. Although less dramatic and less studied, the Arctic winter sea ice cover has also displayed a steady retreat since satellite measurements of sea ice began in 1979 [Cavalieri and Parkinson, 2012]. These wintertime sea ice changes largely result from a retreating Barents Sea ice cover (Figure 1) [Onarheim *et al.*, 2015; Li *et al.*, 2017]. The recent decade has seen reduced sea ice growth leading to an accelerated trend toward lower Barents Sea ice extent, with the sea ice extent in 2016 and 2017 being the lowest on record (Figure 1).

The loss of sea ice in the Barents Sea can potentially affect climate and weather in lower latitudes [Liptak and Strong, 2014; Sorokina *et al.*, 2016], and Arctic ecosystems and fisheries [e.g., Dalpadado *et al.*, 2014]. The location of the sea ice edge in the Barents Sea also impacts shipping opportunities and offshore industry [ACIA, 2005]. It is therefore of great interest to understand winter sea ice variability and trends in the Barents Sea with respect to past variability and to predict the future fate of the winter sea ice cover.

The Barents Sea is a seasonally ice covered Arctic shelf sea, and a transition zone between the temperate Nordic Seas and the cold Arctic Ocean. The ocean climate in the Barents Sea is dominated by the varying influence of the Atlantic water inflow in the Norwegian Atlantic Current, a poleward extension of the Gulf Stream [e.g., Smedsrud *et al.*, 2013]. Variations in the Atlantic inflow exert a dominant influence on the variability and trend of the winter Barents Sea ice cover, by determining the amount of wintertime freezing [Venegas and Mysak, 2000; Vinje, 2001; Årthun *et al.*, 2012; Smedsrud *et al.*, 2013; Onarheim *et al.*, 2015; Li *et al.*, 2017]. Consequently, the Barents Sea ice cover displays pronounced interannual to multidecadal variability as a response to changes in the large-scale ocean circulation and associated changes in poleward ocean heat transport [Venegas and Mysak, 2000; Vinje, 2001; Zhang, 2015]. Low-frequency climate variability, reminiscent of the Atlantic Multidecadal Oscillation, is also evident in Barents Sea temperatures [Skagseth *et al.*, 2008; Levitus *et al.*, 2009].

The presence of substantial decadal to multidecadal sea ice variability in the Barents Sea makes it necessary to consider long time series when evaluating the uniqueness of the ongoing winter Barents Sea ice loss. Hence, in order to assess the occurrence of winter sea ice trends of varying lengths, we will combine a new observational data set covering the time period since 1850 [Walsh *et al.*, 2015, 2017] and multimodel, multicentury climate model control simulations. We also consider future trends in a warming climate, using mainly the Community Earth System Model large ensemble simulation (CESM-LE) [Kay *et al.*, 2015], to assess the possibility of ice-free

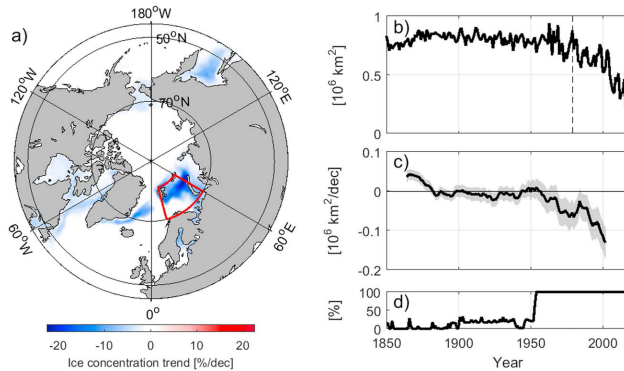


**Figure 1.** (a) Observed winter sea ice concentration trend, 1979–2017. The red box outlines the Barents Sea. (b) Barents Sea winter sea ice extent between 1850 and 2017. The vertical dashed line indicates the year 1979. (c) Successive 30 year trends in Barents Sea winter sea ice extent, 1850–2017. Trends are displayed at the center of each 30-year period. The gray shading indicates the 95% confidence interval. Note that the confidence interval does not take into account uncertainties with respect to data quality. (d) Fraction of winter Barents Sea ice concentration data based on observations. 100% indicates that no data is based on analogs or interpolation by Walsh *et al.* [2015].

conditions in the Barents Sea in winter toward the end of the century. This study thus provides the first detailed assessment of past, present, and future trends in observed and modeled Barents Sea winter sea ice extent.

## 2. Data and Methods

To assess and quantify Barents Sea ice variability and trends, we use a new data set of observed sea ice concentration spanning the time period 1850 to 2013 [Walsh *et al.*, 2015]. Sea ice concentration is satellite derived since 1979, calculated by combining concentration estimates from the Bootstrap and NASA Team algorithms [Meier *et al.*, 2013]. Prior to the satellite era, observations are compiled from, e.g., ship reports and airplane surveys [Walsh *et al.*, 2015, 2017]. To assess the most recent (2014–2017) Barents Sea ice loss, we use satellite-derived sea ice concentrations based on the NASA Team algorithm [Cavalieri *et al.*, 1996; Maslanik and Stroeve, 1999]. For consistency, we replace the Walsh product with the NASA Team product throughout the satellite era, 1979–2013, in the 1850 onward data set; i.e., sea ice concentrations are based on the NASA Team algorithm from 1979 to 2017. Minor differences in winter Barents Sea ice extent, 1979–2013, were found between the two sea ice products; a detrended correlation of 0.98, mean  $\pm$  standard deviation of  $0.64 \pm 0.13 \times 10^6 \text{ km}^2$  and  $0.60 \pm 0.14 \times 10^6 \text{ km}^2$ , and linear trends of  $-0.09 \times 10^6 \text{ km}^2$  per decade and  $-0.10 \times 10^6 \text{ km}^2$  per decade, for the combined (Bootstrap/NASA Team) product and the NASA Team product, respectively. The historical sea ice concentration is mid-monthly and given on a  $0.25^\circ$  latitude by  $0.25^\circ$  longitude grid, whereas the monthly satellite observations are on a 25 km by 25 km grid. The pre-satellite data clearly contain larger uncertainties with respect to trends and variability; however, this uncertainty is not quantified [Walsh *et al.*, 2017]. As a simple measure of data uncertainty, we show in Figure 1d the fraction of the winter Barents Sea ice concentration data which is based on observations, i.e., where the sea ice data is not based on analogs or interpolation by Walsh *et al.* [2015] (100% means that the sea ice concentration in each grid point is based on observations for all winter months). For a detailed description of the different data sources see Walsh *et al.* [2015]. The extended data set is nevertheless valuable for putting the recent sea ice loss into a longer historical perspective.

We consider winter (November–April; we note that results are not sensitive to the chosen definition of the winter season) sea ice extent in the area  $70^\circ\text{--}81^\circ\text{N}$ ,  $15^\circ\text{--}60^\circ\text{E}$  (red box in Figure 1a), following, e.g., Ártun *et al.* [2012]. A large part of the historical observations are of the sea ice edge, making sea ice extent beneficial compared to sea ice concentration or area. Sea ice extent is calculated as the cumulative area of all grid cells where monthly mean sea ice concentration is larger than 15%. Linear trends are thereafter calculated over 10–100 year time periods, although we will mainly consider 30 year trends when discussing temporal changes in the Barents Sea ice cover [cf., Serreze and Stroeve, 2015].

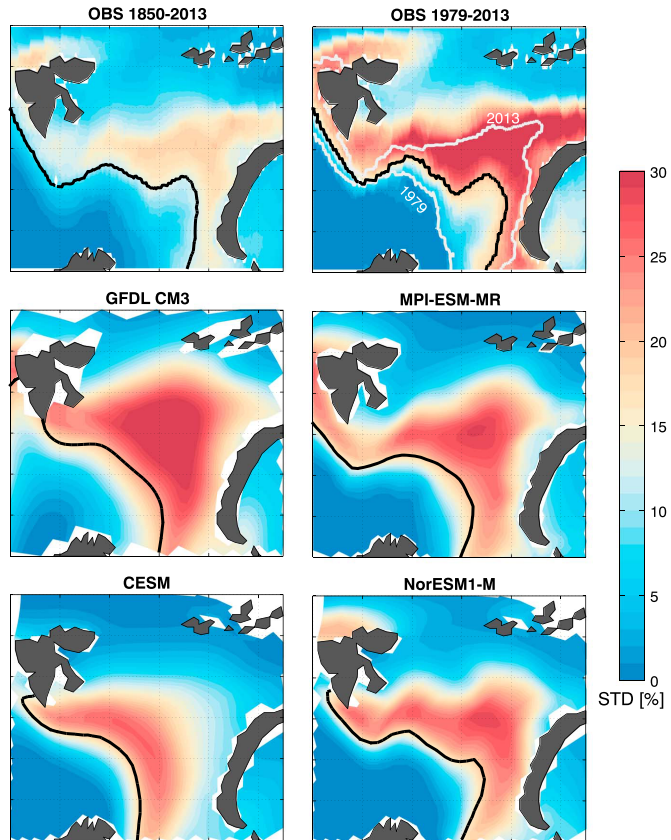


**Figure 2.** Standard deviation of winter sea ice concentration (colors) and mean sea ice edge (15% sea ice concentration; black contour line) in observations [Walsh *et al.*, 2015] and preindustrial climate model control simulations. Note that the data have not been detrended. The observed sea ice edge in 1979 and 2013 are also shown (white contours in the first row).

To evaluate when the Barents Sea approaches ice-free conditions, we define (nearly) ice-free conditions as 10% of the pre-satellite (1850–1978) average winter sea ice extent ( $0.08 \times 10^6 \text{ km}^2$ ). This allows for a small amount of sea ice to remain during parts of the winter, although the ocean is for all practical purposes ice free.

To assess the probability of the occurrence of observed trends as a result of internal variability, we analyze preindustrial control simulations (no external forcing) from four commonly used global climate models available from the fifth phase of the Coupled Model Intercomparison Project (CMIP5) [Taylor *et al.*, 2012]: NorESM1-M [Bentsen *et al.*, 2013] (500 year simulation), GFDL CM3 [Griffies *et al.*, 2011] (500 year simulation), CESM [Kay *et al.*, 2015] (1800 year simulation), and MPI-ESM-MR [Giorgetta *et al.*, 2013] (1000 year simulation). The combination of the four control runs, 3800 years in total, is sufficient to span a broad range of internal variability [e.g., Kay *et al.*, 2011; Li *et al.*, 2017], and the full suite of CMIP5 control simulations is therefore not included here. Keeping in mind that the simulations do not include external forcing, the location of the simulated mean sea ice edge in the Barents Sea is in fairly good agreement with observations in all the models (Figure 2). Consistent with observations, the area of maximum variance in the models stretches toward the northeast along the path of the warm Atlantic water [e.g., Årthun *et al.*, 2012]. The magnitude of variability

in the models is larger than that observed if we consider the time period since 1850, while it is in better agreement with that observed during the satellite period. We note that our results are not sensitive to the differences in grid size. A detailed model evaluation is not performed here, and the reader is referred to, e.g., Sando *et al.* [2014a] (NorESM1), Griffies *et al.* [2011] (GFDL CM3), Jahn *et al.* [2016] (CESM), and Notz *et al.* [2013] (MPI-ESM).

The same four climate models are also used to assess the future development of the Barents Sea ice cover. The simulations considered here use historical forcing for the period 1850–2005 and Representative Concentration Pathway (RCP) [Moss *et al.*, 2010] 8.5 forcing from 2006 to 2100. Instead of using a larger selection of CMIP5 models, we mainly make use of the CESM-LE, from which 40 ensemble members are available for the time period 1920 to 2100. These ensemble members all use the same Earth system model and the same external forcing but have small atmospheric initialization differences. Consequently, the CESM-LE ensemble spread is only generated by internal climate variability, unlike the CMIP5 multimodel spread that results also from different model physics. CESM-LE simulates a realistic Arctic sea ice cover and has previously been used to assess Arctic summer sea ice loss [Swart *et al.*, 2015; Barnhart *et al.*, 2016; Jahn *et al.*, 2016]. To assess scenario uncertainty, we also make use of the CESM medium ensemble (ME) [Sanderson *et al.*, 2015], which consists of 15 ensemble members forced with RCP4.5 from 2006 to 2080.

### 3. Observed Sea Ice Variability and Change 1850–2017

The Northern Hemisphere (NH) winter sea ice extent has linearly decreased by  $1.8 \times 10^6$  km<sup>2</sup> since 1979, with largest trends occurring in the Barents Sea (Figure 1a). Despite the Barents Sea's relatively small area (roughly 4% of the NH's ice covered area), it contributes to 24% of the observed NH winter sea ice loss. The winter Barents Sea ice extent has decreased by  $0.43 \times 10^6$  km<sup>2</sup> since 1979 (Figure 1b). The sea ice loss is associated with a northeastward retreating sea ice edge (Figure 2) and is particularly large in the northeastern Barents Sea (Figure 1a). As a consequence, large parts of the Barents Sea have been ice free in recent winters. The number of months with ice-free conditions has increased from less than one in the 1980s to six in 2016, and November (the first winter month) has been ice free in five of the last 8 years (not shown).

During the most recent decade the Barents Sea ice extent has been less than half of the pre-satellite (1850–1978) mean (Figure 1b). The two most recent winters have had an unprecedentedly small sea ice cover, only 28–32% of the pre-satellite mean, or 40–45% of the satellite mean. Prior to the satellite era, the Barents Sea ice cover shows large interannual variability, and less pronounced decadal to multidecadal variability. The sea ice extent increases slightly from the 1850s to the 1900s, decreases gradually to the 1950s, increases to the 1970s, and displays a rapid decline since. Consistent with Vinje [2001] and Miles *et al.* [2014], there is no clear signal of the 1930s early warming period. The long-term changes are reflected in successive 30 year trends (Figure 1c). The 30 year trends are generally small until the 1980s–1990s, whereas the recent trends are large and unprecedented, exceeding  $-0.13 \times 10^6$  km<sup>2</sup> per decade during the last 30 years. We note that recent 20–40 year trends are also unprecedented.

### 4. Sea Ice Variability and Trends in Preindustrial Control Simulations

To assess the probability of the ongoing winter Barents Sea ice loss to occur as a result of internal variability, we examine trends in preindustrial control simulations from CESM, GFDL CM3, MPI-ESM-MR, and NorESM1-M. The present observed trend is an uncommon feature in these models (Figure 3). The probability of a simulated 30 year trend to be larger than or equal to the most recent observed 30 year trend is less than 0.1% in MPI-ESM-MR, NorESM1-M, and CESM, and slightly higher (2%) in GFDL CM3 (Figure 3). We note that trends are not scaled by the mean sea ice extent in the individual models, but that the results are consistent if we consider a percentage trend. The observed sea ice extent in recent years is also an uncommon feature in the control simulations; the observed sea ice extent in 2016 and 2017 is outside the range of variability in all the preindustrial control simulations considered here (horizontal dashed lines in Figure 4a).

In three out of the four models, the simulated 30 year trends are generally less than half of the current observed trend. The GFDL CM3 simulation has larger trends than the other models and has 30 year trends larger than that observed ten times during the 500 year model run. Hence, according to these models, the chance of the recent observed trend to occur is small in a simulated preindustrial climate. In contrast, the observed decadal trends are less rare in the model simulations, e.g., the probability of a simulated 10 year trend to be larger than or equal to the current observed 10 year trend is 6–25% in all models (not shown). Figure 3 furthermore

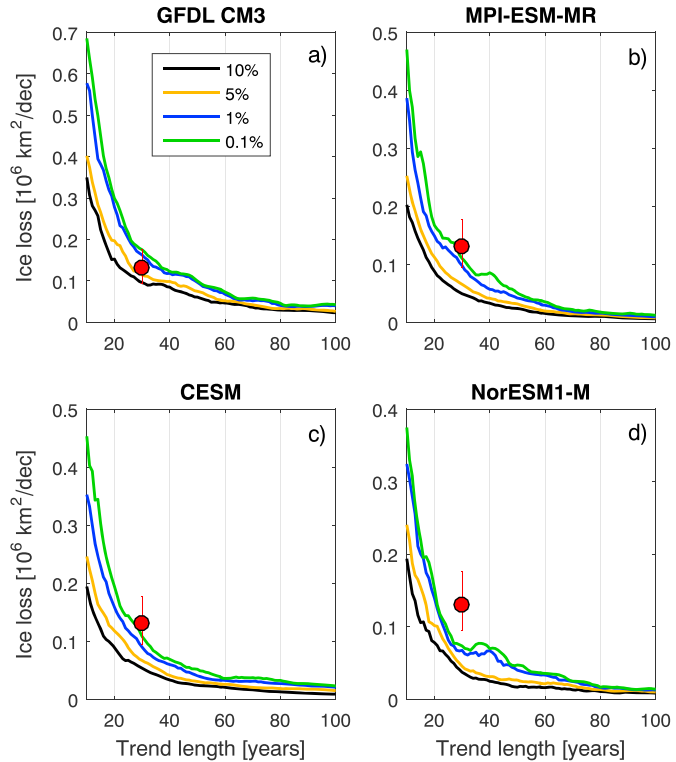


**Figure 3.** The probability (%) of a winter Barents Sea ice extent trend with a specified length (10–100 years) and magnitude to occur in preindustrial control simulations by (a) GFDL CM3, (b) MPI-ESM-MR, (c) CESM (c), and (d) NorESM1-M. Red dots indicate the most recent observed 30 year trend, and corresponding bars show the 95% confidence intervals. Note the different scales on the y-axes.

illustrates that the probability for large trends to occur increases for decreasing time intervals over which the trend is calculated, i.e., the largest trends occur for the shortest time intervals.

### 5. Future Barents Sea Ice Cover

The rapidly shrinking winter Barents Sea ice cover may portend that the Barents Sea is going toward ice-free conditions year round. As a simple estimate of when ice-free winter conditions may occur, we calculate linear and quadratic trends over the most recent 30 year period (1988–2017; both being good fits for the recent observed sea ice evolution) and then extrapolate the trends into the future. This method suggests ice-free conditions in 2023 and 2036 for quadratic and linear trends, respectively. We note that these statistical projections are highly uncertain as they are only based on extrapolating the observed trend and assume that the current sea ice extent trend prevails [e.g., Meier *et al.*, 2007].

To further investigate the future fate of the Barents Sea ice cover in the presence of climate change, we mainly employ the CESM-LE simulation, and also future climate change simulations (single realizations) from GFDL CM3, MPI-ESM-MR, and NorESM1-M. The observed Barents Sea ice extent lies within the ensemble spread of CESM-LE until the recent rapid sea ice loss (Figure 4a). This is consistent with Vinje [2001] and Shapiro *et al.* [2003] who found that the sea ice decline during the 1990s was within the range of observed variability during the last 150 years. However, recent winters fall well below the range of simulated variability in CESM-LE.

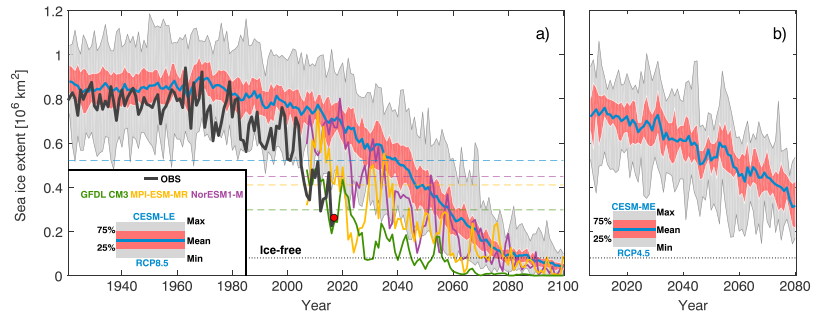


**Figure 4.** Past, present, and future winter Barents Sea ice extent in the (a) CESM-LE and (b) CESM-ME (ensemble mean; blue line; quartiles: red shading; ensemble spread: gray shading). In Figure 4a the future sea ice extent (2007–2100) is also shown for GFDL CM3 (green), MPI-ESM-MR (yellow), and NorESM1-M (purple). Horizontal dashed lines illustrate the minimum sea ice extent for the corresponding preindustrial control simulations. Observed sea ice variability is shown in black, with the red dot highlighting the winter sea ice extent in 2017. The horizontal dotted black line in Figures 4a and 4b marks (nearly) ice-free conditions, defined as 10% of the 1850–1978 average winter sea ice extent.

All models show a gradually declining sea ice cover toward 2100, with shorter (interannual to decadal) time periods of positive trends also present (Figure 4a). The latter is consistent with decadal-long hiatuses in Arctic sea ice loss as a result of internal climate variability [e.g., Kay et al., 2011; Swart et al., 2015; Årthun et al., 2017]. Ice-free conditions are projected to occur for the first time in 2028 in GFDL CM3, 2061 in MPI-ESM-MR, and 2063 in NorESM1-M. For CESM-LE the range of dates when each ensemble member becomes ice free for the first time is 2061–2088, with a median of 2075, meaning that internal variability leads to a prediction uncertainty of 28 years. Similar uncertainty was found in CESM-LE projections of Arctic summer sea ice [Jahn et al., 2016]. For the ensemble mean, representing the externally forced contribution to future sea ice loss, ice-free conditions occur in 2083. All models suggest that the Barents Sea may become ice free in periods, before recovering due to short-term positive trends. At the end of the century, however, the long-term sea ice loss overrides the periods of positive trends, and the Barents Sea thus remains ice free throughout the year (Figure 4a).

The CESM-LE simulation considers the strong forcing scenario RCP8.5, which assumes that emissions will continue to rise throughout the 21st century [Moss et al., 2010]. The medium forcing scenario RCP4.5, which assumes that emissions peak around 2040, also shows a gradually declining winter Barents Sea ice cover (Figure 4b). However, ice-free winters do not occur in any of the CESM-ME ensemble members before the simulations end in 2080. This highlights that future emissions play an essential role in the further decline of the Barents Sea winter sea ice cover.

### 6. Discussion and Conclusion

The Arctic summer sea ice extent has decreased dramatically during the last few decades [Kay et al., 2011; Stroeve et al., 2012a; Overland and Wang, 2013]. However, recent Arctic sea ice changes are also evident in winter [Cavalieri and Parkinson, 2012; Onarheim et al., 2014; Li et al., 2017], and are particularly pronounced in the Barents Sea (Figure 1). Here we have used a new observational data set spanning the time period since 1850 and coupled climate model simulations to assess the uniqueness of the recent winter Barents Sea ice loss and projections for the future. The present winter Barents Sea ice cover is less than a third of the pre-satellite mean. We find that the ongoing Barents Sea ice loss is unprecedented in the historical record (Figure 1c) and an uncommon feature in climate model control simulations (Figure 3). If the most recent 30 year trend persists, simple extrapolation suggests that the Barents Sea might become ice free some time between 2023 and 2036. For a high climate forcing scenario (RCP8.5) the CESM-LE shows ice-free conditions, for the first time, ranging from 2061 to 2088, which is in line with results from MPI-ESM-MR (2061) and NorESM1-M (2063). GFDL CM3 shows ice-free conditions already in 2028, similar to estimates obtained by extrapolating the current observed trend. In contrast, the Barents Sea does not become ice free in the RCP4.5 forced CESM-ME before the end of the simulations in 2080.

The large range in the projected timing of an ice-free Barents Sea (Figure 4) is due to a combination of internal climate variability, model differences, and scenario uncertainty. The intermodel spread in the simulated future Arctic sea ice cover (Figure 4a) [Stroeve *et al.*, 2007; Kay *et al.*, 2011; Stroeve *et al.*, 2012b] might, for instance, be related to differences in the complexity of the sea ice models. Stroeve *et al.* [2007] found that models including more sophisticated sea ice processes were better able to capture the recent observed trend. Similarly, Bathiany *et al.* [2016] argued that the MPI model loses sea ice too quickly in winter due to oversimplified sea ice parametrization. Of the models used here, CESM and NorESM1-M incorporate the relatively sophisticated sea ice model, CICE, but it is not possible to judge based on the results presented here whether these models are more realistic than MPI-ESM-MR and GFDL CM3. Trying to assess which model projection is most reasonable is further complicated by the fact that a realistic representation of the past and present sea ice changes does not imply a correct representation of its future evolution [Notz, 2015].

A possible way of reducing the prediction uncertainty is by examining the CESM-LE for emerging constraints that could indicate which trajectory is most reasonable based on the current sea ice state [e.g., Stroeve and Notz, 2015; Notz, 2015]. We find, however, that the ensemble members in CESM-LE becoming ice free first are not those with small sea ice extent or large sea ice trends at present (and vice versa; not shown), and that we therefore cannot predict which ensemble member becomes ice free first based on the past and present sea ice state. This is consistent with the analysis of the future evolution of the Arctic summer sea ice extent by Jahn *et al.* [2016], which show that common metrics of the past and present sea ice state were unable to reduce the prediction uncertainty from internal variability. As the recent Barents Sea winter sea ice decline has largely been driven by ocean heat transport changes [Árthun *et al.*, 2012; Onarheim *et al.*, 2015; Li *et al.*, 2017], we also examined the predictive skill in Atlantic heat transport (mean, trend, and correlation with sea ice extent) but found no relation to the timing of ice-free conditions (not shown).

The large ensemble spread in CESM-LE projections of future winter sea ice extent indicates that internal variability has a strong influence on the timing of reaching an ice-free Barents Sea. An estimate of the relative contributions of external forcing and internal variability on the most recent sea ice loss can be obtained by comparing the ensemble mean CESM-LE 1988–2017 linear trend with the observed linear trend over the same 30 year time period [cf., Stroeve *et al.*, 2007; Kay *et al.*, 2011]. The averaging across ensemble members cancels out internal variability, and divided by the observed trend, it thus implies the response that results from changes in external forcing. Assuming that the CESM-LE ensemble mean correctly represents the externally forced trend, this calculation indicates that 72% of the recent 30 year trend is due to internal variability. The important role of internal variability is in agreement with Li *et al.* [2017] who found that the observed trend in Barents Sea ice cover during the satellite period has mainly been a result of enhanced ocean heat transport associated with regional internal variability. In summary, internal variability is found to be important for the observed present and modeled future winter sea ice loss in the Barents Sea (Figure 4a). However, modeled internal variability alone cannot explain the recent observed sea ice loss (Figure 3).

Conclusions based on climate model simulations are only as reliable as the model's ability to correctly simulate the governing underlying processes. For the Barents Sea specifically, CMIP5 models generally underestimate ocean heat transport into the Barents Sea and, hence, overestimate the sea ice extent [Li *et al.*, 2017]. Consistently, the models used here also show a slight overestimation, although a comparison with observations is not straightforward as the preindustrial control runs do not include external forcing. Li *et al.* [2017] speculate that these discrepancies are a result of underestimated internal variability in climate models. Consequently, the calculated probability of the current rate of sea ice loss to occur as a result of internal variability (Figure 3) could also be underestimated. The projected timing of ice-free conditions presented here is nevertheless in general agreement with estimates based on downscaled A1B scenarios with a more realistic ocean heat transport and mean sea ice extent [Smetsrud *et al.*, 2013; Sandø *et al.*, 2014b]. However, no detailed analysis of future sea ice loss with respect to past and present trends was performed in these studies.

The recent trend toward less Arctic winter sea ice has predominantly occurred in the Barents Sea (Figure 1), and the Barents Sea could be the first Arctic shelf sea to become ice free year round. With current emissions tracking the RCP8.5 scenario [Peters *et al.*, 2013] the Barents Sea is moving toward ice-free conditions within this century. However, reduced emissions could substantially delay this development (Figure 4). A better understanding of Arctic sea ice variability and trends on different time scales, and the role of internal variability, as provided here, is therefore essential in order to predict future sea ice changes under anthropogenic warming.

### Acknowledgments

This research was supported by the Centre for Climate Dynamics (SKD) at the Bjerkes Centre, the University of Bergen, and by the Research Council of Norway through the projects NORTH and PATHWAY. We thank Helene R. Langehaug, Aleksi Nummelin, and two anonymous reviewers for valuable comments that improved the manuscript. We acknowledge the World Climate Research Programme's Working Group on Coupled Modelling, which is responsible for CMIP, and we thank the climate modeling groups for producing and making available their model output. We also acknowledge the CESM Large Ensemble Community Project for making their data available. Observed sea ice concentrations can be downloaded from the National Snow and Ice Data Center; the NASA Team product from November 1978 to February 2017 from <http://nsidc.org/data/NSIDC-0051>, the near-real-time data for March and April 2017 from <http://nsidc.org/data/NSIDC-0081>, and the 1850 onward data set, 1850–2013, from <http://nsidc.org/data/G10010>. We thank the NSIDC for making their data available.

### References

- ACIA (2005), *Arctic Climate Impact Assessment*, Cambridge Univ. Press, Cambridge, U. K.
- Årthun, M., T. Eldevik, L. H. Smedsrud, Ø. Skagseth, and R. B. Ingvaldsen (2012), Quantifying the influence of Atlantic heat on Barents Sea ice variability and retreat, *J. Clim.*, *25*, 4736–4743.
- Årthun, M., T. Eldevik, E. Viste, H. Drange, T. Furevik, H. L. Johnson, and N. S. Keenlyside (2017), Skillful prediction of northern climate provided by the ocean, *Nat. Commun.*, *8*, 15875.
- Barnhart, K. R., C. R. Miller, I. Overeem, and J. E. Kay (2016), Mapping the future expansion of Arctic open water, *Nat. Clim. Change*, *6*(3), 280–285.
- Bathiany, S., D. Notz, T. Mauritsen, G. Raedel, and V. Brovkin (2016), On the potential for abrupt Arctic winter sea ice loss, *J. Clim.*, *29*(7), 2703–2719.
- Bentsen, M., et al. (2013), The Norwegian earth system model, NorESM1-M. Part 1: Description and basic evaluation of the physical climate, *Geosci. Model Dev.*, *6*(3), 687–720.
- Cavaleri, D. J., and C. L. Parkinson (2012), Arctic sea ice variability and trends, 1979–2010, *Cryosphere*, *6*(4), 881–889.
- Cavaleri, D. J., C. L. Parkinson, P. Gloersen, and H. Zwally (1996), *Sea Ice Concentrations From Nimbus-7 SMMR and DMSP SSM/I Passive Microwave Data*, Digital Media, Natl. Snow and Ice Data Center, Boulder, Colo.
- Dalpadado, P., K. R. Arrigo, S. S. Hjøllø, F. Rey, R. B. Ingvaldsen, E. Sperfeld, G. L. van Dijken, L. C. Stige, A. Olsen, and G. Ottersen (2014), Productivity in the Barents Sea—response to recent climate variability, *9*(5), e95273.
- Giorgetta, M. A., et al. (2013), Climate and carbon cycle changes from 1850 to 2100 in MPI-ESM simulations for the Coupled Model Intercomparison Project phase 5, *J. Adv. Model. Earth Syst.*, *5*(3), 572–597.
- Griffies, S. M., et al. (2011), The GFDL CM3 coupled climate model: Characteristics of the ocean and sea ice simulations, *J. Clim.*, *24*(13), 3520–3544.
- Jahn, A., J. E. Kay, M. M. Holland, and D. M. Hall (2016), How predictable is the timing of a summer ice-free Arctic?, *Geophys. Res. Lett.*, *43*, 9113–9120, doi:10.1002/2016GL070067.
- Kay, J., et al. (2015), The Community Earth System Model (CESM) large ensemble project: A community resource for studying climate change in the presence of internal climate variability, *Bull. Am. Meteorol. Soc.*, *96*(8), 1333–1349.
- Kay, J. E., M. M. Holland, and A. Jahn (2011), Inter-annual to multi-decadal Arctic sea ice extent trends in a warming world, *Geophys. Res. Lett.*, *38*, L15708, doi:10.1029/2011GL048008.
- Levitus, S., G. Matishov, D. Seidov, and I. Smolyar (2009), Barents Sea multidecadal variability, *Geophys. Res. Lett.*, *36*, L19604, doi:10.1029/2009GL039847.
- Li, D., R. Zhang, and T. R. Knutson (2017), On the discrepancy between observed and CMIP5 multi-model simulated Barents Sea winter sea ice decline, *Nat. Commun.*, *8*, 14991.
- Liptak, J., and C. Strong (2014), The winter atmospheric response to sea ice anomalies in the Barents Sea, *J. Clim.*, *27*(2), 914–924.
- Maslanik, J., and J. Stroeve (1999), *Near-Real-Time DMSP SSMIS Daily Polar Gridded Sea Ice Concentrations, Version 1*, NASA Natl. Snow and Ice Data Cent. Distrib. Active Archive Cent., Boulder, Colo.
- Meier, W., F. Fetterer, M. Savoie, S. Mallory, R. Duerr, and J. Stroeve (2013), *updated 2016, NOAA/NSIDC Climate Data Record of Passive Microwave Sea Ice Concentration, Version 2*, Natl. Snow and Ice Data Cent. (NSIDC), Boulder, Colo.
- Meier, W. N., J. Stroeve, and F. Fetterer (2007), Whither Arctic sea ice? A clear signal of decline regionally, seasonally and extending beyond the satellite record, *Ann. Glaciol.*, *46*(1), 428–434.
- Miles, M. W., D. V. Divine, T. Furevik, E. Jansen, M. Moros, and A. E. Ogilvie (2014), A signal of persistent Atlantic multidecadal variability in Arctic sea ice, *Geophys. Res. Lett.*, *41*, 463–469, doi:10.1002/2013GL058084.
- Moss, R. H., et al. (2010), The next generation of scenarios for climate change research and assessment, *Nature*, *463*(7282), 747–756.
- Notz, D. (2015), How well must climate models agree with observations?, *Philos. Trans. R. Soc. A*, *373*(2052), 20140164.
- Notz, D., F. A. Haumann, H. Haak, J. H. Jungclaus, and J. Marotzke (2013), Arctic sea-ice evolution as modeled by Max Planck Institute for Meteorology's Earth system model, *J. Adv. Model. Earth Syst.*, *5*(2), 173–194.
- Onarheim, I. H., L. H. Smedsrud, R. B. Ingvaldsen, and F. Nilsen (2014), Loss of sea ice during winter north of Svalbard, *Tellus A*, *66*, 23933.
- Onarheim, I. H., T. Eldevik, M. Årthun, R. B. Ingvaldsen, and L. H. Smedsrud (2015), Skillful prediction of Barents Sea ice cover, *Geophys. Res. Lett.*, *42*, 5364–5371, doi:10.1002/2015GL064359.
- Overland, J. E., and M. Wang (2013), When will the summer Arctic be nearly sea ice free?, *Geophys. Res. Lett.*, *40*, 2097–2101, doi:10.1002/grl.50316.
- Peters, G. P., R. M. Andrew, T. Boden, J. G. Canadell, P. Ciais, C. Le Quéré, G. Marland, M. R. Raupach, and C. Wilson (2013), The challenge to keep global warming below 2°C, *Nat. Clim. Change*, *3*(1), 4–6.
- Sanderson, B. M., K. W. Oleson, W. G. Strand, F. Lehner, and B. C. O'Neill (2015), A new ensemble of GCM simulations to assess avoided impacts in a climate mitigation scenario, *Clim. Change*, *1–16*, doi:10.1007/s10584-015-1567-z.
- Sandø, A., Y. Gao, and H. Langehaug (2014a), Poleward ocean heat transports, sea ice processes, and Arctic sea ice variability in NorESM1-M simulations, *J. Geophys. Res.*, *119*, 2095–2108, doi:10.1002/2013JC009435.
- Sandø, A. B., A. Melsom, and W. P. Budgell (2014b), Downscaling IPCC control run and future scenario with focus on the Barents Sea, *Ocean Dyn.*, *64*(7), 927–949.
- Serreze, M. C., and J. Stroeve (2015), Arctic sea ice trends, variability and implications for seasonal ice forecasting, *Philos. Trans. R. Soc. A*, *373*(2045), 20140159.
- Serreze, M. C., M. M. Holland, and J. Stroeve (2007), Perspectives on the Arctic's shrinking sea-ice cover, *Science*, *315*(5818), 1533–1536.
- Shapiro, I., R. Colony, and T. Vinje (2003), April sea ice extent in the Barents Sea, 1850–2001, *Polar Res.*, *22*(1), 5–10.
- Skagseth, Ø., T. Furevik, R. Ingvaldsen, H. Loeng, K. A. Mørk, K. A. Orvik, and V. Ozhigin (2008), Volume and heat transports to the Arctic Ocean via the Norwegian and Barents Seas, in *Arctic-Subarctic Ocean Fluxes*, pp. 45–64, Springer, Dordrecht, Netherlands.
- Smedsrud, L. H., et al. (2013), The role of the Barents Sea in the Arctic climate system, *Rev. Geophys.*, *51*, 415–449, doi:10.1002/rog.20017.
- Sorokina, S. A., C. Li, J. J. Wettstein, and N. G. Kwamsto (2016), Observed atmospheric coupling between Barents Sea ice and the warm-Arctic cold-Siberian anomaly pattern, *J. Clim.*, *29*(2), 495–511.
- Stroeve, J., and D. Notz (2015), Insights on past and future sea-ice evolution from combining observations and models, *Global Planet. Change*, *135*, 119–132.
- Stroeve, J., M. M. Holland, W. Meier, T. Scambos, and M. Serreze (2007), Arctic sea ice decline: Faster than forecast, *Geophys. Res. Lett.*, *34*, L09501, doi:10.1029/2007GL029703.
- Stroeve, J. C., M. C. Serreze, M. M. Holland, J. E. Kay, J. Malanik, and A. P. Barrett (2012a), The Arctic's rapidly shrinking sea ice cover: A research synthesis, *Clim. Change*, *110*(3), 1005–1027.

- Stroeve, J. C., V. Kattsov, A. Barrett, M. Serreze, T. Pavlova, M. Holland, and W. N. Meier (2012b), Trends in Arctic sea ice extent from CMIP5, CMIP3 and observations, *Geophys. Res. Lett.*, *39*, L16502, doi:10.1029/2012GL052676.
- Swart, N. C., J. C. Fyfe, E. Hawkins, J. E. Kay, and A. Jahn (2015), Influence of internal variability on Arctic sea-ice trends, *Nat. Clim. Change*, *5*(2), 86–89.
- Taylor, K. E., R. J. Stouffer, and G. A. Meehl (2012), An overview of CMIP5 and the experiment design, *Bull. Am. Meteorol. Soc.*, *93*(4), 485–498.
- Venegas, S. A., and L. A. Mysak (2000), Is there a dominant timescale of natural climate variability in the Arctic?, *J. Clim.*, *13*(19), 3412–3434.
- Vinje, T. (2001), Anomalies and trends of sea-ice extent and atmospheric circulation in the Nordic Seas during the period 1864–1998, *J. Clim.*, *14*(3), 255–267.
- Walsh, J. E., W. L. Chapman, and F. Fetterer (2015), *Gridded Monthly Sea Ice Extent and Concentration, 1850 Onward, Version 1*, Natl. Snow and Ice Data Cent. (NSIDC), Boulder, Colo.
- Walsh, J. E., F. Fetterer, J. Scott Stewart, and W. L. Chapman (2017), A database for depicting Arctic sea ice variations back to 1850, *Geograph. Rev.*, *107*(1), 89–107.
- Zhang, R. (2015), Mechanisms for low-frequency variability of summer Arctic sea ice extent, *Proc. Natl. Acad. Sci.*, *112*, 4570–4575.

